Functional characterization of promoter polymorphisms in the human Cytochrome P450 2B6 gene (*CYP2B6*)

Funktionelle Charakterisierung von Promotorpolymorphismen im humanen Cytochrom P450 2B6-Gen (*CYP2B6*)

DISSERTATION

der Fakultät für Chemie und Pharmazie
der Eberhard-Karls-Universität Tübingen
zur Erlangung des Grades eines Doktors
der Naturwissenschaften

2005

vorgelegt von

Jörg Zukunft

Teile der Arbeit wurden bereits veröffentlicht in:

Zukunft J *et al.* (2005) A natural CYP2B6 TATA box polymorphism (-82T->C) leading to enhanced transcription and relocation of the transcriptional start site. *Mol Pharmacol* **67:** 1772-1782.

Tag der mündlichen Prüfung:	3. Mai 2005
Dekan:	Prof. Dr. S. Laufer
1. Berichterstatter:	PD Dr. U. M. Zanger
2. Berichterstatter:	Prof. Dr. K. W. Bock

“Musik ist Trumpf!
Musik ist Trumpf im Leben.”
(Hazy Osterwald)

Für Tatjana und Richard

TABLE OF CONTENTS

ABSTRACT

Human Cytochrome P450 2B6 (CYP2B6) belongs to the superfamily of Cytochrome P450 enzymes which catalyze a vast variety of biotransformations, mainly oxidations, of numerous endogenous substrates and xenobiotics. Drugs predominantly metabolized by this enzyme include, among others, the anticancer prodrug cyclophosphamide, the narcotic propofol, the antidepressant bupropion, the antimalarial drug artemisinin and the reverse transcriptase inhibitor efavirenz. In several works, a high variability in hepatic expression of CYP2B6 has been observed, part of which can be attributed to induction phenomena similar to the rodent *CYP2B* genes. Additionally, *CYP2B6* has been shown to be highly polymorphic in the coding region as well as in the promoter region, and certain nonsynonymous SNPs have been associated with altered hepatic expression or activity of the protein.

In this work, the impact of promoter polymorphisms on transcription of the human *CYP2B6* gene was investigated. A comprehensive haplotype analysis was conducted using 2.3 kb of promoter sequence data and genotypes for all common nonsynonymous SNPs from 96 individuals of Caucasian origin. Erroneous genotyping for the SNP c.1459C>T in exon 9 was observed with the PCR-RFLP assay described previously by Lang *et al*. (2001) resulting from a mutation in a primer binding site in intron 8, and an alternative assay was developed. The presence and frequency of the major haplotypes present among Caucasians was confirmed except for the *CYP2B6*7* allele which was shown to be a potential artifact caused by faulty genotyping of the mutation c.1459C>T. For functional investigations of the promoter polymorphisms, HepG2-cells and primary rat and human hepatocytes were transfected with luciferase reporter gene constructs driven by 2033 bp of the most frequent promoter variants **1A*, **1J*, **1N* and **22*. The novel haplotype **22* (-1848C>A, -801G>T, -750T>C and -82T>C) showed three- to ninefold enhanced transcriptional activity compared to **1A* representing the wild type in all transfected cells. Constructs containing single mutations surprisingly revealed -82T>C, predicted to disrupt a putative TATA box, to be alone responsible for this effect. *In silico* analysis and electrophoretic mobility shift assay demonstrated conversion of the putative TATA box into a functional C/EBP binding site. Analysis of transcriptional start sites by 5'-RLM-RACE and primer extension showed the mutant promoter to be transcribed from a start site located about 30 bp downstream of the wild type start site, consistent with the use of a noncanonical TATA box at -55 bp. For

genotyping the SNP -82T>C in a large human liverbank, a DHPLC assay was established. The subsequent phenotype-genotype correlation analysis showed that median CYP2B6 mRNA expression and bupropion hydroxylase activity as a selective marker of CYP2B6 catalytic activity were about twofold higher in livers genotyped -82TC as in those genotyped -82TT (20.4 vs. 9.8 a.u., p=0.007, and 201.8 vs. 106.7 pmol/mg*min, p=0.042, respectively). This promoter polymorphism thus contributes to CYP2B6 functional variability and represents a novel mechanism by which mutations can enhance transcription. The SNP -750T>C was also investigated as it was predicted to disrupt a putative HNF1 binding site. Although a reduction in affinity of HNF1 to the promoter was observed in electrophoretic mobility shift assay when the mutation was present, no significant differences in reporter gene assays or hepatic expression were seen in relation to this mutation. In contrast, the *CYP2B6*6B* allele containing this SNP was shown to result in significantly reduced expression in human liver samples at the mRNA, protein and activity level. Thus, median mRNA levels were 11.2 vs. 7.2 a.u. (p=0.017), median microsomal protein content was 14.2 vs. 7.3 pmol 2B6/mg protein (p=0.008), and median bupropion hydroxylase activity was reduced from 121.2 to 79.9 pmol/mg*min (p=0.020) in non-carriers vs. carriers of the *CYP2B6*6* allele. Furthermore, a detailed inter-species comparison of *CYP2B* promoters and transcriptional start sites provided novel insights into evolutionary relationships and constitutive regulation of this gene (Zukunft *et al.*, 2005).

Key words: CYP2B6, CYP2B6*22, CYP2B6*7, transcriptional start site, transcriptional regulation, C/EBP, HNF1

ZUSAMMENFASSUNG

Das humane Cytochrom P450 2B6 (CYP2B6) gehört zu der Superfamilie der Cytochrom-P450-Enzyme, die eine Vielfalt von Biotransformationen, vornehmlich Oxidationen, verschiedenster körpereigener und -fremder Substrate katalysieren. Zu den Arzneistoffen, die fast ausschließlich von diesem Enzym metabolisiert werden, zählen unter anderem das Cytostatikum Cyclophosphamid, das Anästhetikum Propofol, das Antidepressivum Bupropion, das Antimalariamittel Artemisinin und der nichtnukleosidische Reverse-Transkriptase-Hemmer Efavirenz. In verschiedenen Arbeiten wurde eine hohe Variabilität der hepatischen Expression des CYP2B6 beobachtet, die teilweise seiner den *CYP2* Genen der Nager analogen Induzierbarkeit zugeschrieben werden kann. Darüber hinaus wurde gezeigt, dass *CYP2B6* sowohl in der Promotorregion als auch im kodierenden Bereich hochpolymorph ist, und verschiedene zu einem Aminosäureaustausch führende Mutationen wurden mit einer veränderten Expression oder Aktivität des Proteins assoziiert.

In dieser Arbeit wurde der Einfluss von Promotorpolymorphismen auf die Transkription des humanen *CYP2B6*-Gens untersucht. Sequenzierungsdaten von einem 2,3 kb umfassenden Bereich des Promotors sowie Genotypisierungsdaten für alle häufigen nichtsynonymen SNPs von 96 Kaukasiern wurden für eine umfassende Haplotypenanalyse verwendet. Fehlerhafte Genotypisierungen mit der von Lang *et al.* (2001) beschriebenen PCR-RFLP-Methode für die Mutation c.1459C>T wurden beobachtet, die sich auf eine Mutation in einer Primerbindestelle im Intron 8 zurückführen ließen, und eine alternative Methode wurde etabliert. Die Präsenz und Häufigkeiten der wichtigsten Haplotypen bei Kaukasiern konnten bis auf Ausnahme des Allels *CYP2B6*7* bestätigt werden. Für dieses wurde gezeigt, dass es sich wahrscheinlich um ein durch fehlerhaftes Genotypisieren der Mutation c.1459C>T verursachtes Artefakt handelt. Für die funktionelle Untersuchung der Promotorpolymorphismen wurden HepG2-Zellen sowie aus Ratten und Menschen isolierte primäre Hepatozyten mit Reportergenkonstrukten transfiziert, von denen das Luziferasegen unter der Kontrolle von 2033 Basenpaaren der häufigsten Promotorvarianten **1A*, **1J*, **1N* und **22* transkribiert wird. Der neu beschriebene Haplotyp **22* (-1848C>A, -801G>T, -750T>C und -82T>C) zeigte in allen transfizierten Zellen eine drei- bis neunfach erhöhte Transkriptionsaktivität im Vergleich zu **1A*, das den Wildtyp repräsentiert. Überraschenderweise konnte durch Reportergenkonstrukte mit einzelnen Mutationen der SNP -82T>C, der

eine mutmaßliche TATA-box zerstört, als die alleinige ursächliche Mutation identifiziert werden. Computeranalysen und „electrophoretic mobility shift assay“ zeigten, dass die potentielle TATA-box in eine funktionelle C/EBP-Bindestelle umgewandelt wird. Transkriptionsstartanalysen mittels „5’-RLM-RACE“ und „primer extension“ ergaben, dass beim mutierten Promotor die Transkription ungefähr 30 Basen stromabwärts der regulären Transkriptionsstartstelle einsetzt, was auf die Verwendung einer nichtkanonischen TATA-Box bei -55 bp schließen ließ. Eine DHPLC-Methode zur Genotypisierung des SNPs -82T>C in einer umfangreichen humanen Leberbank wurde entwickelt. In der anschließenden Genotyp-Phänotypkorrelation erwies sich, dass die mediane CYP2B6 mRNA-Expression und die Bupropionhydroxylaseaktivität als spezifische Nachweisreaktion für CYP2B6-Aktivität in Lebern mit Genotyp -82TC gegenüber denen mit Genotyp -82TT etwa zweifach erhöht waren (20,4 vs. 9,8 a.u., p=0,007, und 201,8 vs. 106,7 pmol/mg*min, p=0,042). Folglich trägt dieser Promotorpolymorphismus zur funktionellen Variabilität des CYP2B6 bei und stellt einen neuartigen Mechanismus dar, wie eine Mutation die Transkription verstärken kann. Des weiteren wurd der SNP -750T>C untersucht, bei dessen Anwesenheit die Zerstörung einer mutmaßlichen HNF1-Bindestelle vorhergesagt wurde. Obwohl in Gegenwart der Mutation eine Abschwächung der Promotoraffinität von HNF1 im „electrophoretic mobility shift assay“ beobachtet wurde, waren signifikante Unterschiede bezüglich dieser Mutation weder bei den Reportergenversuchen noch bei der hepatischen Expression zu sehen. Im Gegensatz dazu konnte für das Allel *CYP2B6*6B*, das diese Mutation enthält, eine verringerte Expression in humanen Leberproben auf mRNA-, Protein- und Aktivitätsebene beobachtet werden. So war bei Nichtträgern bzw. Trägern des *CYP2B6*6*-Allels die mediane mRNA-Expression 11,2 vs. 7,2 a.u. (p=0,017), der mediane mikrosomale Proteingehalt betrug 14,2 vs. 7,3 pmol 2B6/mg Protein (p=0,008), und die mediane Bupropionhydroxylaseaktivität war von 121,2 auf 79,9 pmol/mg*min (p=0,020) reduziert. Des weiteren wurde ein detaillierte Gegenüberstellung von *CYP2B*-Promotoren und Transkriptionsstartstellen verschiedener Spezies vorgenommen, die neue Einblicke in die evolutionäre Entwicklung und konstitutive Regulation dieses Gens gewährt.

ABBREVIATIONS

ALB	Albumin
AMV	Avian myeloblastosis virus
ANOVA	Analysis of variance
apoE	Apolipoprotein E
APS	Ammonium persulfate
ATP	Adenosine triphosphate
a.u.	Arbitrary units
bp	Basepairs
C/EBP	CCAAT/enhancer binding protein
CAR	Constitutive androstane receptor
CIP	Calf intestinal phosphatase
CMV	Cytomegalovirus
CYP	Cytochrome P450
DCoH	Dimerization cofactor of hepatic nuclear factor 1-alpha
DHPLC	Denaturing high-performance liquid chromatography
DMSO	Dimethyl sulfoxide
DTT	1,4-Dithio-DL-threitol
EDTA	Ethylenediaminetetraacetic acid
EFC	Ethoxy-4-trifluoromethylcoumarin
EMSA	Electrophoretic mobility shift assay
FAM	6-Carboxyfluorescein
HEPES	4-(2-Hydroxyethyl)piperazine-1-ethanesulfonic acid
HIV-1	Human immunodeficiency virus type 1
HNF	Hepatic nuclear factor
HWE	Hardy-Weinberg equilibrium
kb	Kilobases
LAP	Liver-enriched transcriptional activating protein
LIP	Liver-enriched transcriptional inhibitory protein
MGBNFQ	Minor groove binder/Non-fluorescent quencher
NADPH	Nicotinamide adenine dinucleotide phosphate

NR	Nuclear receptor
OARE	Okadaic acid response element
PBREM	Phenobarbital-responsive enhancer module
PBS	Phosphate buffered saline
PCR	Polymerase chain reaction
PEG	Polyethylene glycol
PMSF	Phenylmethanesulfonyl fluoride
PXR	Pregnane-X-receptor
RFLP	Restriction fragment length polymorphism
RIM	Reaction injection mix
RLM-RACE	RNA-ligase mediated rapid amplification of cDNA ends
RT	Reverse transcriptase
RXR	Retinoid-X-receptor
SNP	Single nucleotide polymorphism
TAE	Tris/Acetate/EDTA
TAMRA	Carboxytetramethylrhodamine
TAP	Tobacco acid pyrophosphatase
TBE	Tris/Borate/EDTA
TBP	TATA box binding protein
TE	Tris/EDTA
TEAA	Triethylammonium acetate
TEMED	N-, N-, N'-, N'-Tetramethylethylenediamine
TSS	Transcriptional start site
UDP	Uridine 5'-diphosphate
UGT	UDP-Glucuronosyltransferase
UTR	Untranslated region
XREM	Xenobiotic-responsive enhancer module

I INTRODUCTION

1. The Cytochrome P450 enzymes

With more than 2500 genes described to date in different species from bacteria to human, the Cytochrome P450 (CYP) enzymes constitute one of the biggest gene families (http://drnelson.utmem.edu/CytochromeP450.html). Their name originated from early observations describing them as a pigment (P) with a spectral absorbance maximum at 450 nm seen in the presence of a reducing agent and carbon monoxide (Klingenberg, 1958; Estabrook, 2003). This unique feature distinguishes them from most other hemoproteins, which display an absorption maximum at 420 nm under these conditions. The reason for this unusual behavior is the axial ligand of the prosthetic heme group in the active site. In most hemoproteins like hemoglobin, this ligand represents a nitrogen atom of a histidine residue, whereas in cytochrome P450 enzymes, a sulfur atom of a conserved cysteine residue takes this function.

In eukaryotes, these proteins are embedded in the membrane of either the endoplasmatic reticulum or the mitochondria by an amino-terminal membrane anchor. Their main function is to activate molecular oxygen to introduce hydroxyl groups into unreactive hydrocarbon chains and aromatic rings; these functional groups then facilitate conjugation reactions by UDP-glucuronosyltransferases or other phase II enzymes. The basic stoichiometry of a P450-catalyzed hydroxylation of a substrate S is represented by the following equation:

$$NADPH+H^+ + O_2 + SH \rightarrow NADP^+ + H_2O + SOH$$

The reduction equivalents provided by $NADPH+H^+$ are transferred to the CYP enzyme by the membrane-bound enzyme Cytochrome P450 reductase (Figure 1). Cytochrome b5, a 17 kDa protein, is able to increase the activity of certain CYP-catalyzed reactions; however, the mechanism of this interaction still remains speculative (Schenkman and Jansson, 2003). In addition to hydroxylations, there are also examples of *N*-, *S*-, or *O*-dealkylations, *N*- or *S*-oxidations, deaminations, dehalogenations, epoxidations and peroxidations catalyzed by CYP enzymes (Danielson, 2002).

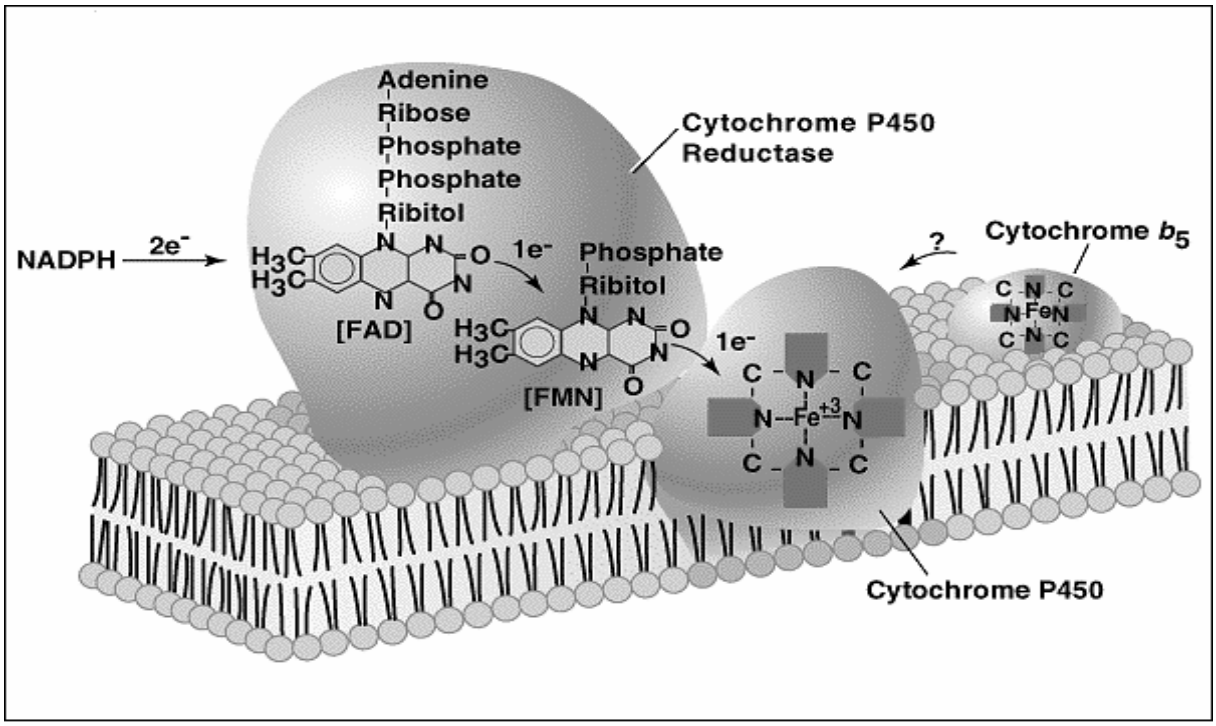

Figure 1: Electron transfer from NADPH + H^+ to Cytochrome P450 enzymes is catalyzed by Cytochrome P450 reductase.

As the tremendous genetic multiplicity of the cytochrome P450 enzymes became apparent, a standardized system of nomenclature has been established to name and assign individual genes into families and subfamilies. Thus, P450 sequences that display greater than 40% amino acid identity are placed into the same family, and sequences that are more than 55% identical are placed into the same subfamily (Nelson *et al.*, 1996). In humans, the cytochrome P450 gene superfamily comprises 57 functional genes and 58 pseudogenes (Nelson *et al.*, 2004), based on the assembly of the human genome published in April 2003 (build 33). The numerous members of the families *CYP1*, *CYP2* and *CYP3,* which account for over 70% of total hepatic CYP content (about 500 pmol/mg, Shimada *et al.*, 1994), represent the most important enzymes of xenobiotic phase I metabolism (Table 1). They exhibit large and overlapping substrate specificity and metabolize many drugs currently in use as well as endogenous steroids, plant alkaloids, environmental toxins and carcinogens.

Family	Functional genes	Functions
CYP1	3	Xenobiotic metabolism
CYP2	16	Xenobiotic and steroid metabolism
CYP3	4	Xenobiotic and steroid metabolism
CYP4	12	Arachidonic acid and fatty acid metabolism
CYP5	1	Thromboxane A2-synthase
CYP7	2	7α-hydroxylase
CYP8	2	Prostacyclin synthase (8A1)
		Bile acid biosynthesis (8B1)
CYP11	3	Steroid biosynthesis
CYP17	1	Steroid biosynthesis (17α-hydroxylase)
CYP19	1	Steroid biosynthesis (aromatase)
CYP20	1	Function unknown
CYP21	1	Steroid biosynthesis
CYP24	1	Vitamin D side-chain oxidation
CYP26	3	Retinoic acid hydroxylase
CYP27	3	Bile acid biosynthesis (27A1)
		Vitamin D3-1α-hydroxylase (27B1)
CYP39	1	7α-hydroxylation of 24-OH-cholesterol
CYP46	1	Cholesterol 24-hydroxylase
CYP51	1	Cholesterol biosynthesis (lanosterol 14α-demethylase)

Table 1: Human CYP families and their functions (adapted from D.R. Nelson's Cytochrome P450 homepage http://drnelson.utmem.edu/CytochromeP450.html)

2. CYP2B6

2.1. Chromosomal localization and gene structure

The family member *CYP2B6* was first described in 1989 (Yamano *et al.*, 1989) as the human orthologue to the phenobarbital-inducible *CYP2B* genes in rodents and mapped to chromosome 19. Two members of the *CYP2B* subfamily are present in the human genome: the functional *CYP2B6* and the paralogous full-sized pseudogene *CYP2B7P1* which is located approximately 50 kb upstream and arose from a tandem duplication. *CYP2B7P1* displays 95%

similarity at the nucleotide level but contains a premature stop codon (CGA>TGA) due to the nonsense mutation c.1132C>T in exon 7. Numerous other members of the *CYP2* family created by several inverted and tandem duplications surround these two genes which appear to have been inserted into the midst of the *CYP2A18P* locus (Hoffman *et al.*, 2001) to create the complex CYP2ABFGST cluster (Figure 2). To date, this conglomerate is known to contain six functional genes and seven pseudogenes from six different *CYP2* subfamilies (Nelson *et al.*, 2004).

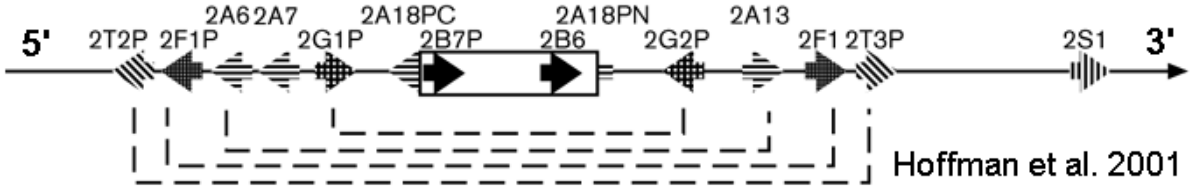

Figure 2: Structure of the *CYP2* gene cluster on chromosome 19. Dashed lines highlight the mirror-image arrangement established by an inverted duplication which was followed by further duplications within the *CYP2A* subfamily. The two *CYP2B* genes have been inserted into the *CYP2A18* locus leading to the present arrangement (Hoffman *et al.*, 2001).

Similar to other members of the *CYP2* family, *CYP2B6* consists of nine exons (Figure 3) encoding a functional protein with 491 amino acids and a molecular weight of about 56 kDa. Remarkable features of the gene are a rather long 3'-UTR of 1.6 kb and an unusual long intron 1 (12.7 kb) that is also present in the *CYP2B7P1* pseudogene.

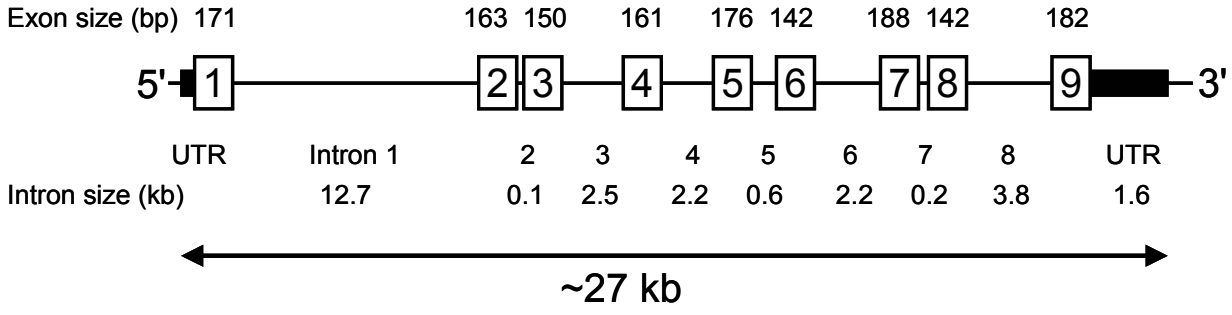

Figure 3: Structure of the human *CYP2B6* gene. Exons are shown as boxes with exon size in bp and intron size in kb. UTR: untranslated region.

2.2. Substrates

Initially underestimated, the number of drugs recognized as CYP2B6 substrates has been constantly increasing and several clinically important substances are now known to be metabolized predominantly by this enzyme (Figure 4). These include the anticancer prodrug cyclophosphamide (Roy *et al.*, 1999), the narcotic propofol (Court *et al.*, 2001), the antidepressant bupropion which is now the most commonly used probe drug for CYP2B6 (Faucette *et al.*, 2000), the antimalarial drug artemisinin (Svensson and Ashton, 1999) and the reverse transcriptase inhibitor efavirenz (Ward *et al.*, 2003). Numerous other substances are at least partially metabolized by this enzyme, and it is likely that more substrates will be identified in the future.

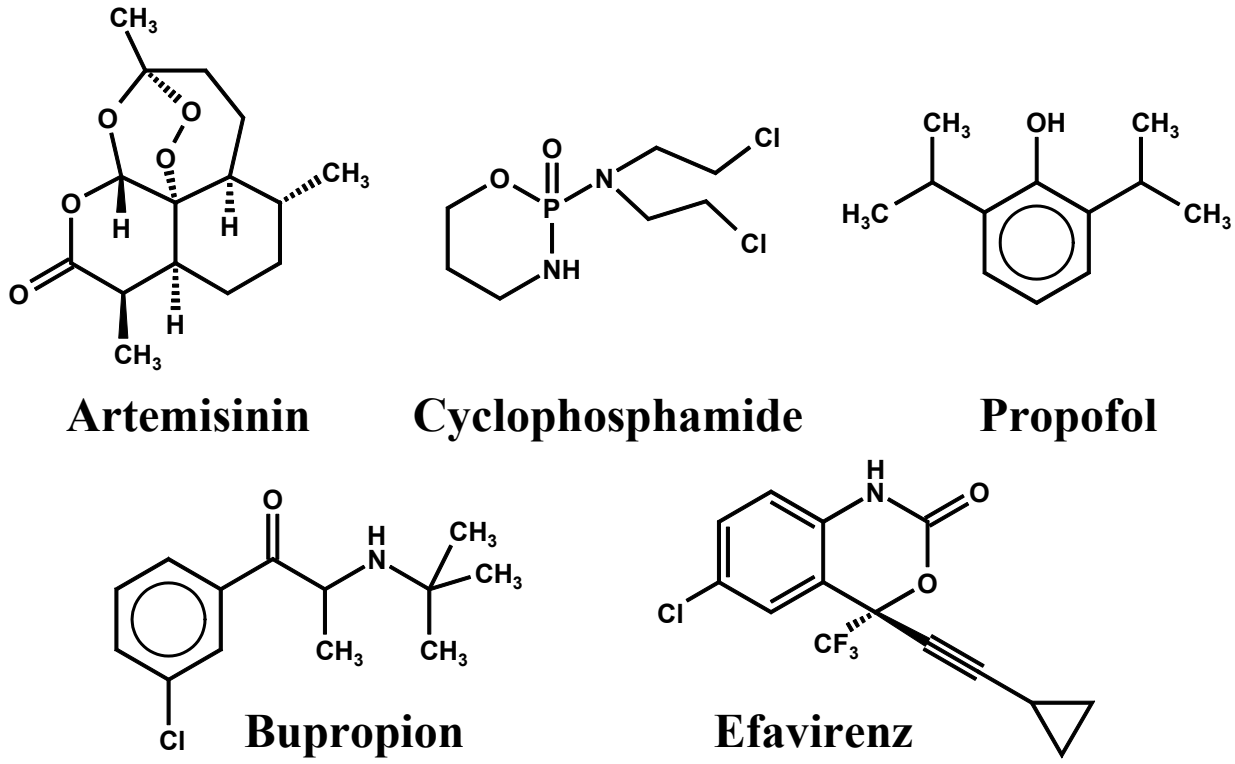

Figure 4: Examples of drugs predominantly metabolized by CYP2B6.

2.3. Expression

Early works suggested that hepatic expression of CYP2B6 might be low or even absent in the majority of individuals (Mimura *et al.*, 1993; Shimada *et al.*, 1994). Facilitated by the improvement of immunological detection techniques and the development of antibodies with high sensitivity and specificity for CYP2B6, subsequent studies demonstrated that the incidence and quantity of its expression is in fact much higher and accounts for 5% on average of total hepatic P450 content. *In vitro* studies using human liver microsomes

(summarized in Table 2) revealed an over 100-fold interindividual variability in hepatic CYP2B6 expression at the mRNA, protein and catalytic activity level (Code *et al.*, 1997; Ekins *et al.*, 1998; Stresser and Kupfer, 1999; Lang *et al.*, 2001; Hesse *et al.*, 2004). Accordingly, population studies demonstrated a broad interindividual variability of *in vivo* pharmacokinetic parameters of several CYP2B6 drug substrates, including cyclophosphamide (Yule *et al.*, 1996), bupropion (Kirchheiner *et al.*, 2003) and efavirenz (Csajka *et al.*, 2003), which could be the cause for non-response or toxicity. CYP2B6 protein has also been described to be expressed at lower levels in extrahepatic tissues like kidney, intestine, and the respiratory tract (Gervot *et al.*, 1999), brain (Miksys *et al.*, 2003), skin (Janmohamed *et al.*, 2001) and leukocytes (Furukawa *et al.*, 2004).

Study	Number of samples	mRNA [a.u.]	Protein content[a]	Enzyme activity[b]
Code *et al.*, 1997	17	n.d.	0.3 – 74	21 – 452[c]
Yang *et al.*, 1998	26	n.d.	0 – 28	n.d.
Ekins *et al.*, 1998	19	n.d.	0.7 – 71	1.8 – 47.6[d]
Stresser and Kupfer, 1999	28	n.d.	2 – 82	n.d.
Gervot *et al.*, 1999	48	n.d.	0.4 – 8	n.d.
Venkatakrishnan *et al.*, 2000	12	n.d.	1.5 – 148	n.d.
Lang *et al.*, 2001	92	n.d.	0.5 – 96	Data not shown
Lamba *et al.*, 2003	60	1 – 12161	0 – 130	0 – 42.5[d]
Hesse *et al.*, 2004	54	1 – 43	0.4 – 180	29 – 2626[e]

Table 2: Variability of CYP2B6 expression in human liver (n.d.: not determined; [a][pmol/mg microsomal protein]; [b][pmol/mg*min]; [c]7-EFC-*O*-deethylase activity; [d]*S*-Mephenytoin *N*-demethylase activity; [e]Bupropion-hydroxylase activity).

2.4. Regulation

Studies conducted by several laboratories in recent years have provided evidence that part of the hepatic CYP2B6 variability is due to its drug-inducible regulation via proximal and distal response elements termed phenobarbital-responsive enhancer module (PBREM) at -1.7 kb (Goodwin et al., 2001) and xenobiotic-responsive enhancer module (XREM) at -8.5 kb (Wang et al., 2003). As shown in Figure 5, these elements contain direct repeats of consensus half-

sites for nuclear receptors (AGKTCA) separated by four nucleotides (DR4 motifs) which act as binding sites for heterodimers of NR1I2 (PXR) or NR1I3 (CAR) with NR2B1 (RXRα). Furthermore, a proximal 24-bp element termed okadaic acid responsive element (OARE) at -233 bp has recently been shown to be involved in CAR-mediated induction (Swales et al., 2005).

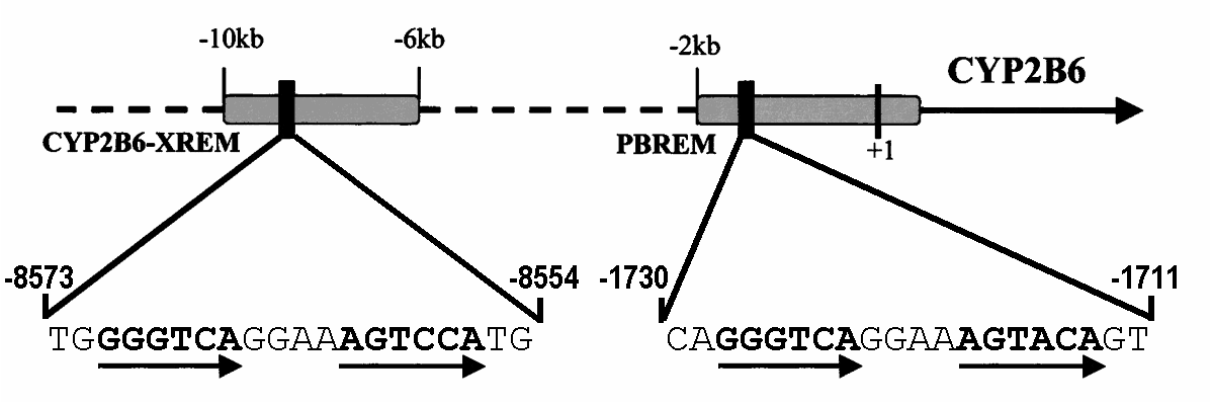

Figure 5: XREM and PBREM in the *CYP2B6* promoter. Base "A" of the initiation codon ATG is designated as +1.

Substances shown to induce CYP2B6 in human hepatocytes *in vitro* include carbamazepine, clotrimazole, phenobarbital, phenytoin, rifampicin and ritonavir (Faucette *et al.*, 2004). Induction was also observed *ex vivo* in human liver samples in several studies: Consumers of carbamazepine (Wolbold *et al.*, 2003, IKP148: L#35 and L#108; Stresser and Kupfer, 1999: H15), phenytoin (Hesse *et al.*, 2004: LV32; Stresser and Kupfer, 1999: H51) and phenobarbital (Yamano *et al.*, 1989: K14; Lamba *et al.*, 2003: HL#650, HL#789) show strikingly elevated amounts of CYP2B6 protein in microsomes. However, *in vivo* induction studies for human CYP2B6 are rare. Ketter *et al.* (1995) reported induction of bupropion metabolism by carbamazepine, and it has been shown that phenytoin alters ifosfamide metabolism presumably by induction of CYP2B6 (Ducharme *et al.*, 1997).

Contrary to the inducible regulation, little is known about the constitutive regulation of *CYP2B6* gene expression. To date, no systematic promoter analysis has been carried out and the transcriptional start site has not been determined.

2.5. Pharmacogenetics of *CYP2B6*

Recent work from a number of laboratories focused on genetic variations as an additional source for interindividual variability in expression (Lang *et al.*, 2001; Lamba *et al.*, 2003; Hesse *et al.*, 2004; Lang *et al.*, 2004). *CYP2B6* was found to be highly polymorphic within exons and introns as well as in its promoter region. Interestingly, none of the studies detected polymorphisms located in the PBREM or XREM suggesting an important role for these conserved regions. Furthermore, no nonsense mutations or gene deletions (which have been described, for example, in the *CYP2D6* gene (Zanger *et al.*, 2004)) have been observed so far; however, some newly discovered rare alleles carrying nonsynonymous SNPs were defined as phenotypic null alleles (Lang *et al.*, 2004) as they were found to result in absent or nonfunctional proteins. Some of the common nonsynonymous polymorphisms, e.g. those of alleles *CYP2B6*5* (R487C) and *CYP2B6*6* (Q172H, K262R) were associated with decreased liver protein expression (Lang *et al.*, 2001; Hesse *et al.*, 2004) or changes in function (Ariyoshi *et al.*, 2001; Jinno *et al.*, 2003; Iwasaki *et al.*, 2004). Indeed, recent clinical studies with efavirenz-treated HIV-1 patients demonstrated significantly elevated plasma levels of this CYP2B6 substrate in individuals homozygous for *CYP2B6*6* (Tsuchiya *et al.*, 2004; Haas *et al.*, 2004; Rotger *et al.*, 2005). In one case report, excessive drug levels in such an individual led to a severe psychosis which disappeared after dose reduction (Hasse *et al.*, 2005). Regarding the *CYP2B6* promoter region, numerous polymorphisms that appear to be linked to the coding SNPs in a complex manner have already been described (Lamba *et al.*, 2003; Hesse *et al.*, 2004); however, these have not been investigated mechanistically with respect to their potential impact on transcription of the *CYP2B6* gene.

3. Aims of this study

A) Haplotype analysis of *CYP2B6*

A comprehensive genotype data set for the promoter and coding region should be used to determine *CYP2B6* haplotypes in a Caucasian population and to identify linkage between exonic and promoter mutations.

B) Functional characterization of promoter mutations

Previous studies have already described promoter polymorphisms in the *CYP2B6* gene; however, no direct attempts were made to investigate their functional relevance. In this work, the impact of promoter mutations on transcription should be examined. Reporter gene constructs containing different *CYP2B6* promoter haplotypes as well as individual promoter SNPs should be generated and used in transfection experiments.

C) Genotype-phenotype correlation

A large collection of well characterized human liver samples was available to study CYP2B6 expression on the mRNA, protein and activity level. By analyzing these expression data in relation to certain SNPs or haplotypes, the effects of mutations on expression *in vivo* should be evaluated.

D) Detection of deletion or duplication alleles of *CYP2B6*

A TaqMan real-time PCR based gene copy number assay should be established to detect deletions or duplications of the *CYP2B6* gene. Until now, such alleles have not been described yet, but it is possible that unequal crossing-over events with the neighboring pseudogene *CYP2B7P1* gave rise to such recombinations, similar to the situation at the *CYP2A6* and *CYP2D6* loci where gene duplications and deletions have already been described (Rao *et al.*, 2000; Zanger *et al.*, 2004).

II MATERIALS AND METHODS

1. DNA and liver samples

Since 1999, a large collection (N>300) of human liver tissue samples and corresponding blood samples (also designated as "liverbank") has been established at the Margarete Fischer-Bosch-Institute of Clinical Pharmacology, Stuttgart (study code IKP148). The liver samples were obtained from non-tumorous tissue from individuals of Caucasian origin undergoing liver surgery for various reasons at the Humboldt University Berlin, Department of General, Visceral and Transplantation Surgery (Wolbold *et al.*, 2003). The preparation of genomic DNA from corresponding blood samples and of liver microsomes had been described earlier (Lang *et al.*, 2001). CYP2B6 protein was quantified by Western blotting with a monoclonal antibody from Gentest Corp. (Woburn, Massachusetts), and enzyme activity in human liver microsomes was detected with 50 µM bupropion as substrate as described (Lang *et al.*, 2001; Richter *et al.*, 2004). The study has been carried out in accordance with the Declaration of Helsinki and approved by the ethics committee of the Medical Faculties of the Charité, Humboldt-University Berlin, and written informed consent was obtained from each patient.

2. PCR conditions

If not noted otherwise, PCR reaction mixes were prepared as follows:

Qiagen 10x PCR buffer	5.0 µl
dNTP mix 2mM each	5.0 µl
Forward primer 100µM	0.5 µl
Reverse primer 100µM	0.5 µl
Qiagen Taq polymerase (5 U/µl)	0.5 µl
DNA	x µl
H_2O to a total volume of	50.0 µl

When genomic DNA was amplified, usually 50 ng were used. Reactions were run in a PTC-200 thermal cycler (MJ Research, Watertown, Massachusetts).

3. Sequencing of double-stranded DNA

For sequencing PCR products or plasmids, the "Thermo Sequenase Fluorescent Labelled Primer Cycle Sequencing Kit with 7-Deaza-dGTP" from Amersham (Buckinghamshire, UK) was used. 5'-IRD800 labeled primers were purchased from MWG (Ebersberg, Germany). For

each sequencing reaction, a mix consisting of 10 µl purified PCR product or plasmid, 1 µl DMSO, 2 µl labeled primer (2 pmol/µl) and 13 µl H_2O was prepared. 4.5 µl of this mix was added to 1.5 µl of the A, C, G and T reagent. Cycle sequencing conditions were as follows:

95°C	2’00’’	
95°C	15’’	} 30x
57°C	30’’	
70°C	1’00’’	
25°C	forever	

After cycling, 6 µl formamide loading dye were added to each reaction of which 1 µl was loaded onto a 5% polyacrylamide gel. Electrophoresis and detection of the sequencing products was performed in a Li-Cor 4000 DNA sequencer (Li-Cor, Lincoln, Nebraska) with 1x TBE as running buffer.

Sequencing gel: 21 g Urea, 6 ml Long Ranger Gel solution (Cambrex, Rockland, Maine), 5 ml 10x TBE, 500 µl DMSO, 50 µl TEMED, H_2O ad 50 ml; after filtration, add 400 µl 10% APS

10x TBE: 162.0 g Tris, 27.5 g boric acid, 9.3 g EDTA in 1000 ml H_2O

4. Genotyping assays

4.1. SNP -2320T>C

1.1 kb of the *CYP2B6* promoter were amplified using the following primers:

2B6(-3010)F `5’-GAA AGA GAC TGG CTG AAT GGA-3’`

2B6(-1894)R `5’-TAT TGT TGC CAT CCC CAT TT-3’`

The resulting fragment was expected to be CYP2B6-specific as similarity of the promoter regions between *CYP2B6* and *CYP2B7P1* does not extend beyond -2300 bp.

Cycling conditions were as follows:

95°C	5’00’’	
95°C	30’’	} 35x
58°C	30’’	
72°C	1’20’’	
72°C	7’00’’	
12°C	forever	

The products were purified using the Qiagen PCR purification kit, eluted in 80 µL Buffer EB and digested as follows:

Roche 10x Buffer D	2.0 µl
purified PCR product	8.0 µl
*Eco*RV (10 U/µl)	1.0 µl
H_2O to a total volume of	20.0 µl

Reactions were incubated at 37°C for two hours and visualized on 2% ethidium bromide-stained agarose gels. *Eco*RV digestion of wild type DNA yielded fragments of 691 bp and 426 bp, whereas the mutation -2320T>C prevented digestion and resulted in an uncleaved fragment of 1117 bp.

4.2. SNP c.1459C>T

Initially, the mutation c.1459C>T was genotyped with a PCR-RFLP assay described by Lang *et al.*, 2001. Briefly, a PCR product with 1401 bp was digested with *Bgl*II resulting in two fragments of 1185 bp and 216 bp only in the presence of the mutation. As this method was suspected to yield incorrect results in certain cases, an alternative assay using a different forward primer was developed. 477 bp of the *CYP2B6* gene containing exon 9 were amplified using the following primers (differences to *CYP2B7P1* underlined):

2B6(25238)F 5′-CAA ATC TGT TGC AGT GGA CAT TTG-3′

CYP2B6-9R 5′-TAA TTT TCG ATA ATC TCA CTC CTG C-3′

Cycling conditions were as follows:

95°C	5’00’’	
95°C	30’’	} 35x
60°C	30’’	
72°C	1’00’’	
72°C	7’00’’	
12°C	forever	

The products were purified using the Qiagen PCR purification kit, eluted in 40 µL Buffer EB and sequenced using the labeled primer seqCYP2B6-9F (5′-IRD800 TGA GAA TCA GTG GAA GCC ATA GA-3′) or digested as follows:

Roche 10x Buffer M	2.0 µl
purified PCR product	8.0 µl
*Bgl*II (10 U/µl)	0.5 µl
H_2O to a total volume of	20.0 µl

Reactions were incubated at 37°C for two hours and visualized on 3% ethidium bromide-stained Metaphor® agarose gels. The mutation c.1459C>T creates a restriction site for *Bgl*II that resulted in two fragments of 263 bp and 214 bp, whereas the wild type product remained uncut.

4.3. SNP g.24322C>T

794 bp of intron 8 of the *CYP2B6* gene were amplified using the following primers (differences to *CYP2B7P1* underlined):

2B6(24062)F 5′-CTG GGT ATG CCA AAG GGA TG-3′

2B6(24855)R 5′-GCC TCC CAA AGT GGG ATT AC-3′

Cycling conditions were as follows:

95°C	5’00’’	
95°C	30’’	} 30x
65°C	30’’	
72°C	1’00’’	
72°C	7’00’’	
12°C	forever	

The products were purified using the Qiagen PCR purification kit, eluted in 40 µL Buffer EB and sequenced using the labeled primer seq2B6(24153) (5′-IRD800 AAC TCA CAC TTG ACA TGG CC-3′) or digested as follows:

Roche 10x Buffer H	2.0 µl
purified PCR product	8.0 µl
*Hin*fI (10 U/µl)	0.5 µl
H_2O to a total volume of	20.0 µl

Reactions were incubated at 37°C for two hours and visualized on 2% ethidium bromide-stained Metaphor® agarose gels. The wild type restriction fragments were 537 bp, 227 bp and 30 bp, whereas the mutation g.24322C>T abolishes a *Hin*fI site yielding products of 567 bp and 227 bp.

4.4. SNP -82T>C (DHPLC assay)

4.4.1. Principle of DHPLC

DHPLC (denaturing high-performance liquid chromatography) identifies mutations based on detection of heteroduplex formation between mismatched nucleotides in PCR-amplified DNA (Figure 6). The duplexes are analyzed by ion-pair reversed-phase HPLC (IP-RP-HPLC). The mobile phase is composed of water, acetonitrile and the ion-pairing agent triethylammonium

acetate (TEAA), the stationary phase consists of a poly(styrene-divinylbenzene) copolymer which binds the DNA. A linear gradient of acetonitrile allows separation of fragments based on presence of heteroduplexes. Under partially denaturing temperatures, the heteroduplexes elute from the column earlier than the homoduplexes because of their reduced melting temperature. As the fragments elute, they are UV-detected at 260 nm.

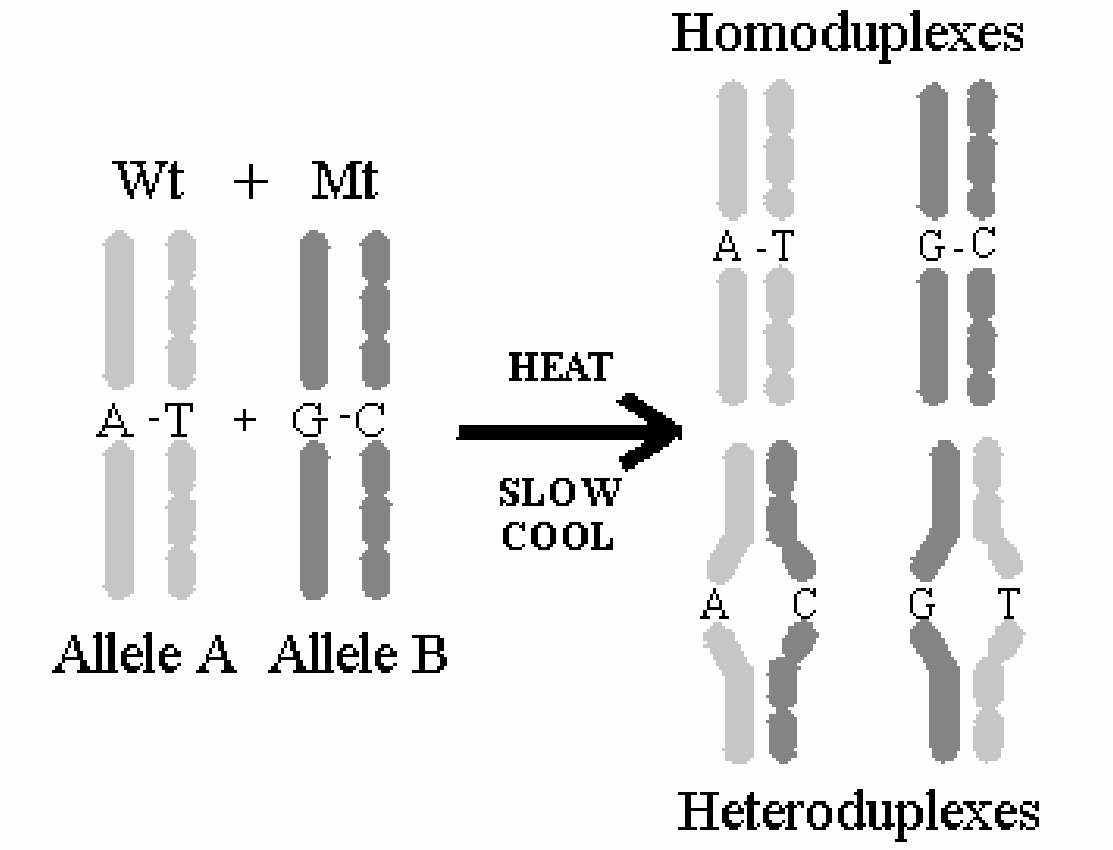

Figure 6: Principle of DHPLC. In the presence of a heterozygous mutation, homo- and heteroduplexes are formed during PCR. Under partially denaturing conditions, these can be separated by HPLC.

4.4.2. Genotyping assay

To identify carriers of the SNP -82T>C in our liverbank, a DHPLC genotyping assay was developed. A 287 bp fragment covering bases -275 to +12 of the *CYP2B6* gene was amplified using the following primers (differences to *CYP2B7P1* underlined):

DH2B6(-275)F 5′-CAC ACA TTC ACT TGC TCA CC-3′

DH2B6(+12)R 5′-GCT GAG TTC CAT GGT CCT G-3′

Cycling conditions were as follows:

95°C	5’00’’	
95°C	30’’	} 35x
62°C	30’’	
72°C	30’’	
72°C	7’00’’	
12°C	forever	

5 µl of the PCR products were injected into the WAVE system (Transgenomic, Omaha, Nebraska) without further purification. The method parameters are described in Table 3.

Method name	2B6-82TC
Oven temperature	61°C
Run time	8.5 min
Flow rate	0.9 ml/min
Gradient	

Step	Time	%A	%B
Loading	0.0	51	49
Start Gradient	0.5	46	54
Stop Gradient	5.0	37	63
Start Clean	5.1	0	100
Stop Clean	5.6	0	100
Start Equilibrate	5.7	51	49
Stop Equilibrate	6.6	51	49

Mobile phase A: 50 ml 2M TEAA, 250 µl acetonitrile, H_2O to 1000 ml
Mobile phase B: 50 ml 2M TEAA, 250 ml acetonitrile, H_2O to 1000 ml

Table 3: DHPLC conditions for genotyping the SNP -82T>C in the *CYP2B6* gene.

To detect homozygous carriers of the mutation, samples were mixed with an equimolar amount of wild type PCR product. To enable heteroduplex formation, mixed samples were denatured at 95°C for ten minutes and cooled down to room temperature at a rate of -1K/min. To generate a template for the wild type or mutant PCR product, the amplification product of a heterozygous carrier (L#110) was cloned into pCR4TOPO, and clones corresponding to the wild type or mutant allele were identified by sequencing. The resulting plasmids pCR4TOPOPCR18/3 (-82C) and /5 (-82T) were used to generate wild type or mutant PCR product.

5. Testing for deviation from Hardy-Weinberg Equilibrium

In large enough randomly mating populations, genotypes for a biallelic SNP should distribute according to the Hardy-Weinberg principle (Hardy, 1908):

$$\mathbf{AA:AB:BB = p^2:2pq:q^2}$$

where A and B represent the two alleles with their respective allele frequencies p and q=1-p. A goodness-of-fit χ^2 test with one degree of freedom was used to test for HWE by comparing the observed number of subjects for each genotype with the expected number of subjects assuming HWE. The χ^2 statistic was calculated as follows:

$$\mathbf{\chi^2=\Sigma(observed-expected)^2/expected}$$

and the corresponding p-value for the χ^2 distribution with one degree of freedom was given.

6. Reconstruction of haplotypes

Genotype data for ten promoter- and four exonic SNPs from 96 Caucasians were used to infer haplotypes using the program PHASE version 2.0.2 (Stephens *et al.*, 2001). The exonic SNP c.777C>A was omitted from the analysis because it was not observed in this population. Runs were conducted five times to ensure model stability. Phase calls with a probability of >95% were considered unambiguous. Identified haplotypes were compared to alleles described by the CYP Allele Nomenclature Committee (http://www.imm.ki.se/CYPalleles/). Novel alleles were designated in concordance with the published inclusion criteria.

7. Construction of plasmids

7.1. Reporter gene vectors pGL3-2B6(-1641) and pGL3-2B6(-2033)

A 2.3 kb fragment of the CYP2B6 promoter region was amplified from genomic DNA of two genotyped Caucasians selected to carry one wild type and three variant alleles representing the most frequent mutations. To minimize the introduction of sequence errors by PCR, the Expand High Fidelity PCR system (Roche, Basel, Switzerland) was used with the following primers (differences to *CYP2B7P1* underlined):

```
                                --MluI--
2B6(-2253)F  5′-TAT GAA TGA GAA Cgc GTG ATA TTC ACT-3′

                                -BglII-
2B6(+16)R    5′-GGA CGC TGA GTT agA Tct TCC TGG TCT G-3′
```

Forward primer 2B6(-2253)F and reverse primer 2B6(+16)R were designed to contain mismatches (in lowercase) to create a *Mlu*I or a *Bgl*II site, respectively. Initially we attempted to prepare reporter gene constructs containing the entire amplified upstream sequence. For this purpose, the 2.3 kb fragment (Figure 7) was cloned into the pCR4-TOPO vector (Invitrogen, Carlsbad, CA). Four different plasmids corresponding to the four different alleles of the two individuals were obtained and designated as WT, A2, A3 and A4 (Table 4). The *Mlu*I/*Bgl*II fragment was then subcloned into the reporter gene vector pGL3-Basic (Promega, Madison, Wisconsin). However, after transformation and plasmid preparation, the desired products were not obtained despite several attempts indicating that they may be unstable or toxic for *E. coli*.

Shortening the insert from the 5'-end was considered a technically feasible approach. The plasmid pGL3-Basic was digested with *Bgl*II and dephosphorylated to reduce religation. A compatible *Bam*HI/*Bgl*II fragment was prepared from the pCR4-TOPO vectors and ligated into the vector yielding the pGL3-2B6(-1641) series. For the pGL3-2B6(-2033) series, pGL3-Basic was sequentially digested with *Sma*I and *Bgl*II and a *Sca*I/*Bgl*II fragment from the pCR4-TOPO vectors was ligated into it. The resulting plasmids could be transformed and propagated in *E. coli* without difficulties.

Plasmid designation pGL3-2B6(-2033)…	Nucleotide changes (compared to genomic reference sequence)
WT	None
A2	-1456T>C, -750T>C
A3	-1848C>A, -801G>T, -750T>C, -82T>C
A4	-1778A>G, -1186C>G, -750T>C
-1848C>A	-1848C>A
-801G>T	-801G>T
-750T>C	-750T>C
-82T>C	-82T>C

Table 4: Vectors of the pGL3-2B6(-2033) series used in transfection assays

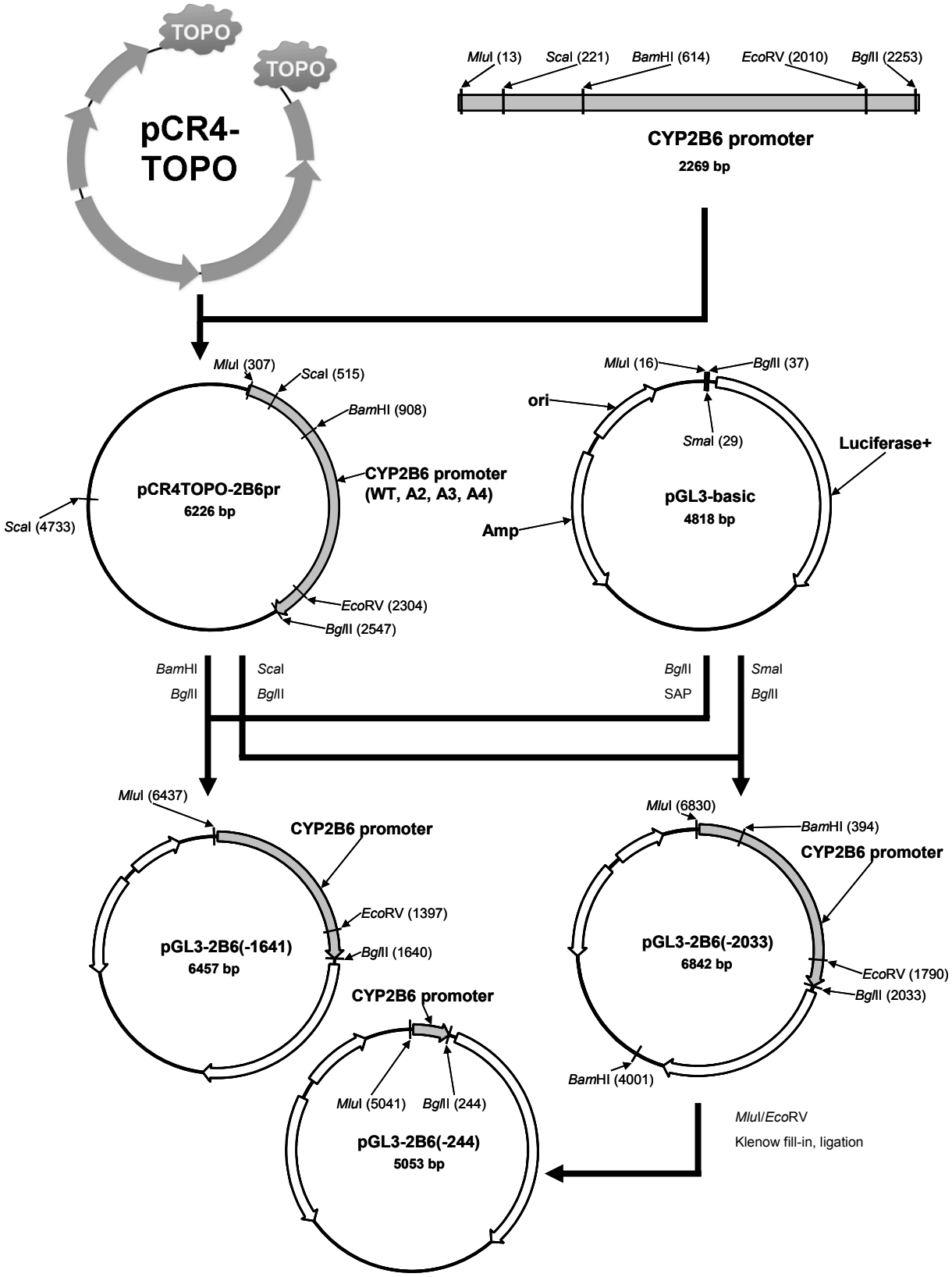

Figure 7: Construction of reporter gene plasmids for transfection assays.

Single mutations were introduced by in vitro mutagenesis into pGL3-2B6(-2033)WT using the QuikChange Mutagenesis Kit (Stratagene, La Jolla, California) and the following mutagenesis primers (mismatches underlined):

2B6-82MTF

5′-GGG GAA TGG ATG AAA TTT CAT AAC AGG GTG CAG AGG C-3′

2B6-82MTR

5′-GCC TCT GCA CCC TGT TAT GAA ATT TCA TCC ATT CCC C-3′

2B6-750MTF 5′-ATC ACG CCC GGC TAA TTT TTG T-3′

2B6-750MTR 5′-ACA AAA ATT AGC CGG GCG TGA T-3′

2B6-801MTF 5′-GGT TCA AGT GAT TCT CTT TCC TCA GCC TCC CGA G-3′

2B6-801MTR 5′-CTC GGG AGG CTG AGG AAA GAG AAT CAC TTG AAC C-3′

2B6-1848MTF 5′-GTA AAG CAC TTC AAG CCT CCC CAT CG-3′

2B6-1848MTR 5′-CGA TGG GGA GGC TTG AAG TGC TTT AC-3′

7.2. Reporter gene vectors pGL3-2B6(-244)WT and -82T>C

500 ng of plasmids pGL3-2B6(-2033)WT and A3 were digested with *Eco*RV and *Mlu*I at 37°C for 90 minutes in a volume of 20 µl. The reactions were incubated at 65°C for 15 minutes to inactivate the restriction enzymes followed by a fill-in of the overhangs using Klenow fragment. After gel electrophoresis on a 1% agarose gel, the 5 kb fragments were extracted using the Qiagen Gel extraction kit and self-ligated using T4 ligase. Reactions contained 8% PEG-6000 in a total volume of 20 µl and were incubated at room temperature for 60 minutes.

7.3. Reporter gene vectors pGL3-2B6(-160)WT and -82T>C

From the vectors pGL3-2B6(-2033)WT or A3, a 175 bp fragment was amplified using the following primers (mismatches in lowercase):

```
                          --BglII-
2B6(11)R     5′-CTG AGT TAG ATC TTC CTG GTC TG-3′

                --MluI-
2B6(-164)F   5′-AcG cgT GGG TTC CCT AAC AAC TT-3′
```

The products were purified by extraction with phenol:chloroform:isoamylalcohol (25:24:1) and subsequent ethanol precipitation, digested with *Bgl*II and *Mlu*I, and cloned into the pGL3-Basic vector. After transformation and propagation of the plasmids, the inserts were sequenced using the standard primers RVprimer3 and GLprimer2.

7.4. Expression plasmids pBJ5HNF1α and pBJ5DCoH

These expression plasmids (kindly provided by Professor Ronald N. Hines) contain the open reading frames for murine HNF1α (Kuo *et al.*, 1990) and DCoH (Mendel *et al.*, 1991), respectively, driven by the SRα promoter (Takebe *et al.*, 1988). DCoH (dimerization cofactor of HNF1α) was shown to stabilize HNF1α dimers and enhance their transcriptional activity. It was predicted that these two proteins form heterotetramers consisting of two molecules of HNF1α and two molecules of DCoH (Mendel *et al.*, 1991). Accordingly, the two expression plasmids were used in an equimolar mixture when cotransfected with reporter gene vectors.

7.5. Expression plasmids pcDNA3-C/EBPβ and pcDNAmHNF1α

For the "TnT T7 Quick Coupled Transcription/Translation System", it is necessary to use templates with a T7 promoter. Therefore, the open reading frame of murine C/EBPβ contained in the plasmid MSV/EBPβ (Cao *et al.*, 1991), provided by Dr. Oliver Burk, was cut out with *Eco*RI and *Xho*I and ligated into the multiple cloning site of pcDNA3.1+. Similarly, the open reading frame of murine HNF1α was cloned from the pBJ5HNF1α plasmid (Kuo *et al.*, 1990), provided by Dr. Ron Hines, into pcDNA3.1+ using the restriction enzyme *Eco*RI.

7.6. Expression plasmids pAC-LAP/LIP

These plasmids were constructed and kindly provided by Dr. Ramiro Jover, Universitat de València, Spain. The intronless genes C/EBPβ-LAP and C/EBPβ-LIP were amplified from human genomic DNA and the PCR products were purified by agarose gel electrophoresis. After digestion with *Eco*RI and *Kpn*I, the fragments were ligated into the adenoviral pAC/CMVpLpA plasmid (Gomez-Foix *et al.*, 1992) previously digested with *Eco*RI and *Kpn*I (Jover *et al.*, 2002). These plasmids contain a CMV promoter and an SV40 polyadenylation site and are therefore suitable for expression in mammalian cells.

8. Cell culture and transient transfection of different cell types

8.1. HepG2 cells

The hepatoma cell line HepG2 was cultured in 75 cm² polystyrene cell culture flasks (Corning, New York, #430720) in minimum essential medium supplemented with 10% fetal calf serum, 1% PenStrep and 1% L-Glutamine (Gibco, Carlsbad, California). The day before transfection, cells were seeded in Multiwell™ 24-well plates (BD Falcon #353047), with a density of approximately 150,000 cells per well and 0.5 ml medium. After transfection,

medium was changed daily. Transient transfections were carried out in triplicate using the effectene transfection reagent (Qiagen, Hilden, Germany) according to the manufacturer's instructions. For normalization, 20 ng/well of the β-galactosidase expression plasmid pCMVβ (Clontech, Palo Alto, California) were cotransfected with 150 ng/well of the respective firefly luciferase reporter plasmid. 48 hours after transfection, medium was removed and cells were washed two times with 0.5 ml 1x PBS. After incubating 20 minutes with 150 µl/well Passive Lysis Buffer (Promega, #E1941), the cells were harvested and reporter activity was measured in the cell extract using the AutoLumat Plus luminometer (Berthold, Bad Wildbad, Germany). Firefly luciferase activity was assayed in 20 µl cell extract. After injection of 300 µl RIM+ buffer, luminescence was measured immediately for four seconds. β-galactosidase activity was assayed in 10 µl cell extract which was incubated with 100 µl β-Gal-Assay buffer for 30 minutes. After injection of 300 µl β-Gal stop mix and a delay of seven seconds, luminescence was measured for five seconds. When additional expression plasmids were cotransfected, 30 ng/well were used if not stated otherwise.

RIM+ buffer:	50 µM luciferin, 2 mM ATP, 10 mM $MgCl_2$, 27 µM CoA, 30 mM DTT in 25 mM Glycylglycine pH 7.8
β-Gal-Assay buffer:	1.25 µg/ml Galacton (Applied Biosystems, Foster City, California), 1 mM $MgCl_2$ in 100 mM sodium phosphate buffer pH 8.0
β-Gal stop mix:	2.5% (v/v) Emerald Enhancer (Applied Biosystems) in 0.2 M NaOH

8.2. Primary human hepatocytes

Primary human hepatocytes were kindly provided by Dr. Andreas Nüssler and Prof. Peter Neuhaus, Charité, Berlin. They were isolated as described (Dorko *et al.*, 1994), plated in collagen-coated 6-well plates with a density of 750,000 cells per well and grown in 2 ml Williams E medium supplemented with 10% dialyzed fetal calf serum (Gibco), 1% PenStrep, 32 U/l insulin, 1.4 µM hydrocortisone and 15 mM HEPES buffer. The day after plating, cells were shipped overnight. Upon arrival, cells were washed with 2 ml 1x PBS and supplied with fresh medium. On the next day, cells were transfected with the Effectene Transfection Kit (Qiagen) using 3.2 µl enhancer and 10 µl effectene per well. For normalization, 40 ng/well of the β-galactosidase expression plasmid pCMVβ were cotransfected with 360 ng/well of the respective firefly luciferase reporter plasmid. Medium was changed daily, with the first change seven hours after transfection. 48 hours after transfection, medium was removed and cells were washed two times with 2 ml 1x PBS. After removal of PBS, 200 µl Passive Lysis Buffer (Promega) was added and cells were transferred to a 1.5 ml reaction tube using a

sterile cell scraper. After 20 minutes incubation on a rocking plate, reaction tubes were centrifuged for five minutes at 20,800 rcf. Firefly luciferase and β-galactosidase activity were assayed as above, except that 20 µl and 40 µl of the cell extract were used, respectively.

8.3. Primary rat hepatocytes

Transfection experiments in primary rat hepatocytes were conducted by Dr. Karen Hirsch-Ernst, Department of Toxicology, University of Göttingen. In brief, primary rat hepatocytes were isolated from adult male Wistar rats (180-220 g) by collagenase perfusion (Seglen, 1976) and prepared for transfection in 6-well plates as described previously (Heder *et al.*, 2001). Transfections were carried out with the effectene transfection reagent (Promega). For normalization, 3 ng/well of the *Renilla reniformis* luciferase expression plasmid pRL-CMV (Promega) were cotransfected with 400 ng/well of the respective firefly luciferase reporter plasmid. Firefly and *Renilla reniformis* luciferase activities were sequentially determined in the same samples of primary rat hepatocyte lysates with the Dual luciferase assay kit (Promega).

9. RNA ligase-mediated rapid amplification of 5'-cDNA ends

To map transcriptional start sites of CYP2B6 or CYP2B6 promoter-driven luciferase transcripts, the GeneRacer Kit (Invitrogen) was used according to the manufacturer's instructions. The GeneRacer technique is based on RNA ligase-mediated rapid amplification of cDNA ends (RLM-RACE) which involves selective ligation of an RNA oligonucleotide to the 5'-ends of decapped full-length mRNA using T4 RNA ligase and a PCR amplification step. The technique is described in detail in Figure 8.

To map the transcriptional start site of *CYP2B6*, total RNA (1-2 µg) of two human livers was isolated as described (Wolbold *et al.*, 2003) and 5'-RLM-RACE was performed according to the manufacturer's instructions. 5'-cDNA ends were amplified using the following primers:

GeneRacer 5'-Primer `5′-CGA ACT GGA GCA CGA GGA CAC TGA-3′`

2B6cDNA(521)R `5′-GAT GGA GCA GAT GAT GTT GGC GGT AA-3′`

Touchdown cycling conditions were:

95°C	5'00''	
95°C	30''	} 5x
72°C	1'30''	
95°C	30''	} 5x
70°C	1'30''	

95°C	30''	} 20x
68°C	30''	
72°C	1'00''	
72°C	7'00''	
12°C	forever	

The sequence of 2B6cDNA(521)R represents bases 521 to 546 of the CYP2B6 mRNA and was intentionally chosen to be identical to the corresponding region in the *CYP2B7P1* pseudogene. Thus, it was possible to analyze potentially present *CYP2B7P1* transcripts simultaneously, as clones obtained from these transcripts could be distinguished from *CYP2B6*-derived clones by sequencing.

To map the transcription start of the *CYP2B6* promoter-driven luciferase mRNA transcripts, 5 µg of total RNA of transfected HepG2 cells, isolated with the RNA Minikit (Qiagen) according to the manufacturer's instructions, was used. Cells were cotransfected with the expression plasmid MSV/EBPβ for murine C/EBPβ (Cao *et al.*, 1991) to enhance transcription, and cDNA ends were amplified with nested PCR using the outer primers

GeneRacer 5'-Primer `5′-CGA ACT GGA GCA CGA GGA CAC TGA-3′` and

luci(350)R `5′-CAC GGT AGG CTG CGA AAT GCC CAT A-3′`

with the touchdown cycling conditions

95°C	5'00''	
95°C	30''	} 5x
72°C	1'30''	
95°C	30''	} 5x
70°C	1'30''	
95°C	30''	} 25x
65°C	30''	
72°C	1'00''	
72°C	7'00''	
12°C	forever.	

1 µl of the PCR product was used as template for nested PCR with inner primers

GeneRacer 5'-NestedPrimer `5′-CGA ACT GGA GCA CGA GGA CAC TGA-3′` and

luci(220)R `5′-AGC TTC TGC CAA CCG AAC GGA CAT TT-3′`

and cycling conditions

95°C	5'00''	
95°C	30''	} 20x
65°C	30''	
72°C	1'00''	
72°C	7'00''	
12°C	forever.	

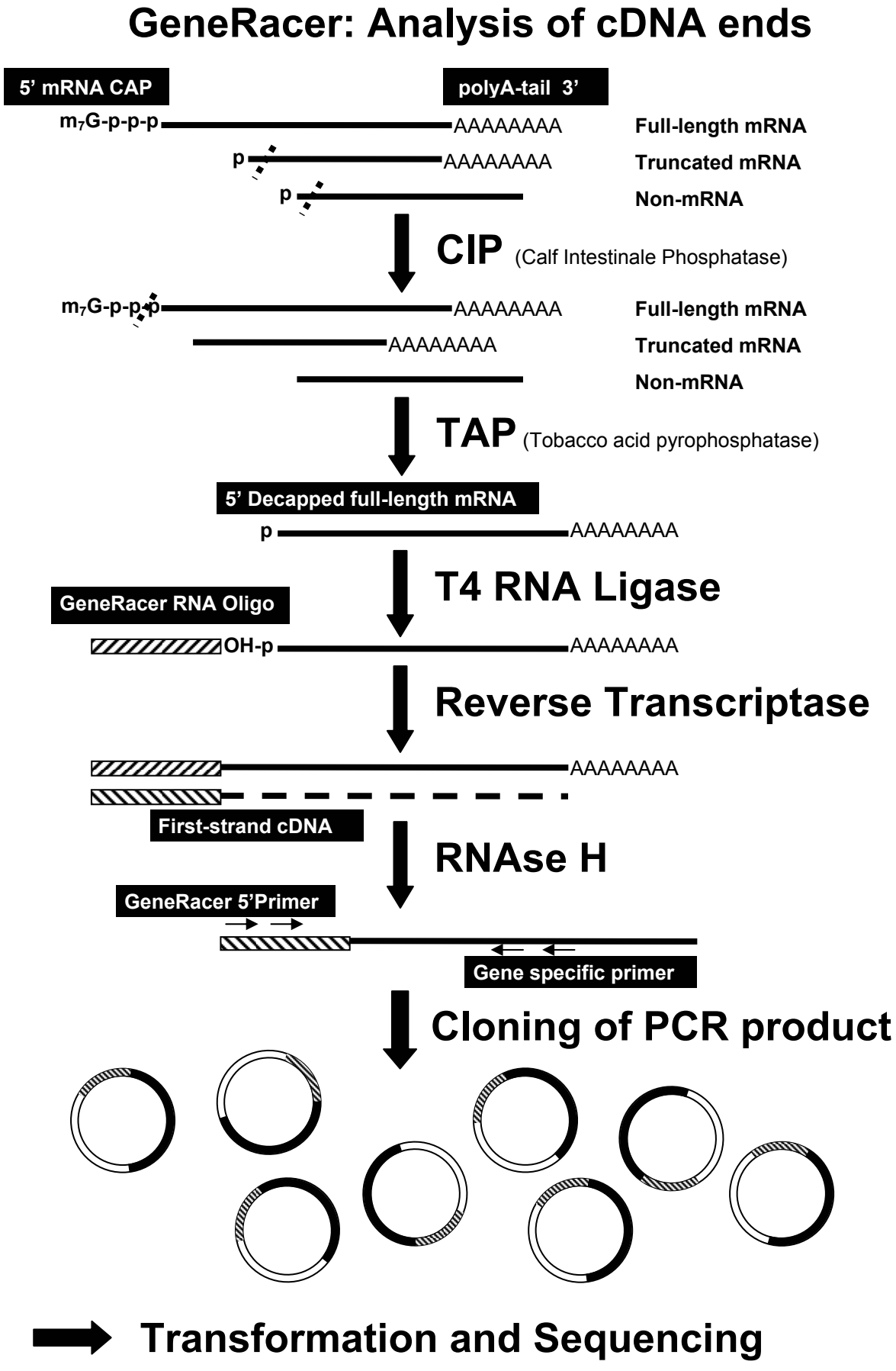
GeneRacer: Analysis of cDNA ends
5' mRNA CAP
polyA-tail 3'
m7G-p-p-p
AAAAAAAA
Full-length mRNA
p
AAAAAAAA
Truncated mRNA
p
Non-mRNA
CIP (Calf Intestinale Phosphatase)
m7G-p-p-p
AAAAAAAA
Full-length mRNA
AAAAAAAA
Truncated mRNA
Non-mRNA
TAP (Tobacco acid pyrophosphatase)
5' Decapped full-length mRNA
p
AAAAAAAA
T4 RNA Ligase
GeneRacer RNA Oligo
OH-p
AAAAAAAA
Reverse Transcriptase
AAAAAAAA
First-strand cDNA
RNAse H
GeneRacer 5'Primer
Gene specific primer
Cloning of PCR product
Transformation and Sequencing

Figure 8: The GeneRacer method.

1. **Total RNA is treated with calf intestinal phosphatase to remove the 5'-phosphates of truncated mRNA and non-mRNA. The 5'-7-methylguanosine cap structure of full-length mRNA is not affected.**
2. **Dephosphorylated RNA is treated with tobacco acid pyrophosphatase to remove the 5'-cap structure from intact, full-length mRNA, leaving a 5'-phosphate.**
3. **The GeneRacer RNA Oligo is ligated to the 5'-end of the decapped full-length mRNA using T4 RNA ligase.**
4. **The ligated mRNA is reverse-transcribed using SuperScript II RT and random primers.**
5. **Treatment with RNAse H leaves the first-strand cDNA which is amplified using PCR with the GeneRacer primers (binding to the Gene Racer Oligo) and gene specific primers binding to the gene of interest.**
6. **The RACE-PCR products are purified and cloned into the pCR4-TOPO vector.**
7. **The resulting clones are transformed and propagated in *E. coli* and sequenced using M13 standard primers.**

10. Primer extension analysis

10.1. Primer labeling

Primer 2B6cDNA(41)R (5'-CCT GTG AGG AGT GCA AGG AAG AGG-3') was labeled with γ-[^{32}P]-ATP, 185 TBq/mmol (Hartmann Analytic, Braunschweig, Germany) using the Primer Extension System – AMV Reverse Transcriptase (Promega) according to the manufacturer's instructions. Salt and unincorporated nucleotides were removed by spin-column chromatography using ProbeQuant G-50 Microcolumns (Amersham Biosciences, Piscataway, New Jersey).

10.2. Primer hybridization and reverse transcription

100 fmol of the labeled primer were added to 100 µg total liver RNA in a volume of 100 µl. Nucleic acids were precipitated by adding 10 µl of 3 M sodium acetate (pH 5.2) and 330 µl ethanol. After 2 hours at -80°C and centrifugation at 14,000 g for 30 minutes, the pellet was dried at room temperature for 20 minutes and dissolved in 6 µl H_2O and 5 µl 2x AMV-RT buffer. The primer was then hybridized for 20 minutes at 58°C and the sample allowed to cool down at room temperature for 10 minutes. Reverse transcription was carried out at 42°C for

30 minutes according to the manufacturer's instructions. Subsequently, 2 µg RNAse was added and incubated at 37°C for 15 minutes. After addition of 80 µl H_2O, the cDNA was extracted with 100 µl phenol:chloroform:isoamylalcohol (25:24:1) and precipitated by adding 10 µl of 3 M sodium acetate (pH 5.2) and 200 µl ethanol. After 2 hours at -80°C and centrifugation at 14,000 g for 30 minutes, the pellet was dried at room temperature for 20 minutes and dissolved in 2 µl loading dye.

10.3. Electrophoresis and detection

The primer extension products were electrophoresed in a sequencing gel (see " Sequencing of double-stranded DNA") using a Hoefer SQ3 sequencer (Pharmacia Biotech) at 1500 V until the bromophenol marker reached the bottom of the gel. After drying, primer extension products were visualized using Fuji imaging plates MS 2325 and a BAS-1800II plate reader (Fuji, Kanagawa, Japan). As size standard, a ^{35}S-labeled sequencing ladder generated with the SeqiTherm EXCEL II DNA Sequencing Kit (Epicentre, Madison, Wisconsin) using a plasmid containing the corresponding genomic fragment as template and the primer 2B6cDNA(41)R, was electrophoresed in parallel.

11. Electrophoretic mobility shift assay (EMSA)

This technique allows characterization of DNA-protein interactions *in vitro*. A double-stranded, radioactively labeled oligonucleotide is incubated with nuclear cell extracts or *in vitro* translated protein. When an interaction occurs, the resulting DNA-protein complex shows decreased mobility in a native polyacrylamide gel causing an upward "shift" of the probe compared to the free DNA probe.

11.1. Annealing and labeling of oligonucleotides

In a 0.5 ml reaction tube, 10 µl of 10x Klenow buffer and 1 nmol of the respective sense and antisense oligonucleotides (Table 5) were diluted to a total volume of 200 µl. The tube was exposed to 95°C for ten minutes, then cooled down slowly to room temperature (-1 K/min) to allow annealing of the oligonucleotides. 10 pmol of the double-stranded oligonucleotide with 4-nt extensions at both ends were labeled with Klenow fragment at the following conditions: 50 mM NaCl, 50 mM Tris pH 7.5, 10 mM $MgCl_2$, 200 µM dATP, dGTP and dTTP, 100 µM α-[^{32}P]-dCTP and 2 U of Klenow fragment. Reactions were incubated at 37°C for one hour. Salt and unincorporated nucleotides were removed by spin-column chromatography using

ProbeQuant G-50 Microcolumns (Amersham Biosciences). The purified labeled probes were diluted with TE/100 to contain 50,000 cpm/µl.

10x Klenow buffer: 500 mM NaCl, 100 mM $MgCl_2$ in 500 mM Tris pH 7.5
TE/100: 100 mM NaCl, 1 mM EDTA in 10 mM Tris pH 7.8

Name	Sequence (extensions in lowercase)	Region in *CYP2B6* promoter
2B6EMSA1	gatccTGGATGAAATTT**T**ATAACAGGGTGCa	-94 to -70 bp
sense/antisense	gatctGCACCCTGTTAT**A**AAATTTCATCCAg	(WT)
2B6EMSA2	gatccTGGATGAAATTT**C**ATAACAGGGTGCa	-94 to -70 bp
sense/antisense	gatctGCACCCTGTTAT**G**AAATTTCATCCAg	(-82C)
2B6EMSA3	gatccCAGGGTCAGGATAAAAGGCCCAGTTa	-64 to -40 bp
sense/antisense	gatctAACTGGGCCTTTTATCCTGACCCTGg	
2B6EMSA4	gatccTACAGAGTGGGTAAAGGGATa	-215 to -196 bp
sense/antisense	gatctATCCCTTTACCCACTCTGTAg	
2B6EMSA5	gatccACTGGGTTGCCCAAGCAGGAa	-183 to -164 bp
sense/antisense	gatctTCCTGCTTGGGCAACCCAGTg	
prHNF1WT	gatccGCCCGG**T**TAATTTTTGTGTTa	-757 to -737 bp
sense/antisense	gatctAACACAAAAATTA**A**CCGGGCg	(WT)
prHNF1MT	gatccGCCCGG**C**TAATTTTTGTGTTa	-757 to -737 bp
sense/antisense	gatctAACACAAAAATTA**G**CCGGGCg	(-750C)
HNF1 apoE	gatccTCTCTGAGAGAATCATTAACTTAATTTa	N.A.
sense/antisense	gatctAAATTAAGTTAATGATTCTCTCAGAGAg	
C/EBP	gatccTGCAGATTGCGCAATCTGCAa	N.A.
sense/antisense	gatctTGCAGATTGCGCAATCTGCAg	
AN15	gatccTACGTTGTTATTTGTTTTTTTCGa	N.A.
AN16	gatctCGAAAAAAACAAATAACAACGTAg	

Table 5: Oligonucleotides for electrophoretic mobility shift assays.

11.2. Preparation of nuclear cell extracts

Nuclear cell extracts from HepG2 cells were prepared by the "mini-extraction" method, which was first described by Schreiber *et al.*, 1989 and modified by Neurath *et al.*, 1997. All steps

were performed on ice. Cells were washed twice with 1x PBS and transferred to a 1.5 ml reaction tube using a sterile cell scraper. After adding 1 ml of buffer A, cells were centrifuged at 750 g for five minutes and the supernatant was taken off. The cell pellet was resuspended in 1 ml buffer A + 0.4% NP-40 and incubated on ice for 10 minutes. The cell lysate was centrifuged at 750 g for five minutes and the supernatant discarded. 200 µl buffer B was added to the pelleted cell nuclei, and the nucleus membranes lysed mechanically by stirring for 30 minutes with a magnetic follower (Roth, #0955, 2x5 mm). The lysate was centrifuged at 7,500 g for 15 minutes and the supernatant transferred to a new reaction tube. Protein concentration was determined using bicinchoninic acid as described (Smith *et al.*, 1985).

Buffer A: 10 mM HEPES pH 7.9, 1.5 mM $MgCl_2$, 10 mM KCl, 0.5 mM PMSF, 1 mM DTT

Buffer B: 20 mM HEPES pH 7.9, 0.42 M NaCl, 1.5 mM $MgCl_2$, 0.2 mM EDTA, 0.5 mM PMSF, 1 mM DTT

PMSF and DTT were added freshly before use.

11.3. *In vitro* translation

The TnT T7 Quick Coupled Transcription/Translation System (Promega) was used for *in vitro* translation according to the manufacturer's instructions. The TnT Quick master mix contains rabbit reticulocyte lysate combined with RNA polymerase, nucleotides, salts and a ribonuclease inhibitor, thus allowing transcription and translation to be performed in a single reaction. The generation of plasmid templates pcDNA3-C/EBPβ and pcDNAmHNF1α is described in Chapter 7.5.

11.4. Incubation and electrophoresis conditions

In vitro translated C/EBPβ or HNF1α (2 µl) was incubated at room temperature for 15 minutes with 2 µg poly(dI-dC) and 5 pmol unlabeled competitor, when included, before adding 2 µl of labeled DNA and incubating for another 20 minutes at room temperature. Binding reactions contained 10 mM HEPES pH 7.8, 60 mM KCl, 0.2% NP-40, 6% glycerol and 2 mM DTT. A 5% polyacrylamide gel (16.5 x 22 x 0.1 cm) was casted as follows:

30% Acrylamid/N- ,N'-Methylenbisacrylamid 37.5/1	5 ml
10x TBE	1.5 ml
TEMED	30 µl
10% APS	300 µl
H_2O to a total volume of	30 ml

The binding reactions were loaded onto the gel which was subjected to electrophoresis at 200 V for 60 minutes prior to sample loading. Electrophoresis was conducted for 1 to 2 hours at room temperature with 0.5x TBE as running buffer. When TBP was used in gel retardation assays, 50 ng protein were incubated with or without 5 pmol unlabeled competitor at 30°C for 15 minutes prior to addition of 2 µl of the labeled DNA probe and further 30 minutes incubation at 30°C. Binding reactions contained 20 mM Tris pH 8.0, 10 mM $MgCl_2$, 2 mM DTT, 80 mM KCl, 2% Ficoll and 0.1% NP-40. The binding reactions were loaded onto 4% polyacrylamide gels; gel and running buffer contained 4 mM $MgCl_2$ and 0.01% NP-40. Running conditions were the same as above. After electrophoresis, gels were dried and radioactive probe visualized using Fuji imaging plates MS 2325 and a BAS-1800II plate reader (Fuji, Kanagawa, Japan).

12. Quantitative real-time PCR

12.1. Synthesis of cDNA

Total RNA was prepared from liver tissue using either the RNeasy Midi Kit (Qiagen) or Trizol reagent (Invitrogen) with subsequent RNA clean-up using the RNeasy Mini Kit (Qiagen). For cDNA synthesis, the Multiscribe Reverse Transcriptase Kit (Applied Biosystems) was used. 520 ng of total RNA were adjusted to a volume of 10 µl, and the following reagents were added:

10x TaqMan RT buffer	2.60 µl
25 mM $MgCl_2$	5.72 µl
dNTP mix (2.5 mM each)	5.20 µl
50 µM Random Hexamers	1.30 µl
RNase inhibitor	0.52 µl

The random hexamers were allowed to anneal at 25°C for 10 minutes. After addition of 0.66 µl MultiScribe Reverse Transcriptase (50 U/µl), samples were incubated at 48°C for 30 minutes and inactivated at 95°C for 5 minutes. The volume was adjusted to 65 µl with RNAse-free water to yield a final cDNA concentration of 8 ng/µl.

12.2. Conditions for RT-PCR

Quantitative real-time PCR was conducted in an ABI Prism 7500 system (Applied Biosystems) using 2x TaqMan universal PCR Master Mix (Applied Biosystems) in a total volume of 25 µl. The cycling conditions were as follows:

50°C	2’00’’	
95°C	10’00’’	
95°C	15’’	} 40x
60°C	1’00’’	

Reactions were performed in duplicate and standards of known quantity were analyzed in every run to calculate a calibration curve for quantification.

12.2.1. β-Actin

For quantification of β-Actin, TaqMan pre-developed assay reagents were used (probe dye: VIC-MGB) with 800 pg cDNA as template. To generate a standard curve, serial 10-fold dilutions of pooled liver cDNA were analyzed over a range from 40 to 0.004 ng.

12.2.2. CYP2B6

For quantification of CYP2B6 mRNA, an amplicon of 89 basepairs spanning intron 4 was amplified using the primers (differences to *CYP2B7P1* underlined)

TQ-CYP2B6FOR 5′-GCT GAA CTT GTT CTA CCA GAC TTT TTC-3′ and

TQ-CYP2B6REV 5′-GAA AGT ATT TCA AGA AGC CAG AGA AGA G-3′

and probe

CYP2B6 MGB-probe 5′-FAM-TGT ATT CGG CCA GCT GT-MGBNFQ-3′

at concentrations of 400 nmol/l each and 40 ng cDNA as template. Specificity against *CYP2B7P1* was confirmed using DNA plasmids of both genes as template. To generate a standard curve, serial 10-fold dilutions of a linearized plasmid containing the open reading frame of *CYP2B6* (kindly provided by Dr. Oliver Burk) were analyzed over a range from 10^{-1} to 10^{-7} ng. β-Actin was used as housekeeping gene to normalize CYP2B6 values, and the lowest normalized value was arbitrarily set to 1.

13. Gene copy number determination of *CYP2B6*

Real-time PCR can be used to quantify the number of copies of a given DNA sequence in a genome relative to a reference gene. In this work, a copy number assay specific for *CYP2B6* was developed to allow for rapid identification of so far unknown deletion or duplication alleles of *CYP2B6*.

13.1. TaqMan real-time PCR conditions

Primers and FAM-labeled probe for *CYP2B6* were designed using the Primer Express software, version 1.5 (Applied Biosystems). They were chosen to be *CYP2B6*-specific

(differences to *CYP2B7P1* underlined) and known polymorphic sites were avoided. Sequences were as follows:

2B6(15748)F 5′-TGT ATT CGG CCA GGT CAG G-3′
2B6(15896)R 5′-CCT GAT TCT TCA CAT GTC TGC G-3′
2B6in4(15800) 5′-FAM-TGA ACA CCC AGA ACA CAC GAG AAA AGG A-TAMRA

For albumin, primers and VIC-labeled probe were used as described previously by Schaeffeler *et al.*, 2003. Primers were purchased from MWG, Ebersberg, Germany, and probes were obtained from Applied Biosystems. Sequences were as follows:

alb ex12 for 5′-TGT TGC ATG AGA AAA CGC CA-3′
alb ex12 rev 5′-GTC GCC TGT TCA ACC AAG GAT-3′
alb ex12 probe 5′-VIC-AAG TGA CAG AGT CAC CAA ATG CTG CAC AG-TAMRA

Real-time PCR was performed using the ABI Prism 7700 sequence detection system. Amplification reactions (25 µl) were carried out in duplicate as one-tube biplex assay with 50 ng of template DNA, 2x TaqMan Universal PCR Master Mix buffer (Applied Biosystems), 300 nM of each primer and 200 nM of each fluorogenic probe. Cycling conditions were:

50°C	2’00’’	
95°C	10’00’’	
95°C	15’’	} 40x
60°C	1’00’’	

Product sizes were 149 bp for CYP2B6 and 72 bp for albumin. In each assay, a standard curve was recorded and a no-DNA control included.

13.2. Evaluation of specificity

To evaluate the specificity of the assay with respect to amplification of *CYP2B6* versus pseudogene *CYP2B7P1*, a PCR product was generated from genomic DNA using the primers

2B6(15569)F 5′-TCT GTG TCC TTG ACC TGC TG-3′ and
2B6(16080)R 5′-TCA TTC TCA TCA ACT CTG TCT CTC A-3′

which were selected to amplify both *CYP2B* genes simultaneously, and cloned into the pCR4-TOPO vector. Two clones carrying the 512 bp-PCR product derived from either *CYP2B6* or *CYP2B7P1* were selected by digestion with *Sty*I and sequenced. Serial tenfold dilutions of these two plasmids designated pCR4TOPO-PCR08-2B6 and -2B7 (10 ng/µl to 0.1 pg/µl) were used as template for real-time PCR.

13.3. Normalization and Quantification

The human albumin gene (*ALB*) was validated as a suitable reference gene to account for variations in the amount of DNA template or different amplification efficiencies. *ALB* was quantified simultaneously in a biplex assay in the same tube, and each reaction was carried out in duplicate. Quantification was performed by the standard curve method. In each assay, standard curves were recorded using serial dilutions (33.3, 16.65, 8.33, 4.16 and 2.08 ng/µl corresponding to 10,000, 5,000, 2,500, 1,250 and 625 copies of genomic templates/µl) of the same calibrator DNA (genomic DNA from J. Zukunft). Gene copy numbers of test samples were interpolated based on standard curves calculated by linear regression and the assumption that calibrator and test samples had two normal copies of the *ALB* gene. The normalized haploid *CYP2B6* gene copy number was defined as N=copy number (*CYP2B6*)/copy number (*ALB*). Assuming that the calibrator DNA possesses two normal copies of the *CYP2B6* gene, a normal diploid test sample is thus expected to yield a ratio of N=1, as compared to N=0.5 for a haploid genotype and N=1.5 for a heterozygous gene duplication.

III RESULTS

1. Sequencing of the *CYP2B6* promoter region

To generate a basis for investigating the role of promoter polymorphisms in CYP2B6 expression, 2.3 kb of upstream sequence in 98 DNA samples from Caucasian liver donors previously studied for exonic polymorphisms and CYP2B6 expression were sequenced by Dr. Thomas Lang at EPIDAUROS Biotechnology AG, Bernried, Germany. As shown in Table 6, the most frequent SNPs in the promoter region were -750T>C (allele frequency 57%) and -1456T>C (26%). The polymorphisms -1778A>G and -1186C>G both occurred with a frequency of 9%, whereas the SNPs -1848C>A, -82T>C and the newly described SNP -801G>T were all found with a frequency of 3%. These frequencies are in good agreement with previously published data. All genotype distributions were in accordance with the Hardy-Weinberg-Equilibrium except for the SNP -591A>G. This deviation indicates that a heterozygous carrier might have been erroneously identified as a homozygous carrier of this mutation (L#68).

SNP	WT/ WT	WT/ MT	MT/ MT	Allele frequency [%] and 95% C.I.		HWE: χ^2 and p-value
-1848C>A	92	6	0	3.1	(1.3 – 6.9)	0.10 (0.75)
-1778A>G	82	15	1	8.7	(5.3 – 13.5)	0.11 (0.74)
-1578C>A	97	1	0	0.5	(0.0 – 3.3)	0.003 (0.96)
-1489G>A	97	1	0	0.5	(0.0 – 3.3)	0.003 (0.96)
-1456T>C	53	40	5	25.5	(19.7 – 32.3)	0.54 (0.46)
-1186C>G	82	15	1	8.7	(5.3 – 13.5)	0.11 (0.74)
-801G>T	92	6	0	3.1	(1.3 – 6.9)	0.10 (0.75)
-750T>C	14	57	27	56.6	(49.4 – 63.6)	3.32 (0.07)
-591A>G	95	2	1	2.0	(0.8 – 5.1)	23.5 (<0.0001)
-82T>C	92	6	0	3.1	(1.3 – 6.9)	0.10 (0.75)

Table 6: Sequenced SNPs in the *CYP2B6* promoter. The base 5' to the initiation codon ATG was numbered -1.

2. Genotyping SNP -2320T>C by RFLP

While the sequencing of the promoter was in progress, a paper describing the SNP -2320T>C was published (Lamba *et al.*, 2003). As this polymorphism was not included in the sequenced fragment, a PCR-RFLP assay was developed to genotype this mutation. A 1.1 kb fragment of the *CYP2B6* promoter was amplified and digested with *Eco*RV. The wild type product yielded two fragments with 691 bp and 426 bp, whereas the mutation -2320T>C prevented digestion and resulted in an uncleaved fragment of 1117 bp (Figure 9).

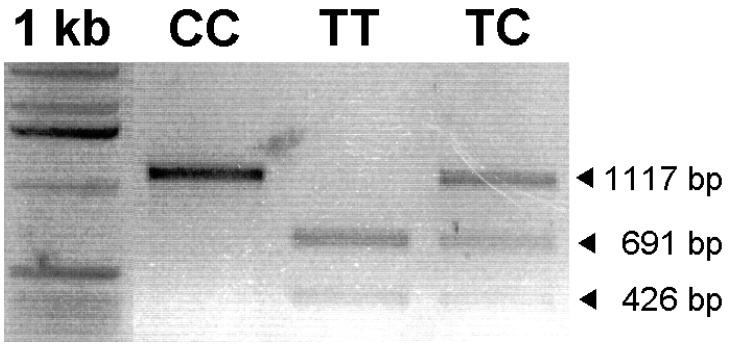

Figure 9: PCR-RFLP assay for the SNP -2320T>C. *Eco*RV digestion of wild type product yielded fragments of 691 bp and 426 bp, whereas the mutation abolished this restriction site and prevented digestion.

110 DNA samples from the liverbank were genotyped (Appendix, Table 10), and the allelic frequency of this SNP was calculated to be 30.5% (95% CI: 24.5% - 37.1%) which is in good accordance with previously published data (Lamba *et al.*, 2003; Hesse *et al.*, 2004). The genotype distribution (52, 49 and 9 for TT, TC and CC) did not deviate from Hardy-Weinberg-Equilibrium (χ^2=0.29, p=0.58).

3. Genotyping SNP c.1459C>T by RFLP

To be able to carry out a haplotype analysis including the promoter and the coding region, all samples that had been sequenced in the promoter had also been genotyped for the most common nonsynonymous SNPs c.64C>T, c.516G>T, c.777C>A, c.785A>G and c.1459C>T by Dr. Thomas Lang and Dr. Kathrin Klein, Institute of Clinical Pharmacology, Stuttgart. However, the distribution of genotypes for the exon 9 SNP c.1459C>T determined by the RFLP-Assay described by Lang *et al.* (2001) deviated significantly from the Hardy-Weinberg-Equilibrium in the Caucasian population described in the publication (χ^2=45, p<0.0001) as well as in the liverbank (χ^2=14, p=0.0002) with an excess of homozygous carriers of the mutant allele (Table 7).

A: Lang *et al.*, 2001

Genotype	observed	expected
c.1459CC	171	159.2
c.1459CT	28	51.6
c.1459TT	16	4.2
Allele frequency: 14.0%		
HWE: χ^2=45, p<0.0001		

B: Liverbank IKP148

Genotype	observed	expected
c.1459CC	86	81.7
c.1459CT	15	23.6
c.1459TT	6	1.7
Allele frequency: 12.6%		
HWE: χ^2=14, p=0.0002		

Table 7: Allele frequencies for the SNP c.1459C>T determined by the PCR-RFLP assay described by Lang *et al.* (2001) for (A) the Caucasian population described in the publication and (B) 107 Caucasians from the liverbank (IKP148).

Five of the six individuals from the liverbank genotyped TT (L#8, 13, 52, 75 and 105) were also heterozygous carriers of the mutations c.516G>T and c.785A>G in exons 4 and 5. The RFLP of these five samples always showed a weak band of undigested PCR product (Figure 10), and their sequencing chromatograms displayed a secondary peak of base C (Figure 11). In contrast, the sample L#23 genotyped TT which does not carry the mutations in exons 4 and 5 displayed unequivocal results in the PCR-RFLP assay and in the sequencing chromatogram.

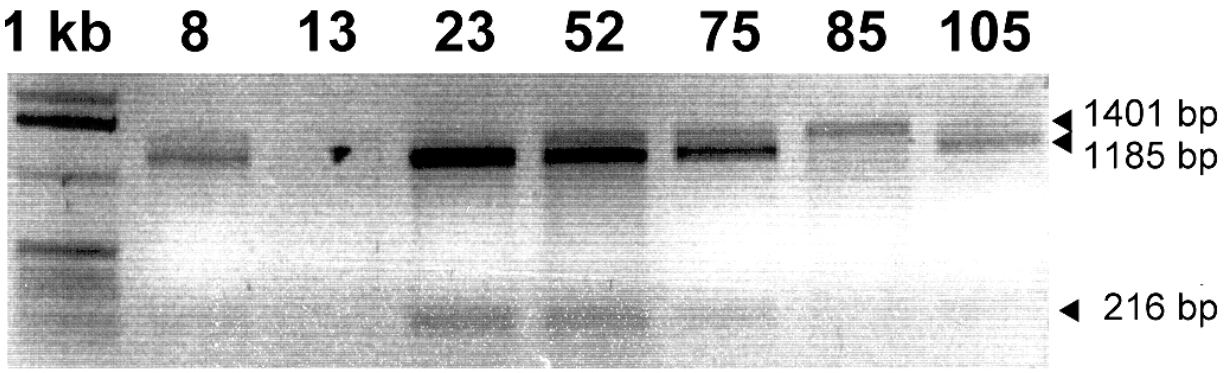

Figure 10: RFLP for the SNP c.1459C>T as described by Lang *et al.*, 2001. A 1401 bp fragment containing exon 9 of *CYP2B6* was amplified. The mutation creates a *Bgl*II site resulting in fragments of 1185 bp and 216 bp. Except L#85 (genotype CC), all samples were genotyped TT. In samples L#8, 52, 75 and 105 which are heterozygous for the exon 4 mutation c.516G>T, a weak band of undigested PCR product was visible.

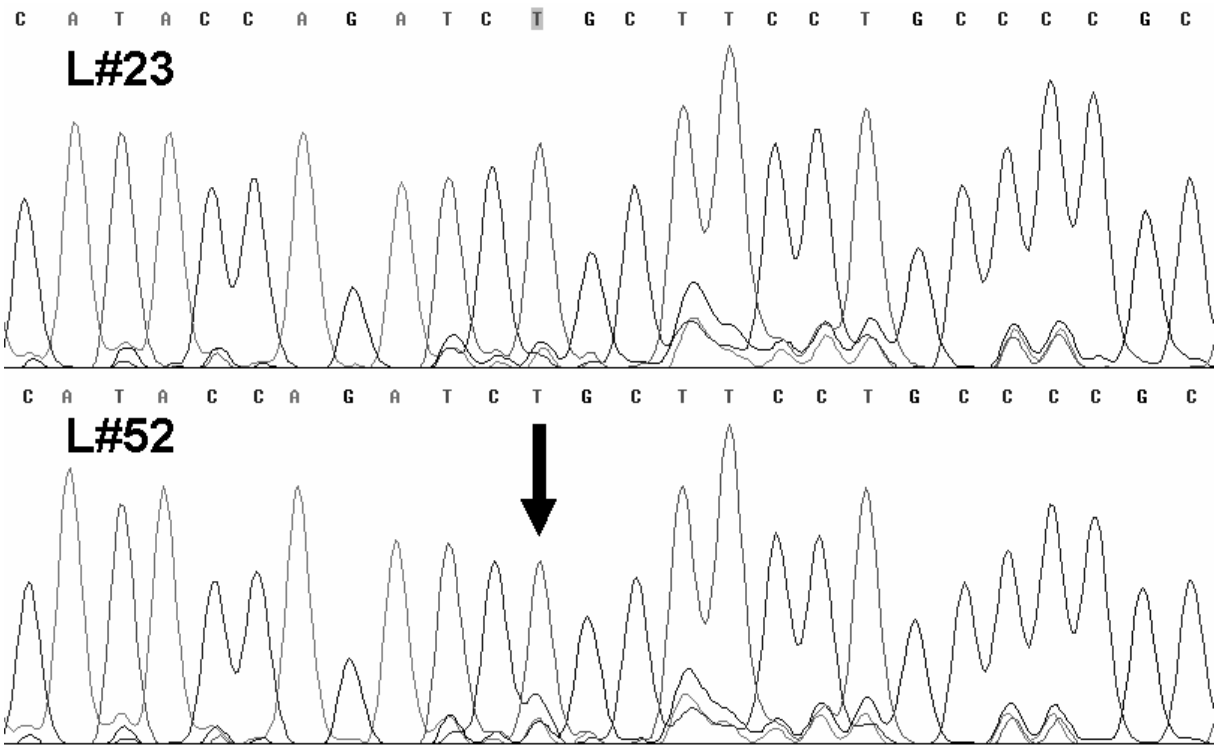

Figure 11: Sequencing chromatogram of two PCR products from Figure 10. In the sample L#52 which is heterozygous for the exon 4 mutation c.516G>T, a secondary peak of base C is visible at base position c.1459 which is not seen in the sample L#23.

The six samples genotyped c.1459TT were reanalyzed by an alternative PCR-RFLP assay in which a different forward primer was used for amplification of a 477 bp fragment (Figure 12).

The TT genotype was confirmed only for L#23, whereas the other five samples were genotyped CT. These results were also verified by sequencing the PCR fragment (data not shown).

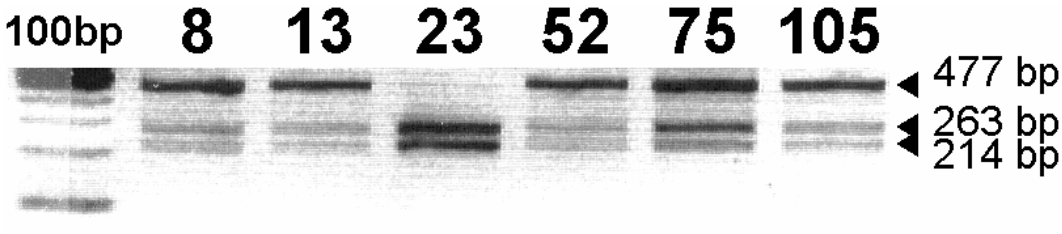

Old genotype	**TT**	**TT**	**TT**	**TT**	**TT**	**TT**
New genotype	**CT**	**CT**	**TT**	**CT**	**CT**	**CT**

Figure 12: Alternative PCR-RFLP assay for the SNP c.1459C>T. The mutation creates a *Bgl*II site resulting in fragments of 263 bp and 214 bp.

The dbSNP database (http://www.ncbi.nlm.nih.gov/entrez/query.fcgi?db=snp) gave a first hint for the reason of these conflicting results. Two SNPs (rs4802104 and rs7259965) were found to be located at the binding site of the primer CYP2B6-9F. Sequencing of this region (Figure 13) indeed demonstrated linkage of the SNP rs7259965 (g.24322C>T) with the SNP c.516G>T, as seen, for example, in samples L#45 and L#48 (Table 8). All five samples that were erroneously identified as homozygous carriers of the exon 9 mutation were shown to be heterozygous carriers of the intron 8 SNP g.24322C>T, indicating that impaired binding of the primer CYP2B6-9F caused wrong results in genotyping the SNP c.1459C>T.

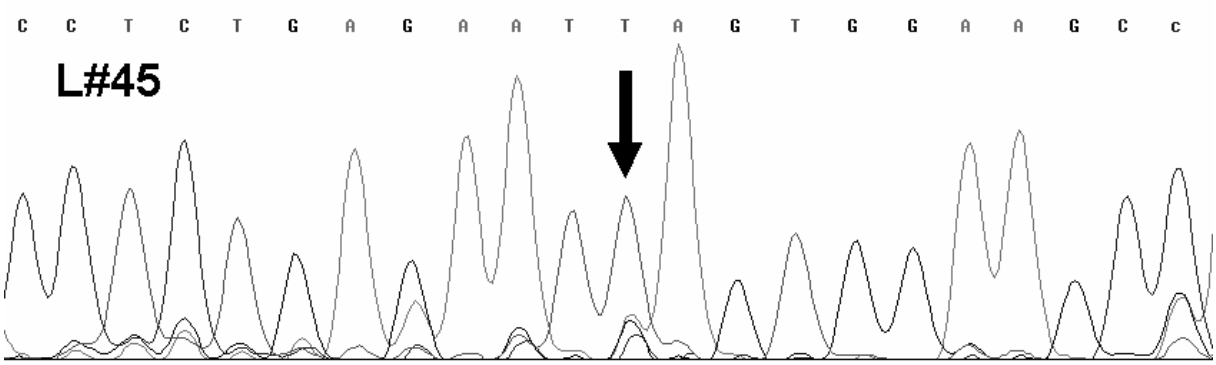

Figure 13: Sequencing chromatogram of a homozygous carrier of the intron 8 SNP g.24322C>T (dbSNP: rs7259965)

L#	**8**	**13**	**23**	39	45	48	50	**52**	59	63	**75**	91	93	97	**105**
Exon 4 c.516G>T	**GT**	**GT**	**GG**	GG	TT	TT	GT	**GT**	GT	GG	**GT**	GG	TT	TT	**GT**
Intron 8 g.24322C>T	**CT**	**CT**	**CC**	CC	TT	TT	CT	**CT**	CT	CC	**CT**	CC	TT	TT	**CT**
Exon 9 c.1459C>T	**CT**	**CT**	**TT**	CT	CC	CC	CC	**CT**	CC	CT	**CT**	CT	CC	CC	**CT**

Table 8: Genotyping results for the SNPs c.516G>T, g.24322C>T and c.1459C>T in selected samples.

The sequencing results were confirmed in a PCR-RFLP assay for the intron 8 SNP g.24322C>T which abolishes a *Hin*fI site (Figure 14).

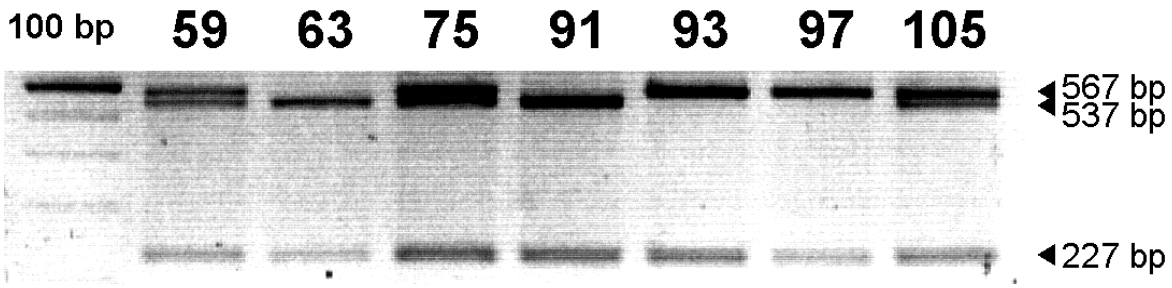

Figure 14: PCR-RFLP assay for the SNP g.24322C>T. *Hin*fI digestion yielded fragments of 537 bp, 227 bp and 30 bp for the wild-type product and fragments of 567 and 30 bp in the presence of the mutation g.24322C>T.

4. Haplotype structure of CYP2B6

From 96 individuals, genotypic data was now available for nine promoter SNPs (obtained by sequencing and RFLP for the -2320T>C SNP) as well as for the most common SNPs in the coding region. Using the PHASE software (Stephens *et al.*, 2001), eleven unambiguous haplotypes from 92 individuals were inferred (Figure 15). Four novel alleles could be defined including allele **22*, which contained the four linked promoter polymorphisms -1848C>A, -801G>T, -750T>C and -82T>C, found at a frequency of 3%. One sample carrying this haplotype (L#110) was sequenced throughout all exons to exclude the presence of further unknown mutations. An allele similar to **4A* but carrying in addition the common promoter SNPs -750T>C and -1456T>C was designated as **4D*. An allele composed of the exon 9 SNP c.1459C>T and the mutation -591A>G was defined as **5C*, whereas a further allele differing from **6A* with regard to the presence of the -750T>C SNP was termed **6C*. The most

common alleles in this Caucasian population were **1A* (frequency 25%), **6B* (22%) and **1H* (20%). Ambiguous haplotype estimates (phase probability <0.95) occurred only in four individuals (L#18, 62, 68, 105). One of these (L#105) was the only carrier of the SNP -1578C>A.

Allele	-2320	-1848	-1778	-1456	-1186	-801	-750	-591	-82	c.64	c.516	c.785	c.1459	Allele frequency [%] and 95% CI (N=184)
**1A*	T	C	A	T	C	G	T	A	T	C	G	A	C	25.0 (19.1 – 32.0)
**1H*	C	C	A	T	C	G	C	A	T	C	G	A	C	19.6 (14.3 – 26.2)
**1J*	C	C	G	T	G	G	C	A	T	C	G	A	C	8.7 (5.2 – 14.0)
**1N*	T	C	A	C	C	G	C	A	T	C	G	A	C	0.5 (0.0 – 3.5)
**2A*	T	C	A	T	C	G	T	A	T	T	G	A	C	7.1 (4.0 – 12.1)
**4D*	T	C	A	C	C	G	C	A	T	C	G	G	C	2.7 (1.0 – 6.6)
**5A*	T	C	A	T	C	G	T	A	T	C	G	A	T	9.2 (5.6 – 14.6)
**5C*	T	C	A	T	C	G	T	G	T	C	G	A	T	1.1 (0.2 – 4.3)
**6B*	T	C	A	C	C	G	C	A	T	C	T	G	C	22.3 (16.6 – 29.1)
**6C*	T	C	A	T	C	G	C	A	T	C	T	G	C	0.5 (0.0 – 3.5)
**22*	T	A	A	T	C	T	C	A	C	C	G	A	C	3.3 (1.3 – 7.3)

Figure 15: Alleles of *CYP2B6*. Bases are numbered according to the recommendations of the Nomenclature Working Group (Antonarakis and the Nomenclature Working Group, 1998). Alleles are designated according to the CYP Allele Nomenclature Committee (http://www.imm.ki.se/CYPalleles/). Names of novel alleles described in this study are printed white on black.

5. Promoter activity in different cell lines

HepG2 cells were transfected with different reporter gene constructs of the pGL3-2B6(-2033) series that contain the firefly luciferase gene driven by the *CYP2B6* promoter (Figure 16A). In this hepatoma cell line, the wild type construct did not show transcriptional activity distinguishable from the pGL3-Basic vector (Figure 16B). In contrast, the construct pGL3-2B6(-2033)A3 consistently showed a transcriptional activity ninefold higher than wild type, whereas the A2 and A4 constructs did not exhibit any detectable promoter activity. We then transfected HepG2 cells with constructs carrying the individual SNPs contained in A3 (Figure 16C). The plasmid pGL3-2B6(-2033)-82T>C showed increased activity of the same magnitude as the A3 construct, whereas the other three SNPs did not alter promoter activity.

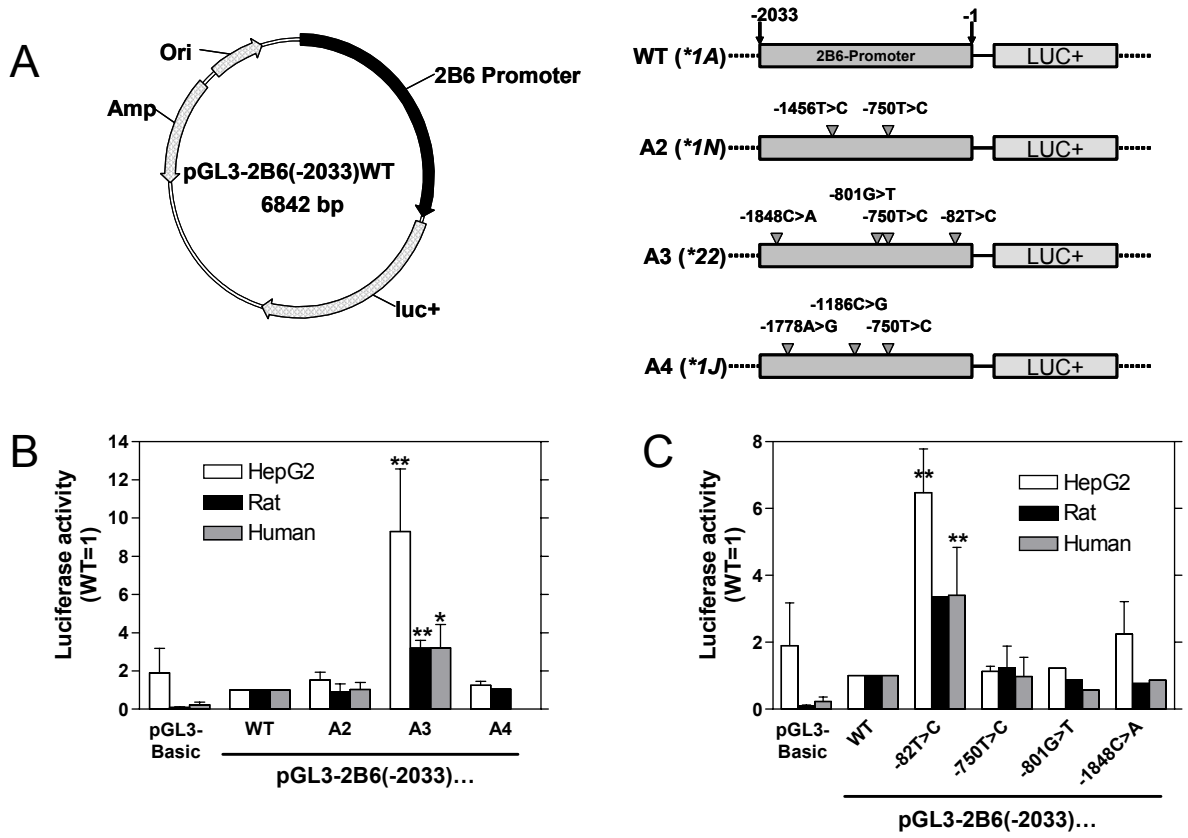

Figure 16: Transcriptional activity of the *CYP2B6* promoter. (A) Firefly luciferase reporter gene plasmids carrying 2033 bp of the wild type (WT) *CYP2B6* 5'-flanking region or different combinations of mutations (A2, A3, A4) representing the haplotypes **1N*, **22* and **1J* of the *CYP2B6* promoter were constructed as described in "Materials and Methods". (B) HepG2 cells and primary rat and human hepatocytes were cotransfected with the various plasmids and a β-galactosidase control plasmid (HepG2, human hepatocytes) or a *Renilla reniformis* luciferase control plasmid (rat hepatocytes). β-galactosidase-normalized or *R. reniformis* luciferase-normalized firefly luciferase activity is shown in relation to the wild type construct which was set to 1.0 for each cell type. (C) Plasmids carrying the individual mutations of the pGL3-2B6(-2033)A3 construct were generated by *in vitro* mutagenesis and analyzed as described under (B). The means and standard deviations of at least two independent experiments are shown; *p<0.05; **p<0.01 (ANOVA followed by Dunnett's multiple comparison test).

To confirm these findings in noncancerous cells, primary rat and human hepatocytes were transfected. The experiments in rat hepatocytes were conducted by Dr. Karen Hirsch-Ernst, Institute of Toxicology, Göttingen, and human hepatocytes were provided by Dr. Andreas Nüssler, Charité, Berlin. In contrast to HepG2 cells, basal promoter activity of the wild type

construct was about tenfold higher compared to pGL3-Basic in both species. The pGL3-2B6(-2033)A3 construct again showed a significant increase in transcriptional activity as compared to the wild type, whereas the other constructs had unchanged activities (Figure 16B). The increase in transcriptional activity of the A3-construct was about threefold, which is somewhat lower than in HepG2 cells. This difference is most likely due to the elevated basal activity of the wild type promoter compared to pGL3-Basic in primary hepatocytes. Similar to the analysis in HepG2 cells, only the single mutation -82T>C conferred enhanced transcriptional activity on the *CYP2B6* promoter (Figure 16C). These results were reproduced in at least three independently performed transfections with different preparations of human hepatocytes.

Primary hepatocytes were also transfected with the plasmid pGL3-2B6(-1641)WT, which contains only 1.6 kb of the promoter and lacks the PBREM of the *CYP2B6* gene. In rat hepatocytes, promoter activity of this shorter construct dropped to 20% of the values obtained with the longer pGL3-2B6(-2033)WT plasmid (Figure 17). In human hepatocytes, however, this difference was not as pronounced; the shorter plasmid still maintained 80% of the transcriptional activity of pGL3-2B6(-2033)WT. This suggests an important role of the PBREM for constitutive *CYP2B6* promoter activity in rat but not in human hepatocytes.

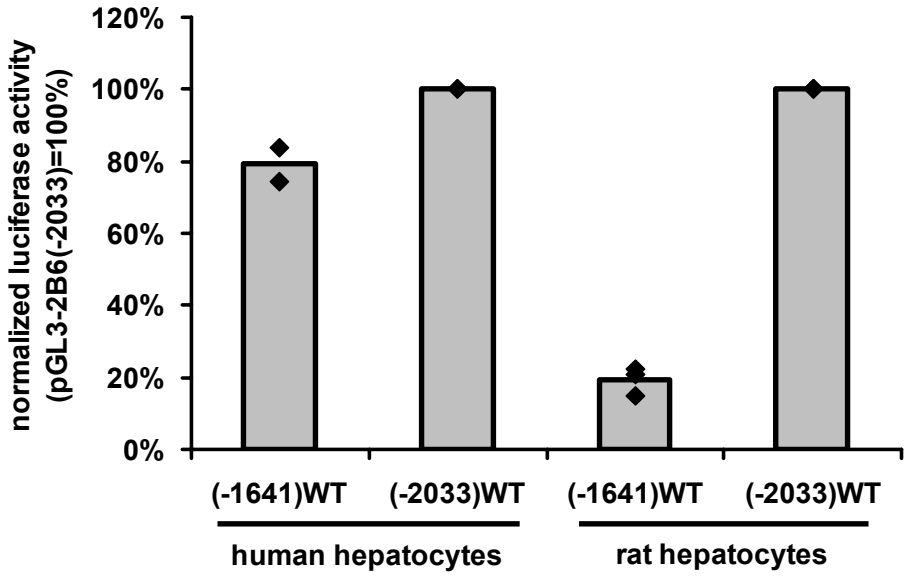

Figure 17: Reporter gene plasmids pGL3-2B6(-2033)WT and (-1641)WT were transfected into primary hepatocytes of rat and human. The activity of pGL3-2B6(-2033)WT was set to 100%.

6. *In silico* analysis of the promoter

The MatInspector Software was used to analyze the polymorphic regions of the novel *CYP2B6*22* allele for transcription factor binding sites. The predicted alterations included the loss of a putative HNF-1 site at -750 bp and disruption of a C/EBP binding site at -801 bp (Figure 18). Remarkably, the mutation -82T>C was not only predicted to disrupt a consensus TATA box, but to simultaneously create a putative C/EBP binding site (Figure 18, bottom). As the transcriptional start site of the human *CYP2B6* gene had not been determined so far, the significance of the loss of the putative TATA box was unclear. Interestingly, an additional noncanonical TATA box was detected at -55 bp (GATAAA). Furthermore, the proximal promoter was scanned for C/EBP binding sites using TESS (Transcription Element Search System, available at http://www.cbil.upenn.edu/tess/), which identified two additional putative C/EBP binding sites at -208 bp and -177 bp.

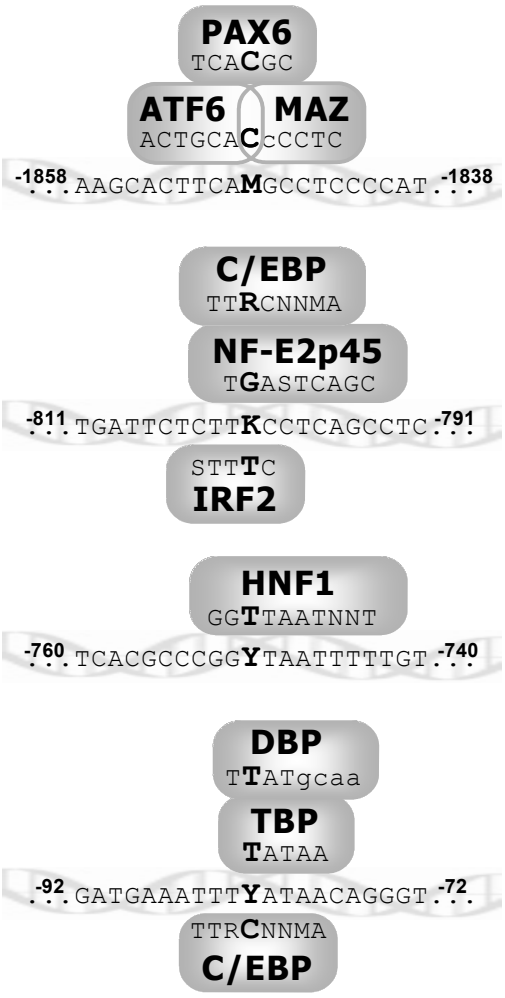

Figure 18: Putative cis-elements in the *CYP2B6* promoter affected by the **22* allele. The promoter region of *CYP2B6* was analyzed using the MatInspector software (Quandt *et al.*, 1995). Transcription factors with their consensus sequences are shown for the reference sequence (above) and the mutated sequence (below), with polymorphic sites in bold. PAX6, Pax-6 paired domain binding site; ATF6, Activating transcription factor 6; MAZ, Myc associated zinc finger protein; C/EBP, CCAAT/enhancer binding protein; NF-E2p45, Nuclear factor, erythroid-derived 2; IRF2, Interferon regulatory factor 2; HNF1, Hepatic nuclear factor 1; DBP, Albumin D-box binding protein; TBP, TATA box binding protein.

7. Electrophoretic mobility shift assays

7.1. C/EBP

Murine C/EBPβ was synthesized *in vitro* using the TnT T7 System (Promega) with the plasmid pcDNA3-C/EBPβ as template. When this protein was incubated with the ^{32}P-labeled oligonucleotide 2B6EMSA1 containing the TATA box at -82, no specific DNA-protein complex was observed (Figure 19, lane 2). However, in the presence of the mutation -82T>C (probe CATAA/2B6EMSA2), a shifted band of a specific DNA-protein complex was observed (lane 8), confirming that a functional C/EBP binding site had been created, as predicted *in silico*. In the presence of HepG2 nuclear extract, two specific complexes with different electrophoretic mobilities as compared to the complex with recombinant C/EBP were formed with mutant, but not with wild type probe. The reason for these differences is most likely related to the multiplicity of cellular C/EBP factors.

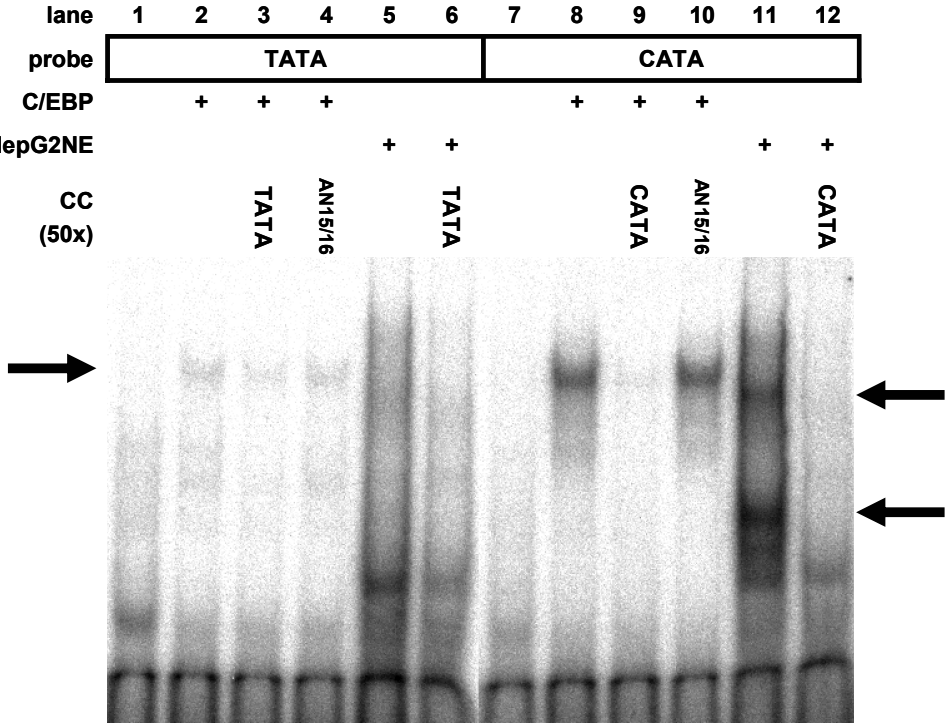

Figure 19: *In vitro* translated C/EBP or nuclear extract of HepG2 cells was incubated with labeled probes representing bases -94 to -70 of the *CYP2B6* promoter (containing a putative TATA box) in absence or presence of the SNP -82T>C (probes TATA and CATA). Unlabeled oligonucleotides were added as cold competitor (CC), as indicated. For unspecific competition, a 25 bp double-stranded oligonucleotide without C/EBP binding sites (AN15/16) was used. Protein-DNA complexes of C/EBP are marked by an arrow.

Additionally, the putative C/EBP binding sites at -208 and -177 bp were examined with the labeled probes EMSA4 and EMSA5 (Figure 20). An interaction between C/EBPβ and DNA indicating the presence of a functional C/EBP *cis*-element was detected with probe EMSA5 representing bases -183 to -164 of the *CYP2B6* promoter, but not with probe EMSA4 representing bases -215 to -196.

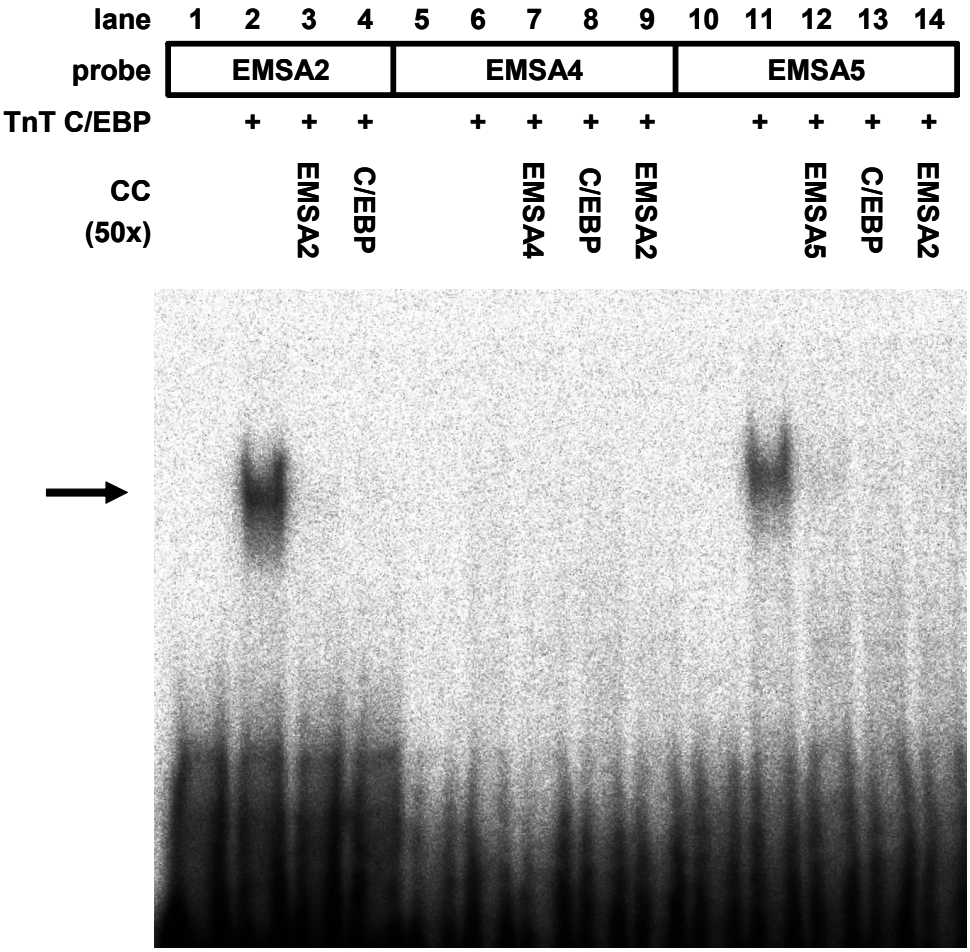

Figure 20: *In vitro* translated C/EBP was incubated with labeled probes representing putative C/EBP binding sites of the *CYP2B6* promoter at -208 bp (EMSA4) or -177 bp (EMSA5). EMSA2 was used as a positive control. The sequence of probe C/EBP used for competition experiments was obtained from Santa Cruz Biotech. Protein-DNA complexes of C/EBP are marked by an arrow. CC: cold competitor.

Specificity of this interaction was further proved by competition experiments (Figure 21): Only those unlabeled probes that represent C/EBP binding sites (C/EBP, EMSA2 and EMSA5) were able to fully displace the labeled probes EMSA2 or EMSA5 from the respective DNA-protein complexes, whereas probes lacking a C/EBP *cis*-element (EMSA1, EMSA4 and AN15/16) were not.

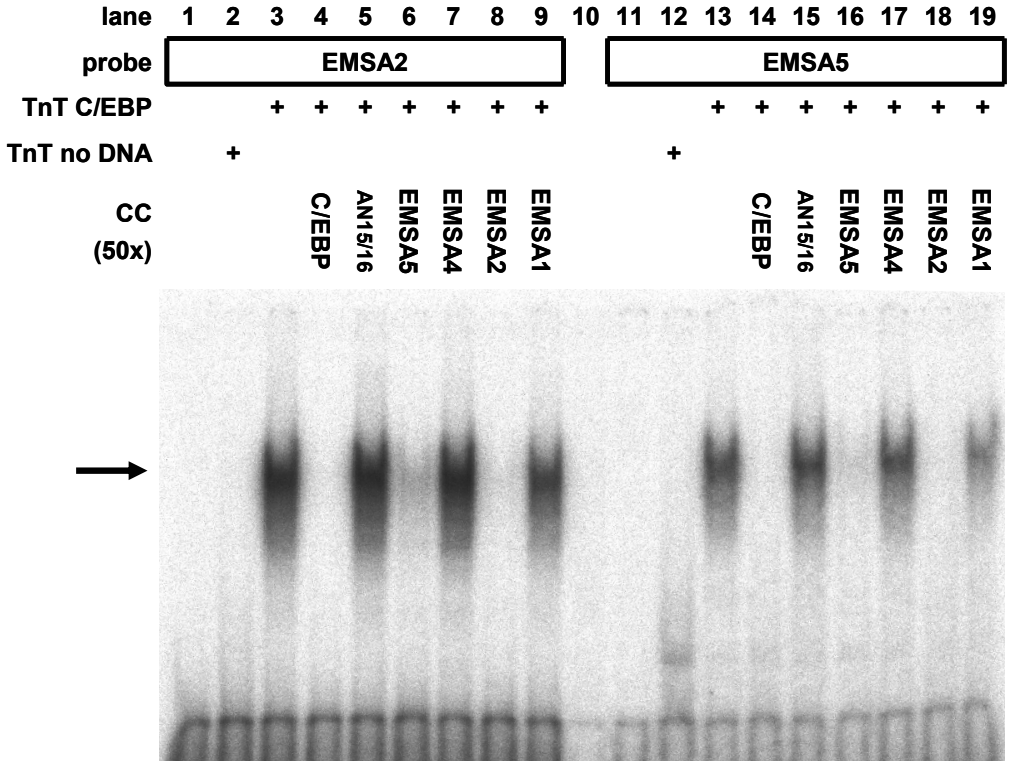

Figure 21: *In vitro* translated C/EBP was incubated with labeled probes EMSA2 and EMSA5 representing putative C/EBP binding sites. Unlabeled probes were added in 50-fold excess for competition experiments (CC: cold competitor). Protein-DNA complexes of C/EBP are marked by an arrow.

7.2.TATA-box binding protein (TBP)

As the *in silico* promoter analysis suggested the presence of two putative TATA boxes, their respective abilities to bind TBP was determined. As evident from Figure 22, strong specific binding of TBP to the GATA motif was visible (oligonucleotide 2B6EMSA3) at -55 bp (lane 10), whereas the TATA motif at -82 bp (oligonucleotide 2B6EMSA1) exhibited markedly weaker binding (lane 2). This interaction was even weaker in the presence of the mutation -82T>C (oligonucleotide 2B6EMSA2, lane 6). In addition, the TATA and CATA motifs were not able to fully compete the GATA-TBP complex even at 50-fold excess (lanes 12, 13). Thus, both the GATA and the TATA motifs were shown to bind TBP and may therefore be able to act as functional TATA boxes, although the affinity of TBP towards the GATA motif seemed to be higher.

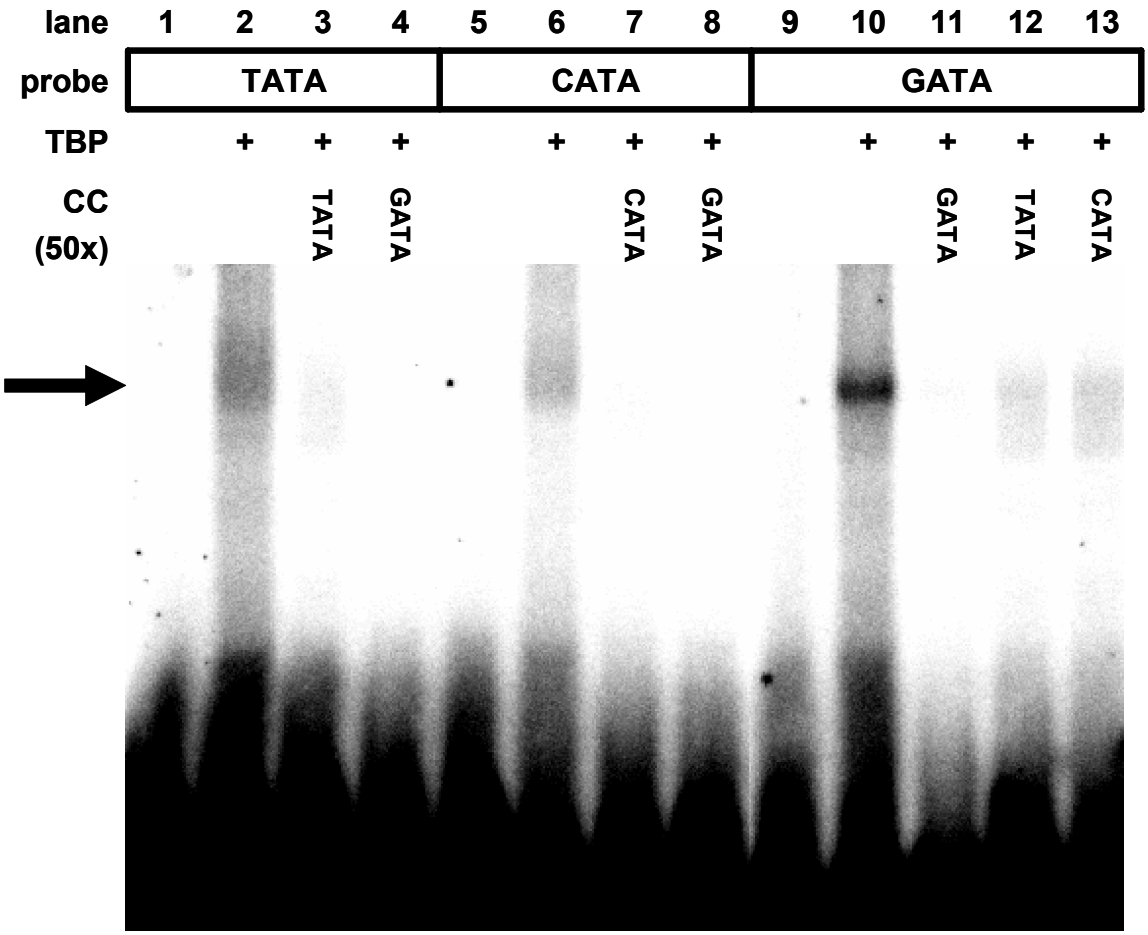

Figure 22: Recombinant TBP was incubated with probes TATA and CATA representing bases -94 to -70 of the *CYP2B6* promoter (containing a putative TATA box) in absence or presence of the SNP -82T>C as well as probe GATA (representing bases -64 to -40 of the *CYP2B6* promoter containing a putative noncanonical TATA box). Unlabeled oligonucleotides were added as cold competitor (CC), as indicated. TBP-DNA complexes are marked by an arrow.

7.3. HNF1

Murine HNF1α was synthesized *in vitro* using the TnT T7 System (Promega) with the plasmid pcDNA3-mHNF1α as template. When this protein was incubated with a labeled oligonucleotide representing the HNF1 binding motif from the apoE promoter (Wade *et al.*, 1994), a strong specific binding that disappeared in the presence of excess of unlabeled DNA was visible (Figure 23), demonstrating the ability of the *in vitro* translated protein to bind DNA. Towards prHNF1WT (representing bases -757 to -737 of the *CYP2B6* reference sequence), HNF1 exhibited weak binding which completely disappeared when the mutation

-750T>C was present (prHNF1MT). Neither prHNF1WT nor prHNF1MT were able to compete the binding of HNF1 to the apoE motif (lanes 4 and 5) in 50-fold excess.

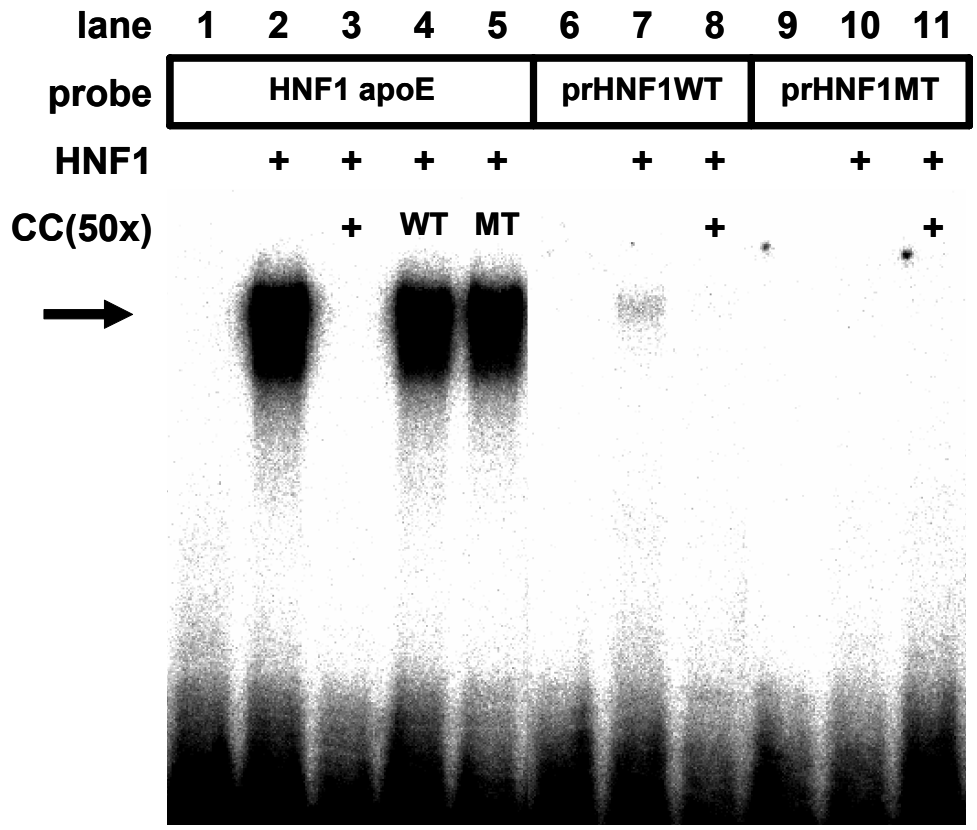

Figure 23: *In vitro* translated HNF1α protein was incubated with a known HNF1 element in the apoE promoter as positive control or oligonucleotides representing a putative HNF1 binding site in the *CYP2B6* promoter containing the base -750T (prHNF1WT) or -750C (prHNF1MT). Unlabeled oligonucleotides were used as cold competitor (CC), WT=unlabeled prHNF1WT, MT=unlabeled prHNF1MT.

8. Transactivation of *CYP2B6* promoter constructs

8.1. Cotransfection of C/EBPβ

As previous work by Jover *et al.* (1998) suggested a role of C/EBP in the regulation of *CYP2B6*, HepG2 cells were transfected with an expression plasmid for murine C/EBPβ and different reporter plasmids containing 2033, 1641 or 244 bp of the *CYP2B6* promoter (Figure 24). Transactivation of the reporter gene constructs was observed for all plasmids and decreased according to the length of the included promoter sequence from 67-fold for the pGL3-2B6(-2033)WT construct to 8-fold for the plasmid pGL3-2B6(-244)WT. This suggested the presence of multiple C/EBP binding sites in the proximal *CYP2B6* promoter, as predicted by *in silico* analysis and electrophoretic mobility shift assays.

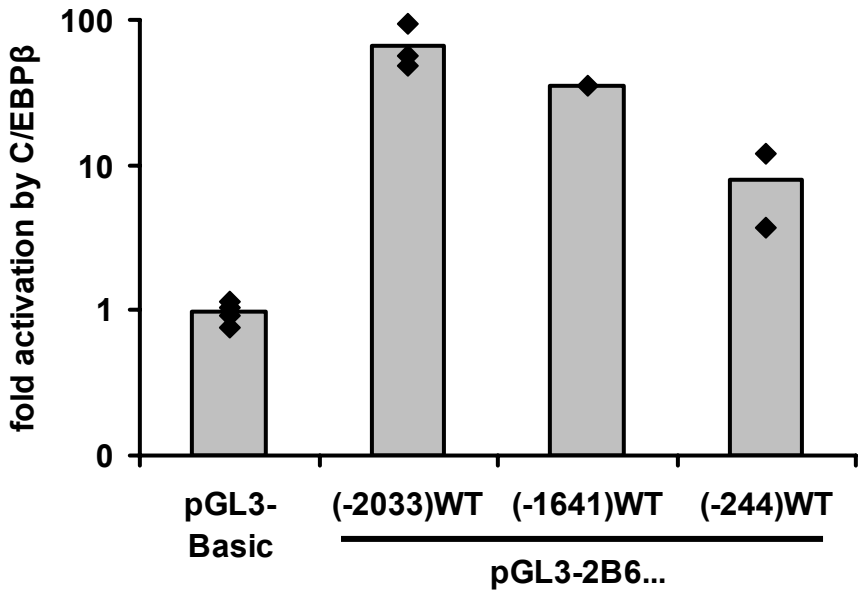

Figure 24: Transactivation of reporter gene plasmids by C/EBPβ. HepG2 cells were transfected with reporter gene plasmids containing the *CYP2B6* promoter region and an expression plasmid for C/EBPβ. The transactivation of the respective plasmids is shown.

To confirm the hypothesis that the transcription factor C/EBP is involved in the increased promoter activity caused by the mutation -82T>C, an expression vector for C/EBPβ-LIP was cotransfected in human hepatocytes with reporter plasmids containing 2033, 245 or 160 bases of the *CYP2B6* promoter. As C/EBPβ-LIP lacks the activation domain of C/EBPβ-LAP but still possesses the DNA binding and dimerization domain (Jover *et al.*, 2002), it was expected to behave as a dominant-negative transcriptional agonist against endogenous C/EBP. As seen

in Figure 25, the basal activity of the plasmids pGL3-2B6(-245)WT and (-160)WT were four- and sixfold lower than pGL3-2B6(-2033)WT, and in all constructs, the mutation -82T>C increased activity about threefold. Surprisingly, cotransfection of the presumably dominant-negative expression vector pAC-LIP resulted in an approximately threefold increase in transcriptional activity in all constructs indicating the presence of either residual transactivating activity or unspecific effects caused by the DNA binding of C/EBPβ-LIP. When the expression vector pAC-LAP encoding for C/EBPβ-LAP was cotransfected with the pGL3-2B6(-160) vectors, a 40-fold transactivation was observed (data not shown) suggesting the presence of C/EBP binding sites even within this short section of the promoter.

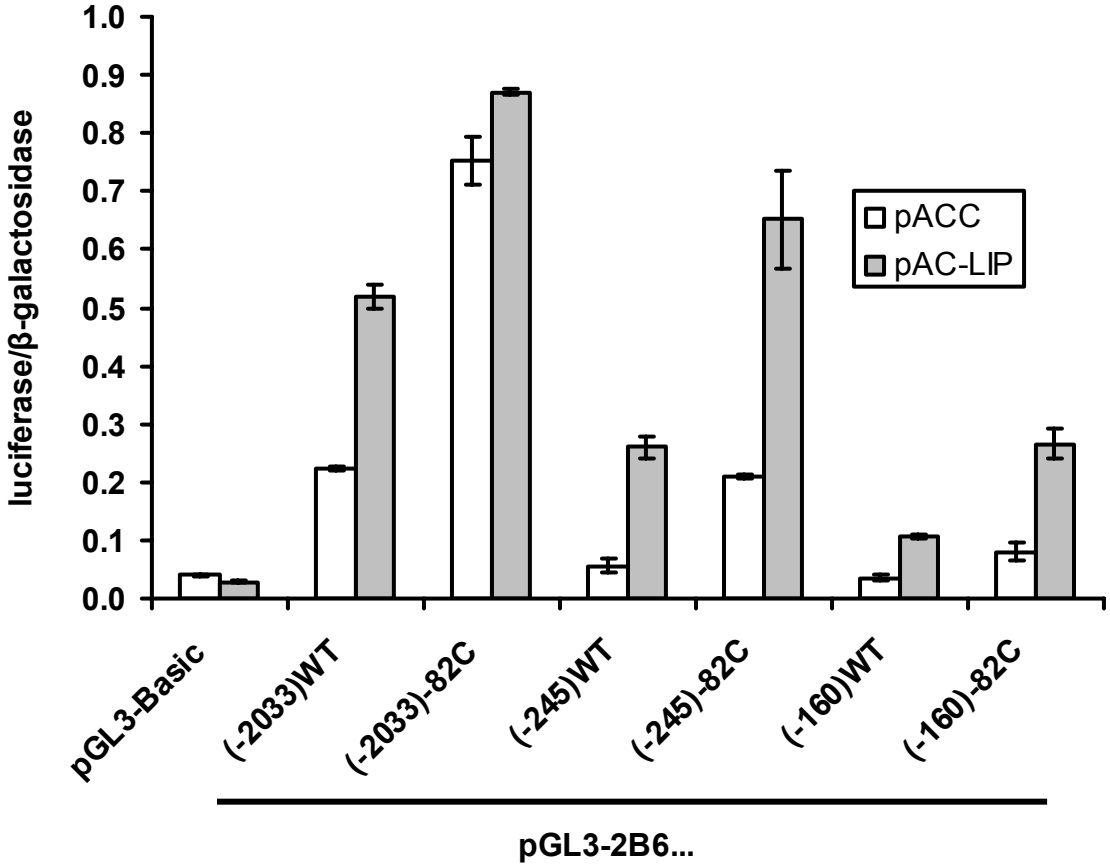

Figure 25: Cotransfection of the expression vector pAC-LIP encoding C/EBPβ-LIP which lacks the transactivation domain of C/EBPβ-LAP. The values and the means of duplicates of a single experiment are shown.

8.2. Cotransfection of HNF1α

As *in silico* analysis revealed a putative HNF1 binding site around -750 bp which was also suggested by other authors (Lamba *et al.*, 2003; Hesse *et al.*, 2004), expression plasmids for murine HNF1α and the dimerization cofactor DCoH were cotransfected with pGL3-2B6(-2033)WT and -750T>C, respectively. No transactivation of the reporter gene plasmids was observed in HepG2 cells, as their β-galactosidase normalized luciferase activities remained below the values of the control vector pGL3-Basic (Figure 26).

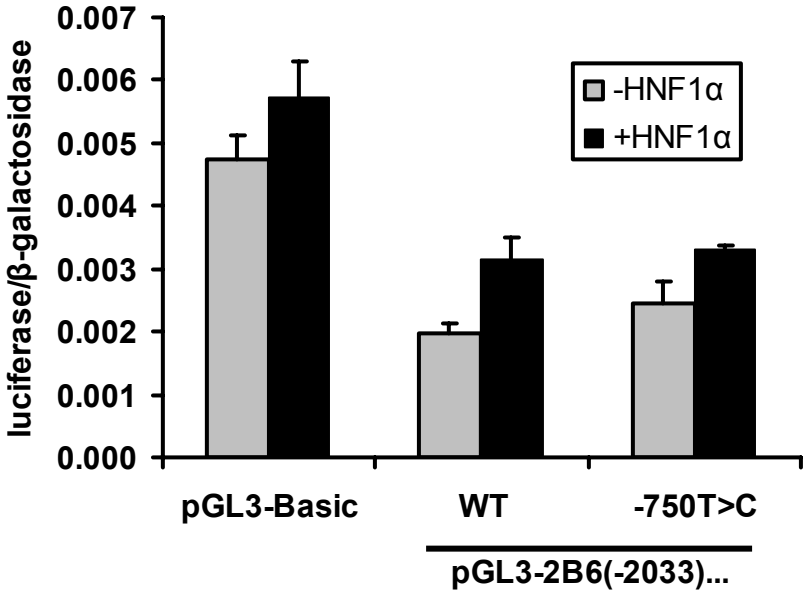

Figure 26: HepG2 cells were transfected with pGL3-2B6(-2033)WT or -750T>C and expression plasmids for HNF1α and DCoH. Data are presented as means + S.D. of triplicates in a single experiment.

9. Analysis of transcriptional start sites by 5'-RACE

9.1. CYP2B6 transcripts in human liver RNA

To investigate whether the two putative TATA boxes are involved in transcription, analysis of the transcriptional start site was performed using 5'-RLM-RACE and human liver RNA of two persons with different genotypes at -82 bp (Figure 27). From both persons, 24 clones were prepared and sequenced. Of those, 18 (L#64) and 14 (L#78) were derived from 5'-full-length transcripts of CYP2B6 mRNA; the remaining plasmids represented either splicing variants of CYP2B6 or unspecific products.

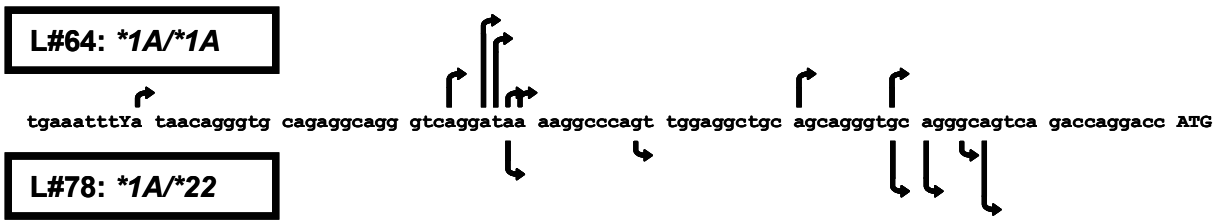

Figure 27: The TSS of *CYP2B6* was determined in cDNA of two human livers with different genotype using 5'-RLM-RACE. The length of the arrows corresponds to the number of clones representing the respective TSS.

We found two different transcriptional start regions of the *CYP2B6* gene around -54 bp and -20 bp. The usage of these sites appeared to be strongly dependent on genotype: for the individual with the wild type promoter (upper arrows), 13 out of 18 transcripts originated from -57 to -51 bp. Additional minor transcriptional start sites were mapped to -81 bp, -30 bp and -22 bp. In contrast, 11 out of 14 analyzed transcripts of the **1A/*22* individual started between -22 bp and -15 bp (lower arrows), whereas only two clones were derived from transcripts using the transcriptional start site at -52 bp.

In addition, we also found a transcript of the recently described splice variant SV4 (Lamba *et al.*, 2003) that contained the cryptic exon 3A, as well as a transcript of a new splice variant that used an alternate acceptor site in exon 4 without including the cryptic exon 3A. The resulting transcript contained a 32 bp deletion leading to a frameshift and a predicted premature stop codon in exon 5 (Figure 28). In RNA of both livers, no transcripts of the pseudogene *CYP2B7P1* were found among the 34 clones analyzed.

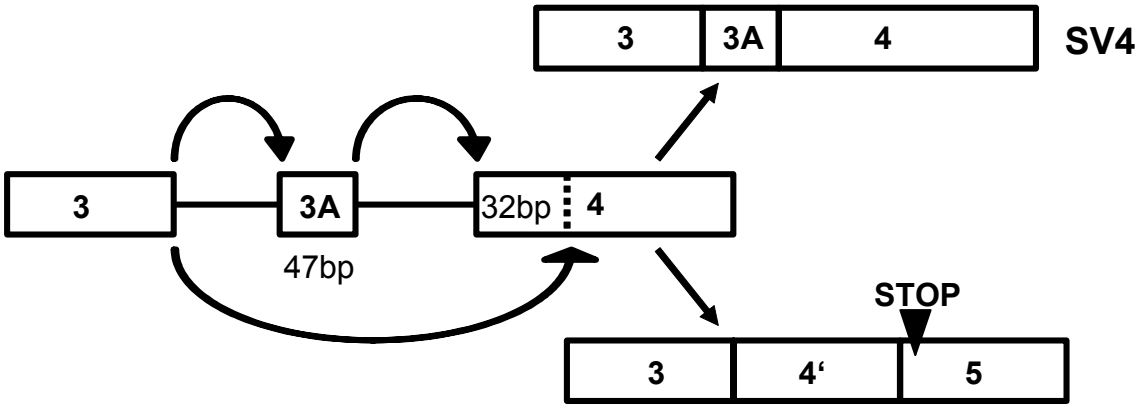

Figure 28: Alternative splicing products of *CYP2B6* found in this study.

9.2. Luciferase transcripts in transfected HepG2 cells

To exclude the possibility that other factors than genotype including gender, age or drug exposure were responsible for the differential use of the two transcriptional start sites, we also analyzed luciferase transcripts driven by 2.0 kb of the *CYP2B6* promoter in transfected HepG2 cells. In cells transfected with pGL3-2B6(-2033)WT, the major transcriptional start site was mapped to a region from -57 bp to -49 bp, which was used by 16 of 21 analyzed clones (Figure 29, upper arrows). The remaining five clones were derived from transcripts utilizing a transcriptional start site at -43 bp which was not used in human liver RNA except by the splice variant SV4 in L#78. In contrast, when pGL3-2B6(-2033)A3 was transfected, shorter transcripts with a transcriptional start site at -24 bp dominated (14 of 24 clones, Figure 29, lower arrows), whereas transcriptional start sites at -54 bp and -53 bp were found in only four clones. Also here, six transcripts originated from a transcriptional start site at -43 bp. This result confirmed the pivotal role of the promoter genotype in determining the transcriptional start site of *CYP2B6*.

Figure 29: HepG2 cells were transfected with two reporter gene constructs reflecting the two different alleles *CYP2B6*1A* and **22*. The TSS of the transcribed luciferase gene driven by 2033 bp of the CYP2B6 promoter was mapped and displayed as in Figure 27.

10. Analysis of transcriptional start sites by primer extension

To validate the results obtained in the 5'-RLM-RACE experiments, primer extension analyses were performed with ~100 µg total RNA of the liver samples L#64 and L#78 (Figure 30). In the sample L#64, transcriptional start sites were localized around -53 bp, which were not seen in the liver genotyped -82TC (L#78). In this sample, two other transcriptional start sites at -22 and -20 bp were clearly recognized. These results demonstrate excellent agreement between the two methods applied for analysis of transcriptional start sites.

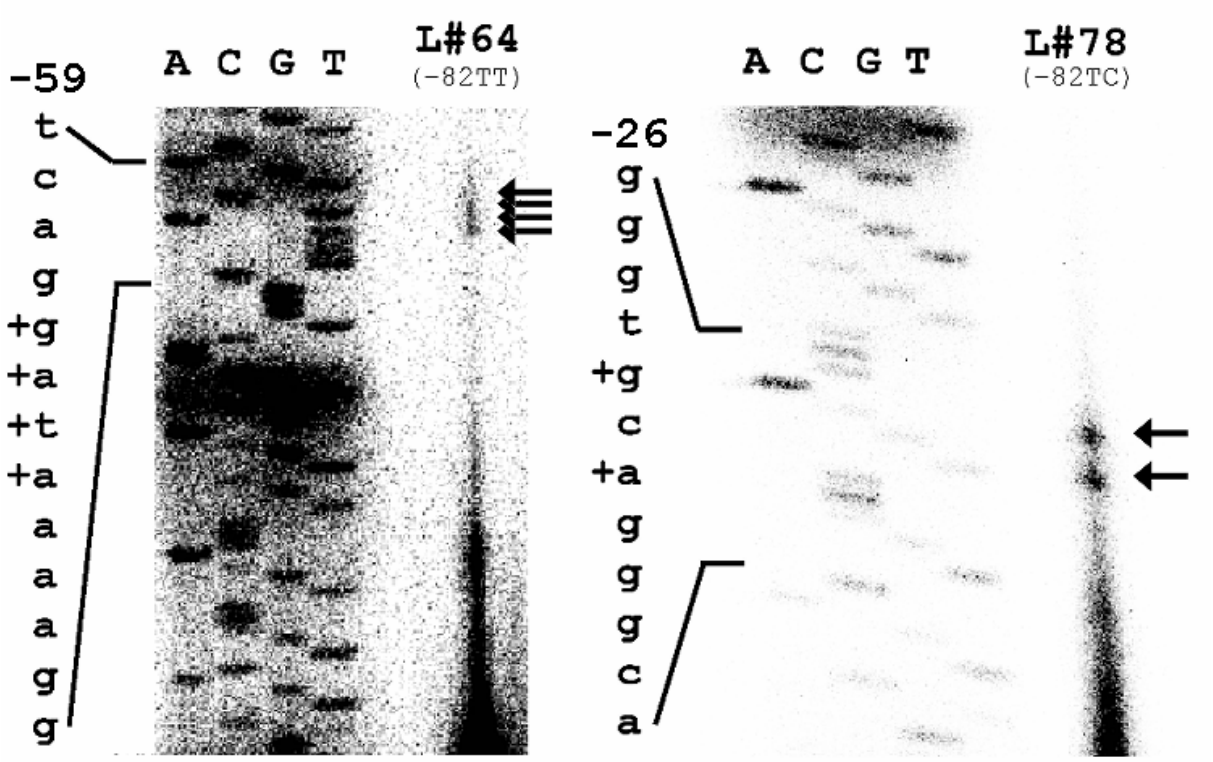

Figure 30: Primer extension analyses. Primer extension was performed with ~100 µg total liver RNA of two individuals with different genotypes at -82 bp and a ^{32}P-labeled primer located 41 bp downstream from the translation initiation site. The corresponding genomic fragment was sequenced using the same primer. Primer extension products are marked by arrows, and the corresponding transcriptional start sites (TSS) in the sequence are marked by +.

11. CYP2B6 mRNA expression in human liver samples

In a panel of 97 RNA samples from the liverbank, CYP2B6 mRNA expression was measured by quantitative real-time PCR. For normalization, β-actin was used as housekeeping gene to account for differences in RNA quality and cDNA synthesis, and the lowest value (L#48) was arbitrarily set to 1 (Appendix, Table 11). Median CYP2B6 mRNA expression was 9.8 a.u. with a range from 1 to 105 a.u. (Figure 31). This result is in good agreement with the 43-fold interindividual variability found by Hesse *et al*. (2004), but much lower than the >3000-fold variation described by Lamba *et al*. (2003). The highest and fourth highest values were measured in two individuals taking carbamazepine (indicated by arrows), underlining the ability of this drug to induce CYP2B6 expression *in vivo*. The correlation between CYP2B6 mRNA and apoprotein levels was relatively poor (r_S=0.4127, p<0.0001), an observation that was also described by Hesse *et al*. (2004). No difference in median mRNA expression was found between males and females (10.24 vs. 9.75 a.u.).

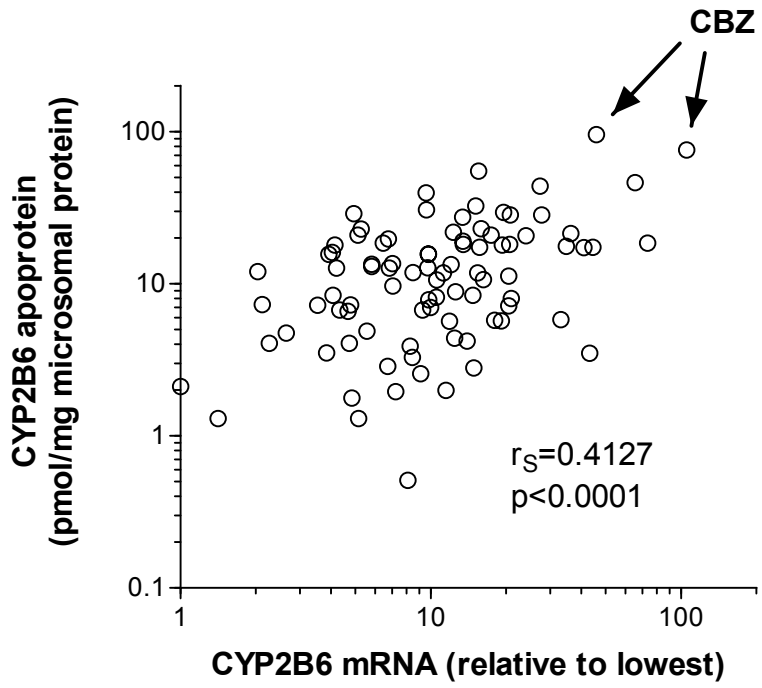

Figure 31: Correlation between CYP2B6 mRNA content and apoprotein expression. Two individuals known to have taken the CYP-inducing antiepileptic carbamazepine are marked by arrows. The spearman correlation coefficient is given.

12. Genotype-phenotype correlations

12.1. Genotyping SNP -82T>C by DHPLC

Of the approximately 300 samples of the liverbank, 98 had been sequenced in the promoter region, and only six of those were heterozygous for the SNP -82T>C. To increase the group size for a subsequent genotype-phenotype analysis, the remaining DNA samples of the liverbank were genotyped for this SNP by a DHPLC assay. When the mutation was present, formation of heteroduplexes occurred and additional peaks appeared in the chromatogram (Figure 32). 182 additional samples were analyzed; six of those were heterozygous carriers of the mutation (Appendix, Table 9). No homozygous carrier of the mutation was identified. The allele frequency in the entire liverbank (182 + 98 samples) was therefore calculated to be 2.1% (95% CI: 1.2% -3.8%).

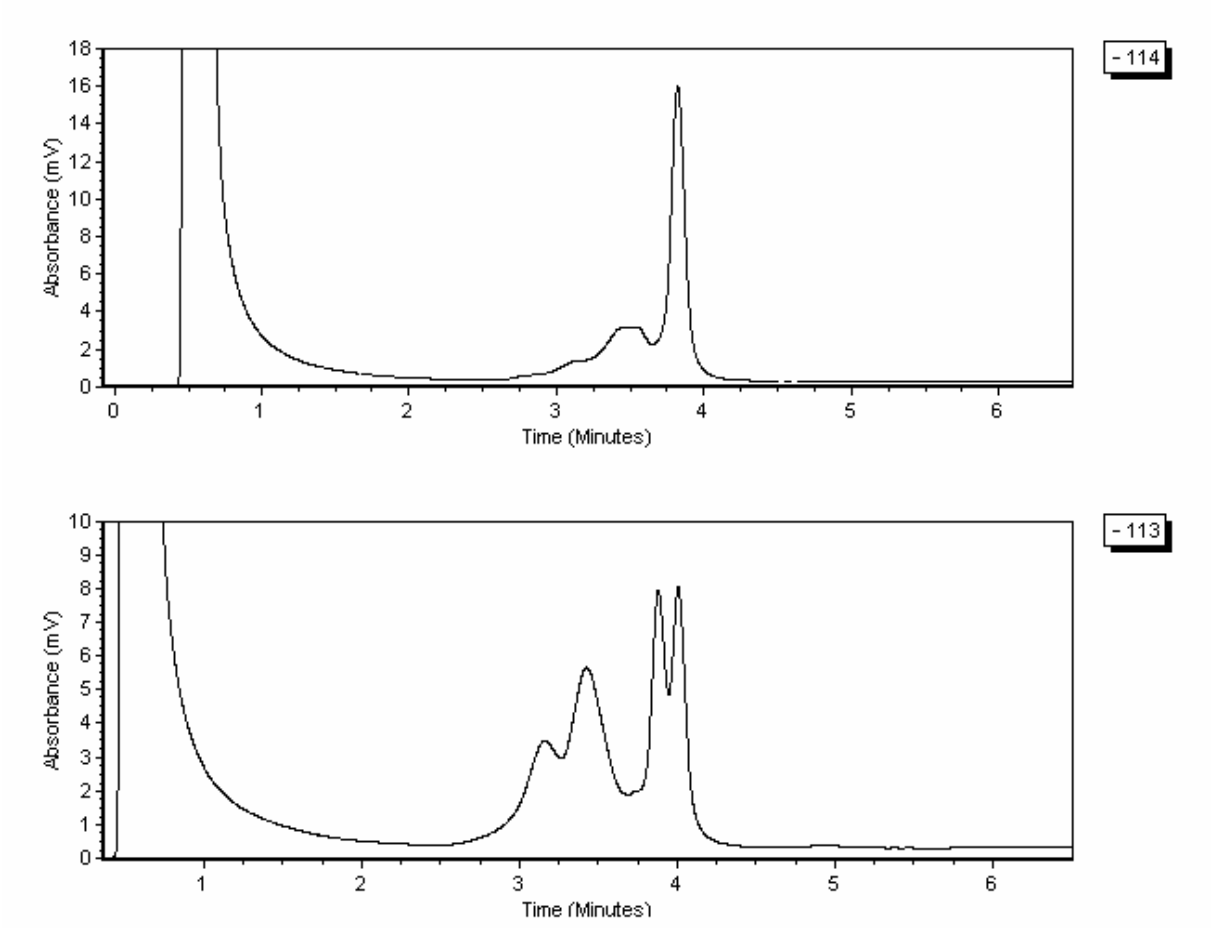

Figure 32: DHPLC chromatograms of L#114 (-82TT) and L#113 (-82TC). In the chromatogram of the heterozygous sample (bottom), additional peaks appear due to formation of heteroduplexes.

12.2. Promoter polymorphism -82T>C

To investigate whether the promoter genotype has functional consequences *in vivo*, CYP2B6 mRNA and apoprotein expression as well as enzyme activity were analyzed in the liverbank. Patients with known severe liver diseases (viral hepatitis, cirrhosis) or alcohol abuse as well as two individuals known to be induced by treatment with carbamazepine (Ketter *et al.*, 1995) were excluded from this investigation. As shown in Figure 33, median CYP2B6 mRNA expression in livers genotyped -82TC was more than doubled compared to those genotyped -82TT (20.4 vs. 9.8 a.u., p=0.007). Similarly, the median apoprotein content in livers with genotype -82TC was 66% higher compared to those genotyped -82TT (17.6 vs. 10.6 pmol/mg microsomal protein), although this difference did not reach statistical significance. However, the median CYP2B6 bupropion hydroxylase activity in microsomes of livers genotyped -82TC again was almost twofold higher than in those with genotype -82TT (201.8 vs. 106.7 pmol/mg*min, p=0.042). Unfortunately, no -82CC homozygotes could so far be identified.

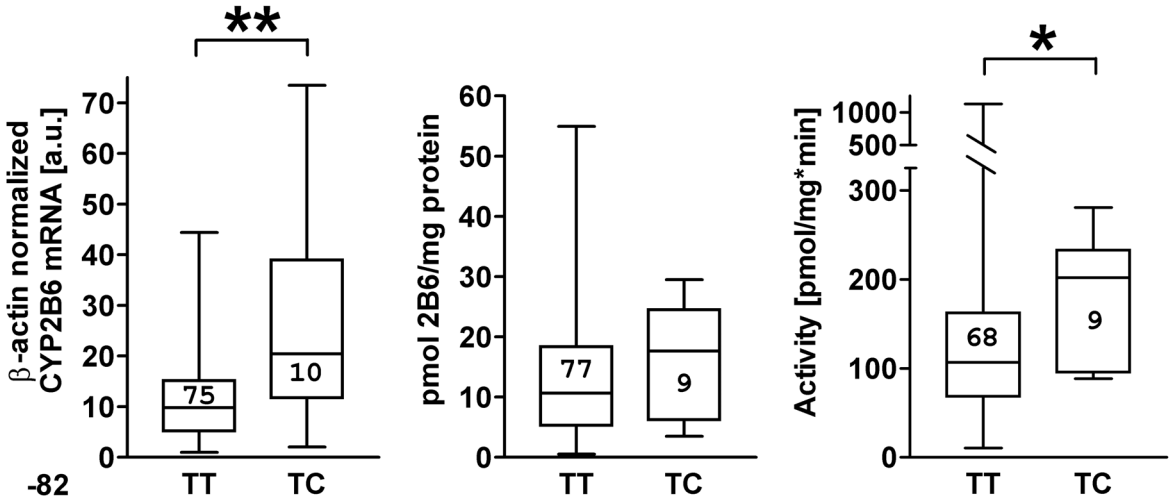

Figure 33: CYP2B6 mRNA expression in total liver RNA and apoprotein expression as well as bupropion hydroxylase activity as a selective marker for CYP2B6 catalytic activity in human liver microsomes were measured as described in "Materials and Methods". Median values in samples genotyped -82TT were compared to those with genotype -82TC. Data are presented as quartiles, and the group size is given in the respective boxplot. Statistical significance is indicated (p<0.01, *p<0.05; Mann-Whitney U-test).**

12.3. Promoter polymorphism -750T>C

In livers with genotype -82TT, we also investigated a possible influence of the -750T>C polymorphism, which disrupts a putative HNF1 binding site and which had previously been reported to be associated with decreased expression and enzyme activity (Lamba *et al.*, 2003). A trend for decreased median CYP2B6 protein content and activity dependent on the -750 genotype could indeed be confirmed (Figure 34). Thus, genotypes -750TT, TC and CC had 17.3, 10.6 and 7.3 pmol of CYP2B6 apoprotein per mg of microsomal protein, respectively, and 119.6, 107.9 and 76.6 pmol/mg*min bupropion hydroxylase activity, respectively. These differences were however not statistically significant. Furthermore, this trend was not seen in mRNA expression which was 9.1, 11.2 and 8.3 a.u. for -750TT, TC and CC groups.

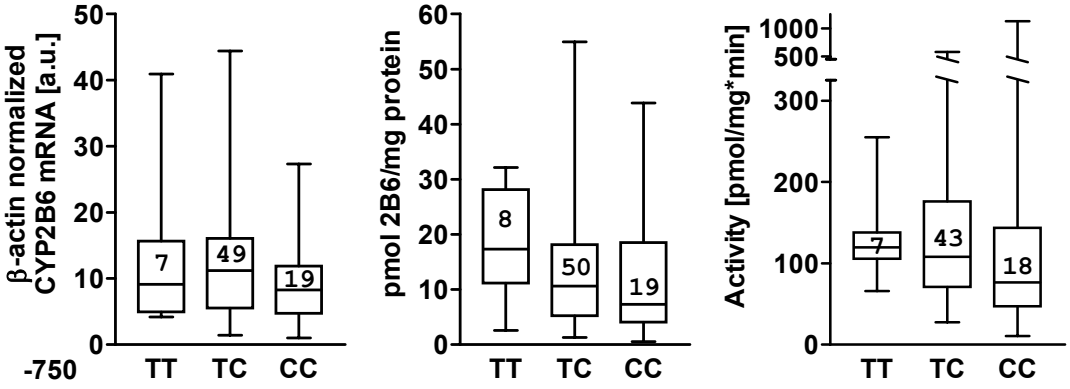

Figure 34: CYP2B6 hepatic expression and activity in relation to -750 genotype in livers with genotype -82TT. Data are presented as in Figure 33.

12.4. The *CYP2B6*6* allele

The -750T>C polymorphism has been shown to be a component of several haplotypes (Figure 15), e.g. *CYP2B6*1H* or **6B*. These haplotypes could therefore be more informative than the SNP alone because it is not known whether the SNP -750T>C or other linked mutations in the promoter or coding region influence expression. The *CYP2B6*6* allele has already been shown to decrease expression of CYP2B6 and to result in slower elimination of its substrate efavirenz (Tsuchiya *et al.*, 2004; Haas *et al.*, 2004). Indeed, significant differences between non-carriers and carriers of this allele were observed in our population (Figure 35): mRNA expression was reduced from 11.2 to 7.2 a.u. (p=0.017), and apoprotein expression was almost halved (14.2 vs. 7.3 pmol/mg microsomal protein, p=0.008). Accordingly, catalytic activity in human liver microsomes was reduced from 121.2 to 79.9 pmol/mg*min (p=0.020).

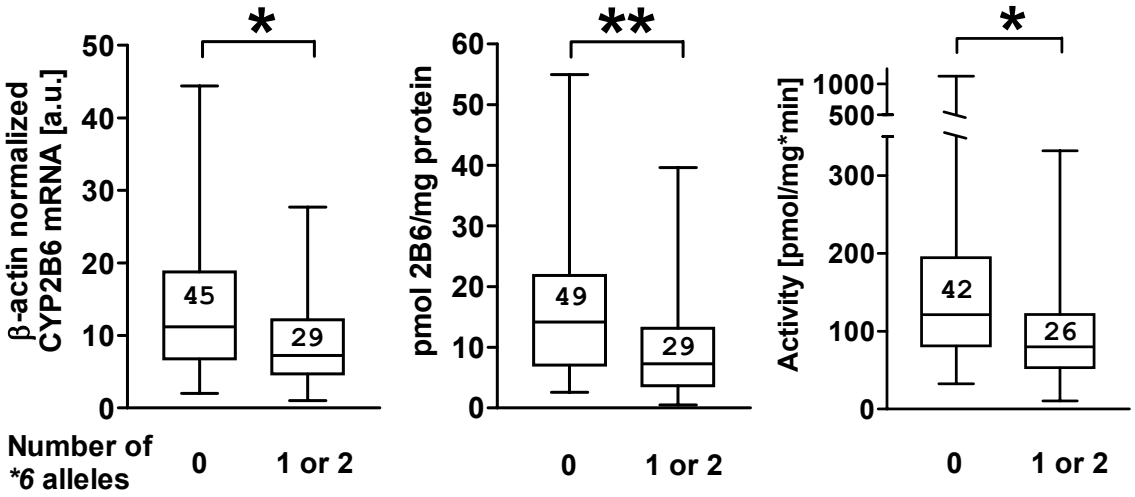

Figure 35: CYP2B6 hepatic expression and activity in relation to the number of **6* alleles. Data are presented as in Figure 33. Statistical significance is indicated (p<0.01, *p<0.05; Mann-Whitney U-test).**

13. Comparison of CYP2B promoters between different species

Nine different promoters of four different species (*Mus musculus*, *Rattus norvegicus*, *Pan troglodytes* and *Homo sapiens*) were extracted from the UCSC genome browser (available at http://www.genome.ucsc.edu/) and aligned up to -95 bp (Figure 36). Except for *Cyp2b9*, all promoters analyzed contain a C at the position corresponding to -82T in human *CYP2B6*. The transcriptional start sites in several rodent genes (*CYP2B2*, *CYP2B3*, *Cyp2b9*, *Cyp2b10* and *Cyp2b19*) were mapped at around -25 bp (Hoffmann *et al.*, 1992; Jean *et al.*, 1994; Lakso *et al.*, 1991; Honkakoski *et al.*, 1996; Suzuki *et al.*, 2002), similar to the transcriptional start site of the *CYP2B6*22* allele, whereas major transcriptional start sites of *CYP2B6*1A* were found at -53 and -54 bp (this study).

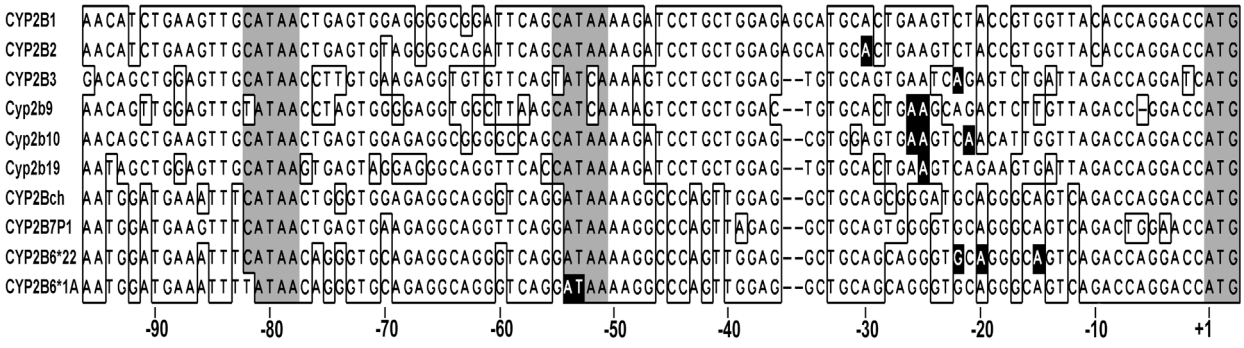

Figure 36: Alignment of *CYP2B* promoters in different species. Bases are numbered relative to the translation start ATG of *CYP2B6*. Available transcriptional start sites of

***CYP2B* genes are printed white on black (Hoffmann *et al.*, 1992; Jean *et al.*, 1994; Lakso *et al.*, 1991; Honkakoski *et al.*, 1996; Suzuki *et al.*, 2002). Putative C/EBP binding sites, TATA boxes and the translational start sites are shaded in dark grey. The orthologue to human *CYP2B6* in chimpanzee was designated *CYP2Bch*.**

14. Gene copy number of *CYP2B6*

14.1. Specificity of the assay for *CYP2B6* versus *CYP2B7P1*

To evaluate the specificity of the gene copy number assay regarding amplification of *CYP2B7P1*, plasmids containing the amplified region of *CYP2B6* and *CYP2B7P1* were used as templates for TaqMan real-time PCR. Amounts of template DNA ranged from 50,000 to 0.5 pg per reaction. As seen in Figure 37, the C_t-values for similar template amounts of the two constructs differ about 25. Assuming an amplification efficacy of 90%, the specificity of the assay for *CYP2B6* versus *CYP2B7P1* equals $1.9^{25} \approx 10{,}000{,}000 : 1$.

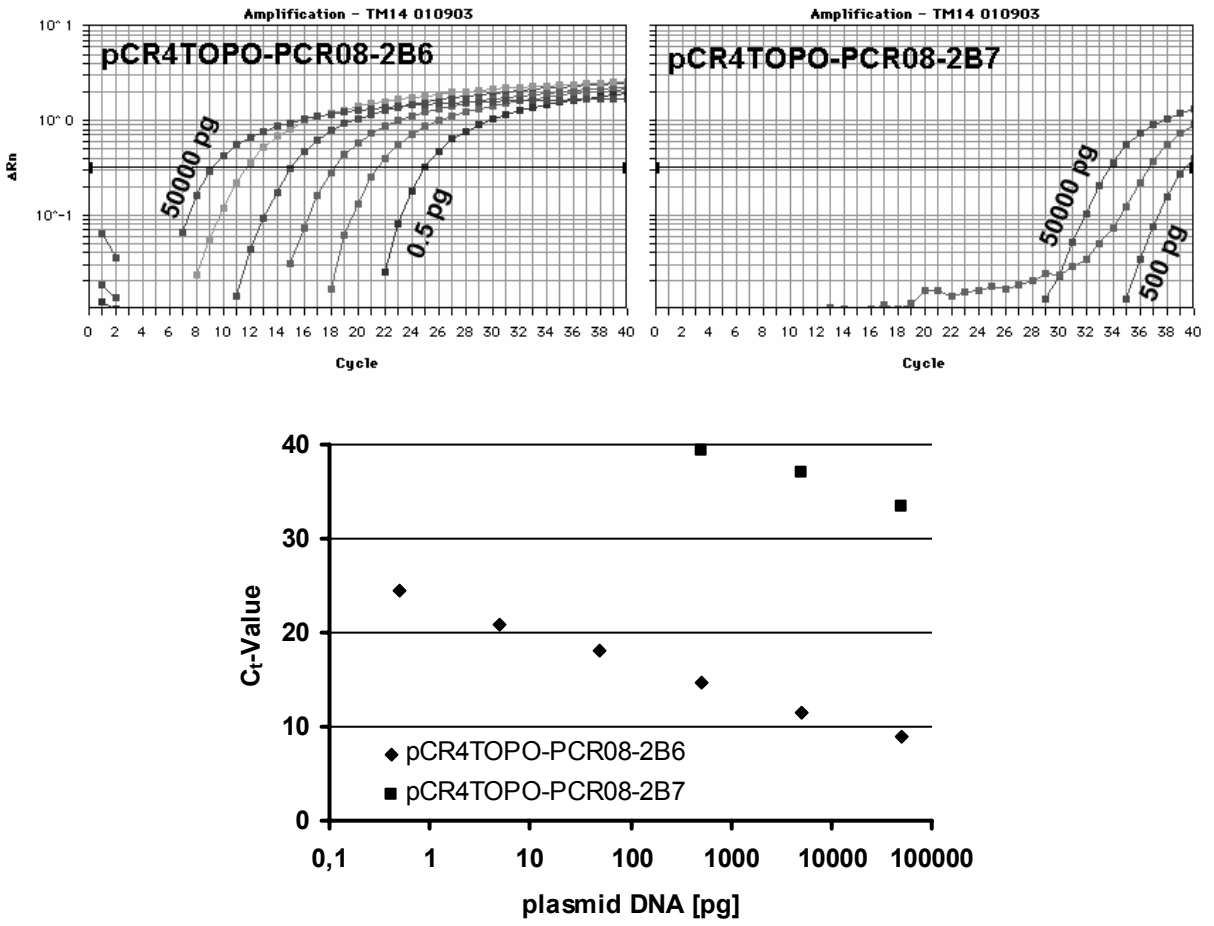

Figure 37: The specificity of the gene copy number assay for *CYP2B6* against *CYP2B7P1* was evaluated using plasmids containing the respective genomic regions as template.

14.2. Generation of standard curves

In each PCR assay, a standard curve was generated using 5 µl of serial dilutions (33.3, 16.65, 8.33, 4.16 and 2.08 ng/µl) of the same calibrator DNA corresponding to 50,000, 25,000, 12,500, 6,250 and 3,125 copies of genomic template. Figure 38 shows an example of two standard curves for the *CYP2B6* and the *ALB* gene, which had been chosen as an internal reference gene, run in a single-tube biplex assay. The difference of the C_t-values between each twofold dilution step equals approximately one.

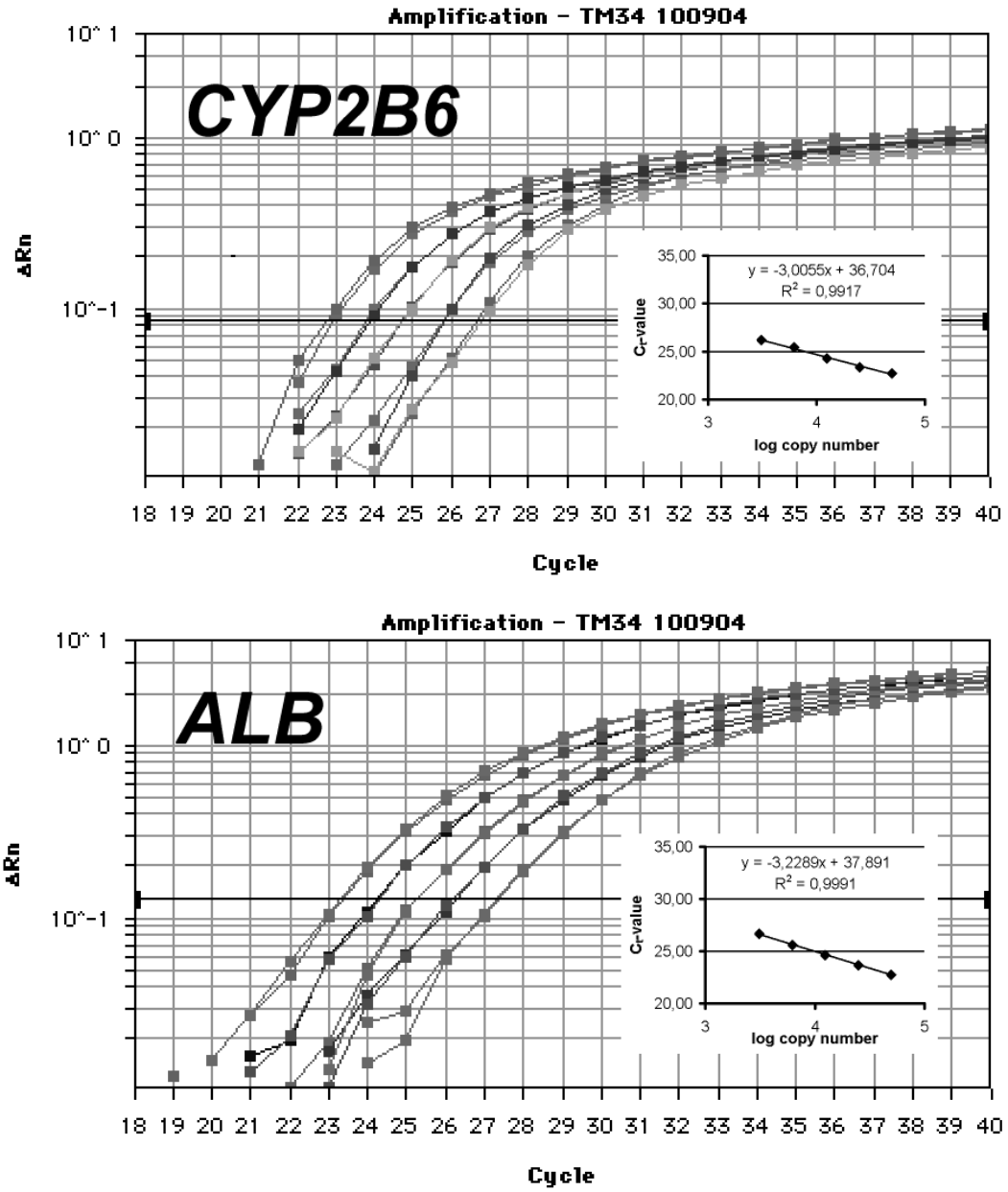

Figure 38: Standard curves for *CYP2B6* and *albumin* determined in a single-tube biplex assay. Serial two-fold dilutions of genomic DNA corresponding to 50,000 to 3,125 copies were used as template.

14.3. Copy number determination in a panel of DNA samples

30 DNA samples from the liverbank (IKP148) with low or high CYP2B6 expression were selected to be tested for *CYP2B6* gene deletions or duplications. Also, 94 additional randomly chosen samples were screened. Samples were assayed up to five times using a TaqMan real-time PCR-based gene copy number assay. The mean normalized haploid *CYP2B6* copy number was 0.9059 with a standard deviation of 0.1202 (Figure 39). The three lowest values were 0.6996 (L#129), 0.6418 (L#133) and 0.5519 (L#116), and the remaining values ranged from 0.7512 to 1.250.

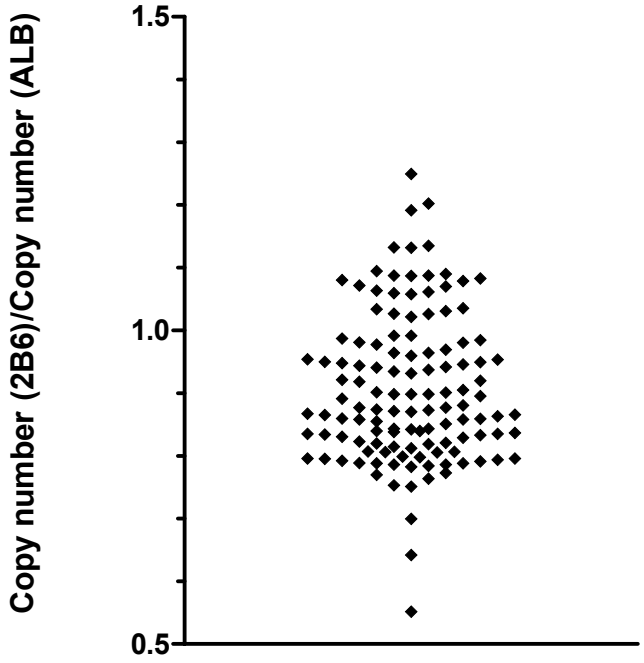

Figure 39: The gene copy number of *CYP2B6* in 124 DNA samples was determined as described in "Materials and Methods". The normalized haploid gene copy number of *CYP2B6* is given.

IV DISCUSSION

1. Influence of promoter polymorphisms on *CYP2B6* expression

Hepatic expression of CYP2B6 is highly variable and may depend on many exogenous and endogenous factors including drug exposure, diet, sex, age, and various physiologic and genetic factors. In this work, the contribution of common promoter variants to this variability was investigated by using reporter gene assays and studies in human liver samples and it was found that the mutation -82T>C is associated with significantly increased expression and function of CYP2B6 even in heterozygous carriers. Although two previous studies have addressed the potential impact of *CYP2B6* promoter variants, they used only descriptive methods to relate haplotypes to liver expression and activity, and no direct attempts were made to investigate their functional relevance (Lamba *et al.*, 2003; Hesse *et al.*, 2004). This study is based on a comprehensive haplotype analysis using 2.3 kb of promoter sequence data and genotypes for all common nonsynonymous SNPs from 96 individuals of Caucasian origin (49 males/47 females). One novel SNP (-801G>T) as well as four novel alleles (**4D*, **5C*, **6C* and **22*) were identified and the presence and frequency of the major haplotypes present among Caucasians was confirmed. The three variant alleles **1J*, **1N* and **22* were selected to be represented by reporter gene constructs because they comprised the promoter SNPs with frequencies over 3%. When the plasmids pGL3-2B6(-2033)WT, A2, A3 and A4 were transfected into three liver cell types (HepG2, primary rat and human hepatocytes), only the A3 construct showed increased transcriptional activity (Figure 16). In HepG2 cells, transcriptional activity of the wild type construct was not distinguishable from empty control vector pGL3-Basic, consistent with the fact that these cells do not express endogenous CYP2B6 (Gervot *et al.*, 1999). Although we can not exclude the possibility that individual SNPs of the constructs with unchanged activity (A2 and A4) may have an effect on transcription, these would be expected to be functionally compensatory in their allelic combinations.

2. Pleiotropic effects of SNP -82T>C

The considerably increased transcription rate of the A3-construct representing the **22* allele was entirely attributable to the TATA box disrupting SNP -82T>C. This result seemed initially quite surprising, because known TATA box polymorphisms appear to decrease

transcription rate, as seen for example in the *UGT1A1*28* or *CYP2A6*9* alleles (Bosma *et al.*, 1995; Pitarque *et al.*, 2001). Our detailed promoter analysis revealed an unusual and unique scenario that appears to take place when -82T is changed into -82C (Figure 40): The TATA box at -82 bp is predominantly used for transcription of the wild type *CYP2B6* gene, as shown by mapping the transcriptional start sites at around -54 bp using two independent methods (Figure 27, Figure 30). As indicated by electrophoretic mobility shift assay, the mutation -82T>C seems to decrease binding of TBP while simultaneously increasing affinity for C/EBP. The enhanced binding of C/EBP would then promote usage of the alternative noncanonical TATA box at -55 bp, generating shorter transcripts initiated from transcriptional start sites around -20 bp in both transfected cells and human liver (Figure 27, Figure 29). The observation that the shorter transcripts originating from the mutant promoter by far dominate over the longer wild type transcripts in liver RNA of a heterozygous individual as well as the increased mRNA expression in carriers of the -82T>C mutation strongly support the higher transcription rate of the **22* allele also *in vivo*.

Figure 40: Model of the mechanism of the -82T>C polymorphism. The SNP -82T>C converts the TATA box used by the human gene at -82 bp to a functional C/EBP binding site. Bound C/EBP supports binding of TBP to the alternative noncanonical TATA box at -55 bp, resulting in enhanced transcription from a transcriptional start site further downstream.

3. *CYP2B6*22*: a gain-of-function allele

Using a collection of human liver samples, an impact of the mutation -82T>C on phenotype could be clearly demonstrated (Figure 33). Median hepatic CYP2B6 mRNA expression was more than doubled in heterozygous carriers of the -82T>C mutation compared to -82TT individuals (20.4 vs. 9.8 a.u., p=0.007); accordingly, median apoprotein content was 66% higher (17.6 vs. 10.6 pmol/mg microsomal protein). The increased promoter activity even

became manifest in median bupropion hydroxylase activity as a selective marker of human CYP2B6 catalytic activity (Faucette *et al.*, 2000), which was also nearly doubled in the -82TC group (201.8 vs. 106.7 pmol/mg*min, p=0.042). However, a considerable variability within the TT and TC groups suggests the involvement of other factors than the -82 polymorphism. These could be either induction phenomena or additional genetic factors, as only heterozygous carriers of the mutation could be included in this study. Indeed, the lowest mRNA expression and enzyme activity in the -82TC group was found in a carrier of the **5* allele which had been shown to result in decreased expression (Lang *et al.*, 2001). Nonetheless, these data demonstrate a close concordance between the *in vitro* reporter gene experiments and hepatic expression *in vivo* and characterize the novel *CYP2B6*22* allele as a gain-of-function allele. Promoter mutations that increase transcriptional activity have already been described, for example the *UGT1A9*22* allele (Yamanaka *et al.*, 2004) or a C>G polymorphism in the *CYP7B1* promoter (Jakobsson *et al.*, 2004). However, no TATA box mutations resulting in enhanced transcription or relocation of the transcriptional start site have been described so far. The clinical significance of this allele as well as its occurrence in other populations should be further investigated as it may result in a CYP2B6 "ultrarapid metabolizer" phenotype. In the case of CYP2D6, the well characterized and clinically relevant ultrarapid metabolizer phenotype results from a heterozygous gene duplication which increases gene dose by just 50% (Ingelman-Sundberg, 1999). Clinical implications of *CYP2B6*22* may include, for example, enhanced bioactivation of cyclophosphamide, shortened duration of action of propofol, and treatment failure in HIV therapy with efavirenz.

4. Inter-species comparison of *CYP2B* promoters

The comparison of different mammalian *CYP2B* promoters and transcriptional start sites (Figure 36) further supports the model presented in Figure 40 and reveals further insights into evolutionary relationships. Except for *Cyp2b9*, all promoters analyzed contain a C at the position corresponding to -82T in human *CYP2B6*, and in the rat *CYP2B1* promoter, this region was indeed characterized as a functional C/EBP site (Park and Kemper, 1996). The transcriptional start sites in several rodent genes (*CYP2B2*, *CYP2B3*, *Cyp2b9*, *Cyp2b10* and *Cyp2b19*) were mapped at around -25 bp (Hoffmann *et al.*, 1992; Jean *et al.*, 1994; Lakso *et al.*, 1991; Honkakoski *et al.*, 1996; Suzuki *et al.*, 2002), indicating usage of the respective noncanonical TATA boxes at -55 bp similar to the human *CYP2B6*22* allele. According to this analysis, the mouse *Cyp2b9* gene would however be expected to use the TATA box at -82 bp and initiate transcription around -54 bp. That this is not the case suggests that the C/EBP

site of this gene is conserved despite its -82T genotype. Apparently, -82T is compatible with C/EBP binding in the murine but not in the human sequence context, which shows an additional sequence difference at -83 bp. Interestingly, the murine -83G is compatible with the C/EBP consensus sequence, whereas the human -83T is not. Remarkably, even in chimpanzee and in the paralogous pseudogene *CYP2B7P1* the -82C is found, suggesting that the disruption of the putative C/EBP binding site occurred after the speciation of *Homo* and *Pan* and after the duplication of the *CYP2B* gene in human on the *CYP2* gene cluster on chromosome 19 (Hoffman *et al.*, 2001). This would indicate that the -82C may represent the ancestral state. From an evolutionary point of view, it may be speculated that a high constitutive activity may have been disadvantageous due to the known promutagen-activating properties of CYP2B6 (Code *et al.*, 1997). It remains unclear why the human GATA motif at -55 bp does not act as a functional TATA box in the absence of the mutation -82T>C, albeit exhibiting much stronger binding to TBP than the TATA motif at -82 bp in electrophoretic mobility shift assay. Probably the flanking sequences of the GATA motif at -55 bp are not as suitable for binding other members of the Polymerase II complex as those in the TATA box at -82 bp and therefore require stabilization by C/EBP to be functional.

5. Extension of the *CYP2B6*22* allele into the *CYP2A6* locus

A haplotype-phenotype association study was conducted for the *CYP2A6* gene by Haberl *et al.* at EPIDAUROS AG, Bernried, Germany. In this study, five of six samples heterozygous for a certain *CYP2A6* haplotype cluster (haplotypes 10,14,15, and 24), and only these, were also carriers of the *CYP2B6*22* allele (Haberl *et al.*, submitted). This suggests strong linkage of these two haplotypes and the existence of a haplotype block that extends over 150 kb from the 5'-region of *CYP2B6* into exon 9 of *CYP2A6* (Figure 2). A similar example has been described at the *UGT1* locus on chromosome 2 where the frequent co-occurrence of the alleles *UGT1A1*28, 1A6*2* and *1A7*7* (haplotype II) in Caucasians and Egyptians (Kohle *et al.*, 2003) defined a haplotype block with a range of at least 90 kb.

6. Expression of the pseudogene *CYP2B7P1*

Pseudogenes are complete or partial copies of genes that are unable to code for functional polypeptides, and in the human genome, already 20,000 pseudogenes have been identified (Torrents *et al.*, 2003). Recent works have described the expression of the pseudogene *CYP2D7* mRNA in liver (Endrizzi *et al.*, 2002) and the presence of a functional variant of this pseudogene in certain individuals (Pai *et al.*, 2004). Another publication revealed an

important role of an expressed pseudogene in regulation of mRNA stability of its homologous coding gene (Hirotsune *et al.*, 2003). Therefore it would be also interesting to know whether the pseudogene *CYP2B7P1* is expressed in liver. When determining the transcriptional start site of *CYP2B6* in liver with the GeneRacer Kit (Chapters II.9. and III.9.), the primer for the amplification of *CYP2B6* 5'-cDNA ends was designed to be 100% identical with the corresponding region of the *CYP2B7P1* cDNA, allowing transcripts of this gene to be analyzed simultaneously. From 34 clones sequenced, none was derived from a *CYP2B7P1* transcript, supporting the notion that this pseudogene plays a minor role in the liver transcriptome. Of course this method does not measure *CYP2B7P1* expression in a quantitative manner, and there is evidence in the literature that this pseudogene is indeed expressed in liver, as shown by isolation of a *CYP2B7P1*-derived cDNA clone from human liver RNA (Yamano *et al.*, 1989). In lung, *CYP2B7P1* seems to be even the dominant isoform (Gervot *et al.*, 1999; Czerwinski *et al.*, 1994). It would be interesting to know how the two human *CYP2B* genes are regulated in this tissue-specific manner.

7. The putative HNF1 binding site at -750 bp

As previous work suggested an impact of the common SNP -750T>C (which was predicted to disrupt a putative HNF1 binding site) on CYP2B6 expression (Lamba *et al.*, 2003; Hesse *et al.*, 2004), the influence of this polymorphism on phenotype was also investigated. For individuals genotyped -82TT, a trend for lower CYP2B6 enzyme activity and protein expression was observed dependent on the mutation -750T>C, although not statistically significant (Figure 34). Per contra, a decrease in mRNA levels in relation to -750 genotype was not observed. As the SNP -750T>C is a component of several haplotypes (**1H*, **6B* etc.), it is possible that not this particular SNP itself but one of the alleles that include this mutation alter expression. Indeed, when comparing carriers and non-carriers of the **6* allele which includes the -750T>C mutation (Figure 35), significant differences at all three levels of expression were observed. This shows that in certain cases haplotypes can be more informative than SNPs, in particular when a mutation is part of different haplotypes.

Further experiments were conducted to determine a possible role for HNF1 in the regulation of CYP2B6. In electrophoretic mobility shift assay, a weak binding of *in vitro* translated murine HNF1α to the promoter region around -750 bp was visible, which disappeared in the presence of the mutation -750T>C. In contrast, no difference between wild type promoter and the construct carrying this single mutation was observed in our reporter gene experiments

(Figure 16), neither in primary hepatocytes that are likely to express HNF1 nor in cotransfection experiments with expression plasmids for murine HNF1α and DCoH (Figure 26). It is unlikely that sequence differences between murine and human HNF1α are the reason for the lack of transactivation, as the protein sequences are 100% identical in the DNA binding domain (data not shown), but there are other possible explanations for these ambiguous results. First, the structural requirements of HNF1 activation might not be met in the reporter gene assays due to the lack of chromatin or insufficient coverage of the required DNA region by the reporter gene plasmids. Second, the absence of essential cofactors or the presence of inhibitory factors could prevent transactivation by HNF1. Another reason might be that the affinity of HNF1 to the *cis*-element is not high enough to generate considerable transactivation. In any case, these results can not definitely rule out an involvement of HNF1 in CYP2B6 transcription, and further studies would be necessary to fully elucidate the relevance of this transcription factor and the -750T>C polymorphism for the regulation of *CYP2B6*.

8. Constitutive regulation of *CYP2B6* by C/EBP

Previous work suggested an important role of C/EBP in the regulation of *CYP2B6*, as reexpression of C/EBP in HepG2 cells by stable transfection induces expression of CYP2B6 (Jover *et al.*, 1998). In this work, it could be shown that *CYP2B6* promoter constructs of different sizes are transactivated by cotransfection of C/EBPβ (Figure 24). The extent of the transactivation gradually increased with increasing length of the included promoter fragment, suggesting the presence of multiple C/EBP binding sites in the promoter. As 245 bp of the CYP2B6 promoter were sufficient to observe transactivation by C/EBPβ in reporter gene assays, this particular region was further investigated. Two binding sites were predicted by *in silico* analysis, and for one of these at -177 bp, binding of C/EBP could indeed be confirmed by electrophoretic mobility shift assay. Interestingly, a higher score denoting higher similarity to the consensus sequence was assigned to the putative site at -208 bp, which did not bind C/EBP in electrophoretic mobility shift assay. This shows that even for well characterized transcription factors like the C/EBP family, *in silico* prediction still fails to deliver reliable results, and experimental verification remains mandatory. To eliminate the putative C/EBP binding site in pGL3-2B6(-244) at -177 bp, a reporter plasmid containing only 160 bp of the promoter was generated. This construct was not expected to be transactivated by C/EBP unless the mutation -82T>C creates a C/EBP binding site; however, both plasmids pGL3-2B6(-160)WT and -82C were transactivated by C/EBPβ to the same extent (data not shown)

suggesting the presence of another C/EBP binding site in the proximal region close to the TATA box at -82.

9. Transactivation by C/EBPβ-LIP

C/EBPβ-LIP represents an isoform of human C/EBPβ that is able to bind DNA and to form dimers with other C/EBP isoforms, but lacks the amino-terminal activation domain (Jover *et al.*, 2002). Therefore, it was expected to act as a transcriptional antagonist of endogenous C/EBPβ-LAP (the "full-length" form) or C/EBPα when transfected into human hepatocytes. However, when cotransfected with reporter gene plasmids containing the *CYP2B6* promoter, the transcriptional activity of these constructs was unexpectedly increased in human hepatocytes by C/EBPβ-LIP, albeit to a much lesser extent than by C/EBPβ-LAP. This unanticipated activating effect of C/EBPβ-LIP was also observed with *CYP3A4* promoter constructs in HeLa cells (R. Jover, personal communication). These findings might be explained by a residual transactivating activity of C/EBPβ-LIP, although this has not been reported previously. There is also the possibility that DNA-bound LIP improves accessibility for other transcription factors to the promoter. Third, the dimerization or DNA binding domain of C/EBPβ-LIP could be able to recruit other transactivating factors when bound to DNA. These transcription factors would then increase transcriptional activity independent of the activating domain of C/EBPβ.

10. Detection of a genotyping error by HWE testing

As shown previously, deviation from Hardy-Weinberg equilibrium of a genotype distribution can be indicative for genotyping errors (Hosking *et al.*, 2004), which in turn can give rise to false positive results in association studies (Xu *et al.*, 2002). In the course of this work, erroneous genotyping of the SNP c.1459C>T in exon 9 of the *CYP2B6* gene by the PCR-RFLP assay described by Lang *et al.* (2001) was suspected as the observed genotype distribution strongly deviated from HWE. Six individuals of the liverbank genotyped c.1459TT were reanalyzed using an alternative PCR-RFLP assay described in this work. The TT genotype was confirmed for only one sample, whereas the other five were genotyped CT. The reason for the erroneous genotyping was further analyzed. It could be shown by sequencing and PCR-RFLP that the binding site for primer CYP2B6-9F in intron 8 is polymorphic due to the contained SNP g.24322C>T (dbSNP: rs7259965) which was furthermore shown to be linked to the *CYP2B6*6* allele. This resulted in ambiguous genotyping in samples with genotype *CYP2B6*5/*6* (Figure 41): Amplification of the exon 9

wild type product derived from the **6* allele was less efficient due to impaired binding of the forward primer. Therefore, the wild type product was underrepresented in the PCR product mixture, as amplification of the mutated exon 9 on the **5* allele was not affected. The subsequent analysis of the PCR product thus showed pseudohomozygosity for c.1459T, both in the RFLP and in the sequencing chromatogram.

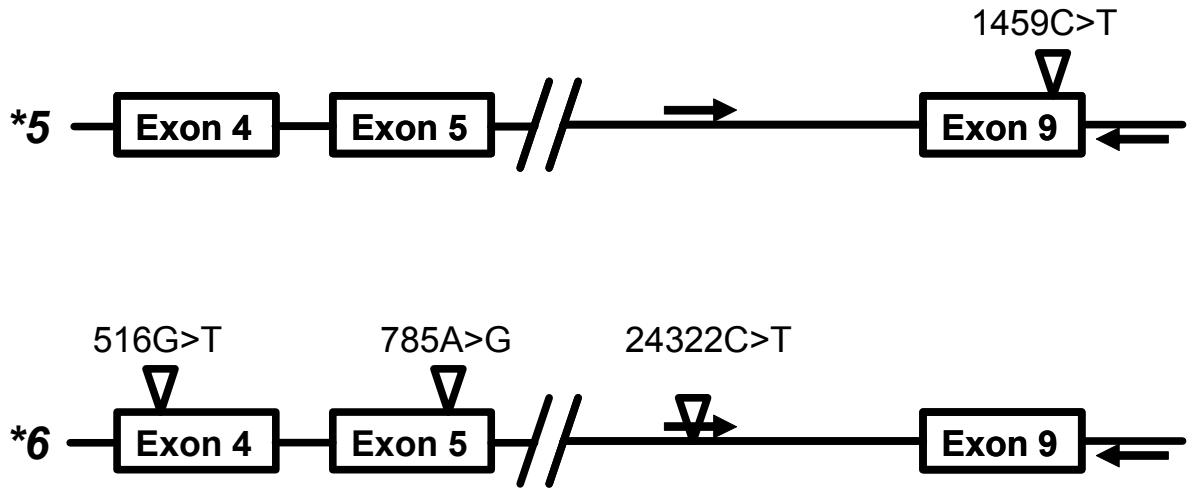

Figure 41: False genotyping of the exon 9 SNP c.1459C>T in individuals with genotype *CYP2B6*5/*6* is caused by impaired binding of primer CYP2B6-9F on the **6* allele. Preferential amplification of the mutated exon 9 product from the **5* allele results in pseudohomozygosity for the mutation c.1459C>T.

These findings emphasize the usefulness of Hardy-Weinberg equilibrium testing when assessing the plausibility of genotyping results in randomly selected populations. Also, the database of single nucleotide polymorphisms (dbSNP, http://www.ncbi.nlm.nih.gov/SNP/) can serve as a helpful tool to avoid polymorphic sites in primer design. In dbSNP build 122, the mean spacing of SNPs was 360 bases, therefore, assuming a mean primer length of 25 bp, about 7% (25/360) of chosen primers can be expected to bind to polymorphic sites in the genome. This could be avoided by checking the dbSNP database and redesign primers that would bind to polymorphic sites.

11. *CYP2B6*7*: An artifact?

The *CYP2B6*7* allele was first described in 2001 by Lang *et al*. In this study, 215 Caucasian individuals were genotyped for several exonic mutations by PCR-RFLP, including the exon 9 SNP c.1459C>T. As shown above, the method used yields incorrect results in **5/*6* individuals, erroneously assigning them a TT genotype instead of CT. In 215 individuals, the

c.1459TT genotype was only observed either alone (3 individuals, **5*/**5*) or in combination with the heterozygous mutations c.516G>T and c.785A>G of the *CYP2B6*6* allele (13 individuals, assigned genotype: **5/*7*). It is likely that the latter samples were actually heterozygous for c.1459C>T, defining their genotype as **5*/**6* instead of **5*/**7*. The fact that no sample was genotyped **5*/**6* further favors this hypothesis as the expected number of such individuals in this study would have been 12 (=2*p(**6*)*p(**5*)*N). Furthermore, the analysis of cDNA from a putative carrier of the *CYP2B6*7* allele assumed homozygosity for c.1459TT and did not further test for the presence of this mutation in those cDNA clones carrying the mutations c.516G>T and c.785A>G. There have been other population studies determining frequencies for *CYP2B6* alleles (Hiratsuka *et al.*, 2002; Kirchheiner *et al.*, 2003; Lamba *et al.*, 2003; Xie *et al.*, 2003; Jacob *et al.*, 2004), and even a long-PCR-based method has been established to directly detect the **7* allele (Futatsugawa *et al.*, 2004). However, none of these works except one (Hesse *et al.*, 2004) could unambiguously identify a carrier of the *CYP2B6*7* allele. But, as Hesse *et al.* used the same primers as Lang *et al.* for amplification of exon 9, the single individual identified as carrier of the alleles **5*/**7* was most likely in fact carrier of **5*/**6*. Taken together, these facts indicate that the allele *CYP2B6*7* is an artifact caused by faulty genotyping of the SNP c.1459C>T in **5*/**6* individuals.

12. Possible deletions of *CYP2B6*

Using a TaqMan real-time PCR based assay, the gene copy numbers of *CYP2B6* and *albumin* as reference gene were determined in 124 DNA samples. The mean normalized haploid *CYP2B6* gene copy number was 0.9059, somewhat lower than the expected value of 1.0. This indicates that amplification efficiency of the *CYP2B6* fragment might be lower or more dependent on DNA quality than that for *albumin*. The standard deviation of 0.12 is comparable to that obtained by Schaeffeler *et al.*, 2003, who assessed gene copy number of *CYP2D6*. When taking out the three lowest values, numbers ranged from 0.75 to 1.25, also similar to the distribution seen in the group with two gene copies of *CYP2D6* in the publication of Schaeffeler *et al.* There was no evidence for gene duplications, as the highest haploid gene copy number was 1.25, but three values were reproducibly lower than 0.75 suggesting the presence of only one gene copy of *CYP2B6* in these samples. These findings need however to be confirmed using alternative methods like Southern blotting or long PCR.

V APPENDIX

1. Genotyping results for the SNP -82T>C in the *CYP2B6* gene

L#	-82	L#	-82	L#	-82	L#	-82
112	TT	152	TT	192	TT	232	TT
113	TC	153	TT	193	TT	233	TT
114	TT	154	TT	194	TT	234	TT
115	TT	155	TT	195	TT	235	TT
116	TT	156	TT	196	TT	236	TT
117	TT	157	TT	197	TT	237	TT
118	TT	158	TT	198	TT	238	TT
119	not done	159	TT	199	TT	239	TT
120	TT	160	TT	200	TT	240	TT
121	TT	161	TT	201	TT	241	TT
122	TT	162	TT	202	TT	242	TT
123	TT	163	TT	203	TT	243	TT
124	not done	164	TT	204	TT	244	TT
125	TT	165	TT	205	TT	245	TT
126	TT	166	TT	206	TT	246	TT
127	TT	167	TT	207	TT	247	TT
128	TT	168	TT	208	TT	248	TT
129	TT	169	TT	209	TT	249	TT
130	TT	170	TT	210	TT	250	TT
131	TT	171	TT	211	TT	251	TT
132	TT	172	TT	212	TT	252	TT
133	TT	173	TT	213	TC	253	TT
134	TT	174	TT	214	TT	254	not done
135	TT	175	TT	215	TT	255	TT
136	TT	176	TT	216	TT	256	TT
137	TT	177	TT	217	TT	257	TT
138	TT	178	TT	218	not done	258	TT
139	TT	179	TT	219	TT	259	TT
140	TC	180	TT	220	TT	260	TT
141	TC	181	TT	221	TT	261	TT
142	TT	182	TT	222	TT	262	TT
143	TT	183	not done	223	TT	263	TT
144	TT	184	TT	224	TT	264	TC
145	TT	185	TT	225	TT	265	TT
146	TT	186	TT	226	TT	266	TT
147	TT	187	TT	227	TT	267	TT
148	TT	188	TT	228	not done	268	TT
149	TT	189	TT	229	TT	269	TT
150	TT	190	TT	230	TT	270	TT
151	TT	191	not done	231	TT	271	TT

L#	-82	L#	-82	L#	-82	L#	-82
272	TT	280	TT	288	TT	296	TT
273	TT	281	TT	289	TT	297	TT
274	TT	282	TT	290	TT	298	TT
275	TT	283	TT	291	TT	299	TT
276	TT	284	TT	292	TT	300	TT
277	TT	285	TT	293	TT		
278	TT	286	TT	294	TT		
279	TT	287	TC	295	TT		

Table 9: DHPLC genotyping results for SNP -82T>C

2. Genotyping results for the SNP -2320T>C in the *CYP2B6* gene

L#	-2320	L#	-2320	L#	-2320	L#	-2320
1	TT	29	CC	57	TT	85	TC
2	TT	30	TC	58	TC	86	TT
3	TT	31	TT	59	TT	87	CC
4	TC	32	TT	60	TC	88	TT
5	not done	33	TT	61	TT	89	TT
6	TC	34	TT	62	TC	90	TT
7	TC	35	TT	63	TT	91	TT
8	TT	36	TC	64	TT	92	TC
9	TT	37	TT	65	TC	93	TT
10	TT	38	TT	66	TC	94	TC
11	TT	39	TT	67	CC	95	CC
12	TC	40	CC	68	TC	96	TT
13	TT	41	CC	69	TC	97	TT
14	TC	42	TC	70	TC	98	TC
15	TC	43	TC	71	not done	99	TT
16	TT	44	TC	72	TT	100	TC
17	TC	45	TT	73	TC	101	TC
18	TC	46	TC	74	TC	102	TT
19	TT	47	TC	75	TT	103	TC
20	TT	48	TT	76	TC	104	TC
21	TC	49	TT	77	TT	105	TT
22	TC	50	TT	78	TT	106	CC
23	TT	51	TC	79	TT	107	CC
24	TT	52	TT	80	TC	108	TT
25	TT	53	TC	81	TT	109	TC
26	TC	54	TC	82	TT	110	TC
27	TC	55	TT	83	TC	111	CC
28	TC	56	TC	84	TC	112	TC

Table 10: RFLP genotyping results for SNP -2320T>C.

3. Results of quantitative real-time PCR

L#	CYP2B6 mRNA	CYP2B6 mRNA rel to L#110	β-actin	CYP2B6 mRNA normalized to β-actin	CYP2B6 mRNA normalized to β-actin rel to L#48
1					
2	4.33E-04	25.471	469.52	9.222E-07	7.027
3	1.75E-04	10.294	55.54	3.151E-06	24.010
4	1.48E-03	87.059	1161.24	1.274E-06	9.712
5	9.47E-04	55.706	644.16	1.470E-06	11.202
6	1.38E-04	8.118	105.48	1.308E-06	9.969
7	4.69E-04	27.588	287.42	1.632E-06	12.434
8	5.62E-04	33.059	592.35	9.488E-07	7.230
9					
10					
11					
12	1.11E-03	65.294	800.87	1.386E-06	10.561
13	4.47E-04	26.294	296.19	1.509E-06	11.500
14	5.59E-04	32.882	339.45	1.647E-06	12.548
15	5.34E-04	31.412	291.43	1.832E-06	13.962
16	5.21E-04	30.647	257.86	2.020E-06	15.396
17	8.19E-05	4.818	69.41	1.180E-06	8.991
18	5.32E-04	31.294	196.47	2.708E-06	20.633
19	1.21E-03	71.176	332.93	3.634E-06	27.694
20	3.28E-04	19.294	486.48	6.742E-07	5.138
21	2.15E-04	12.647	167.21	1.286E-06	9.798
22	3.95E-04	23.235	851.49	4.639E-07	3.535
23	5.09E-04	29.941	425.46	1.196E-06	9.116
24	3.23E-04	19.000	467.76	6.905E-07	5.262
25	2.44E-04	14.353	821.32	2.971E-07	2.264
26	1.41E-04	8.294	276.04	5.108E-07	3.892
27	1.02E-03	60.000	234.96	4.341E-06	33.080
28	4.75E-04	27.941	246.14	1.930E-06	14.705
29	2.25E-03	132.353	627.13	3.588E-06	27.339
30	9.93E-04	58.412	415.31	2.391E-06	18.219
31	1.69E-04	9.941	316.60	5.338E-07	4.068
32	7.55E-04	44.412	587.75	1.285E-06	9.788
33	6.09E-04	35.824	344.20	1.769E-06	13.482
34	4.81E-04	28.294	537.31	8.952E-07	6.821
35	7.15E-03	420.588	1187.30	6.022E-06	45.888
36	6.02E-05	3.541	113.45	5.306E-07	4.043
37	5.34E-05	3.141	103.86	5.142E-07	3.918
38	2.54E-04	14.941	378.87	6.704E-07	5.109
39	5.30E-04	31.176	962.79	5.505E-07	4.195
40					
41	1.22E-03	71.765	968.33	1.260E-06	9.600
42					

L#	CYP2B6 mRNA	CYP2B6 mRNA rel to L#110	β-actin	CYP2B6 mRNA normalized to β-actin	CYP2B6 mRNA normalized to β-actin rel to L#48
43	3.81E-04	22.412	191.94	1.985E-06	15.126
44					
45					
46	2.23E-04	13.118	351.41	6.346E-07	4.836
47	4.19E-04	24.647	201.14	2.083E-06	15.873
48	6.96E-05	4.094	530.35	1.312E-07	1.000
49	6.79E-03	399.412	791.34	8.580E-06	65.382
50	2.24E-04	13.176	356.69	6.280E-07	4.785
51	1.13E-04	6.647	128.07	8.823E-07	6.723
52	6.09E-04	35.824	550.65	1.106E-06	8.427
53	2.65E-04	15.588	249.34	1.063E-06	8.099
54	1.16E-03	68.235	421.85	2.750E-06	20.953
55	1.59E-04	9.353	74.61	2.131E-06	16.239
56	6.04E-04	35.529	238.80	2.529E-06	19.273
57	7.19E-04	42.294	409.37	1.756E-06	13.383
58					
59	9.56E-04	56.235	761.02	1.256E-06	9.572
60					
61					
62	1.14E-04	6.706	82.65	1.379E-06	10.510
63	1.56E-04	9.176	168.82	9.241E-07	7.041
64	7.65E-04	45.000	142.44	5.371E-06	40.924
65	3.39E-04	19.941	126.10	2.688E-06	20.485
66					
67	3.25E-04	19.118	208.65	1.558E-06	11.869
68	1.31E-04	7.706	705.90	1.856E-07	1.414
69	4.85E-04	28.529	300.83	1.612E-06	12.285
70	4.12E-04	24.235	153.41	2.686E-06	20.464
71					
72	1.11E-03	65.294	407.02	2.727E-06	20.781
73	9.28E-05	5.459	127.36	7.286E-07	5.552
74					
75	1.02E-03	60.000	432.95	2.356E-06	17.952
76	7.09E-04	41.706	1145.06	6.192E-07	4.718
77	3.07E-04	18.059	565.66	5.427E-07	4.136
78	1.24E-03	72.941	483.75	2.563E-06	19.532
79	3.23E-04	19.000	1208.65	2.672E-07	2.036
80	5.73E-04	33.706	645.59	8.876E-07	6.763
81	2.20E-04	12.941	387.93	5.671E-07	4.321
82	7.50E-04	44.118	365.15	2.054E-06	15.651
83	7.16E-04	42.118	351.42	2.037E-06	15.525
84	4.42E-04	26.000	581.00	7.608E-07	5.797
85	6.50E-04	38.235	583.18	1.115E-06	8.493
86	2.43E-04	14.294	106.34	2.285E-06	17.413
87	1.28E-04	7.529	72.61	1.763E-06	13.433
88	3.63E-04	21.353	349.27	1.039E-06	7.920

L#	CYP2B6 mRNA	CYP2B6 mRNA rel to L#110	β-actin	CYP2B6 mRNA normalized to β-actin	CYP2B6 mRNA normalized to β-actin rel to L#48
89	1.26E-04	7.412	103.67	1.215E-06	9.261
90	9.39E-05	5.524	123.27	7.617E-07	5.804
91	1.54E-04	9.059	238.18	6.466E-07	4.927
92					
93	1.02E-04	6.000	165.32	6.170E-07	4.701
94					
95	1.01E-03	59.412	1192.03	8.473E-07	6.456
96					
97	8.44E-04	49.647	3027.85	2.787E-07	2.124
98					
99	4.10E-04	24.118	669.97	6.120E-07	4.663
100	3.55E-05	2.088	6.09	5.829E-06	44.419
101	3.27E-05	1.924	22.22	1.472E-06	11.214
102					
103	2.53E-04	14.882	197.21	1.283E-06	9.776
104	1.32E-04	7.765	83.42	1.582E-06	12.057
105	1.72E-04	10.118	88.24	1.949E-06	14.853
106	3.89E-04	22.882	773.54	5.029E-07	3.832
107					
108	1.34E-04	7.882	9.71	1.380E-05	105.157
109	8.20E-05	4.824	75.50	1.086E-06	8.276
110	1.70E-05	1.000	29.96	5.674E-07	4.324
111					
112	1.81E-04	10.647	521.41	3.471E-07	2.645
113	3.00E-05	1.765	11.37	2.639E-06	20.105
140	2.79E-04	16.412	61.18	4.560E-06	34.749
141	1.19E-04	7.000	25.03	4.754E-06	36.228
213	2.47E-04	14.529	98.30	2.513E-06	19.147
264	2.42E-04	14.235	42.75	5.661E-06	43.135
287	1.41E-04	8.294	14.63	9.638E-06	73.439

Table 11: Results of quantitative real-time PCR

4. Oligonucleotides used in this work

Oligonucleotide	Sequence (5' – 3')
Genotyping -2320T>C	
2B6(-3010)F	GAA AGA GAC TGG CTG AAT GGA
2B6(-1894)R	TAT TGT TGC CAT CCC CAT TT
Genotyping c.1459C>T	
2B6(25238)F	CAA ATC TGT TGC AGT GGA CAT TTG
CYP2B6-9R	TAA TTT TCG ATA ATC TCA CTC CTG C
seqCYP2B6-9F	IRD800-TGA GAA TCA GTG GAA GCC ATA GA
Genotyping g.24322C>T	
2B6(24062)F	CTG GGT ATG CCA AAG GGA TG
2B6(24855)R	GCC TCC CAA AGT GGG ATT AC
seq2B6(24153)	IRD800-AAC TCA CAC TTG ACA TGG CC
DHPLC	
DH2B6(-275)F	CAC ACA TTC ACT TGC TCA CC
DH2B6(+12)R	GCT GAG TTC CAT GGT CCT G
Cloning	
2B6(-2253)F	TAT GAA TGA GAA CGC GTG ATA TTC ACT
2B6(-164)F	ACG CGT GGG TTC CCT AAC AAC TT
2B6(11)R	CTG AGT TAG ATC TTC CTG GTC TG
2B6(+16)R	GGA CGC TGA GTT AGA TCT TCC TGG TCT
2B6(15569)F	TCT GTG TCC TTG ACC TGC TG
2B6(16080)R	TCA TTC TCA TCA ACT CTG TCT CTC A
In vitro mutagenesis	
2B6-82MTF	GGG GAA TGG ATG AAA TTT CAT AAC AGG GTG CAG AGG C

Oligonucleotide	**Sequence (5' – 3')**
2B6-82MTR	GCC TCT GCA CCC TGT TAT GAA ATT TCA TCC ATT CCC C
2B6-750MTF	ATC ACG CCC GGC TAA TTT TTG T
2B6-750MTR	ACA AAA ATT AGC CGG GCG TGA T
2B6-801MTF	GGT TCA AGT GAT TCT CTT TCC TCA GCC TCC CGA G
2B6-801MTR	CTC GGG AGG CTG AGG AAA GAG AAT CAC TTG AAC C
2B6-1848MTF	GTA AAG CAC TTC AAG CCT CCC CAT CG
2B6-1848MTR	CGA TGG GGA GGC TTG AAG TGC TTT AC

5'-RACE & Primer extension

2B6cDNA(521)R	GAT GGA GCA GAT GAT GTT GGC GGT AA
luci(220)R	AGC TTC TGC CAA CCG AAC GGA CAT TT
luci(350)R	CAC GGT AGG CTG CGA AAT GCC CAT A
2B6cDNA(41)R	CCT GTG AGG AGT GCA AGG AAG AGG

EMSA (as=antisense)

2B6EMSA1 sense	GAT CCT GGA TGA AAT TTT ATA ACA GGG TGC A
2B6EMSA1 as	GAT CTG CAC CCT GTT ATA AAA TTT CAT CCA G
2B6EMSA2 sense	GAT CCT GGA TGA AAT TTC ATA ACA GGG TGC A
2B6EMSA2 as	GAT CTG CAC CCT GTT ATG AAA TTT CAT CCA G
2B6EMSA3 sense	GAT CCC AGG GTC AGG ATA AAA GGC CCA GTT A
2B6EMSA3 as	GAT CTA ACT GGG CCT TTT ATC CTG ACC CTG G
2B6EMSA4 sense	GAT CCT ACA GAG TGG GTA AAG GGA TA
2B6EMSA4 as	GAT CTA TCC CTT TAC CCA CTC TGT AG
2B6EMSA5 sense	GAT CCA CTG GGT TGC CCA AGC AGG AA
2B6EMSA5 as	GAT CTT CCT GCT TGG GCA ACC CAG TG
prHNF1WT sense	GAT CCG CCC GGT TAA TTT TTG TGT TA
prHNF1WT as	GAT CTA ACA CAA AAA TTA ACC GGG CG
prHNF1MT sense	GAT CCG CCC GGC TAA TTT TTG TGT TA
prHNF1MT as	GAT CTA ACA CAA AAA TTA GCC GGG CG
HNF1 apoE sense	GAT CCT CTC TGA GAG AAT CAT TAA CTT AAT TTA
HNF1 apoE as	GAT CTA AAT TAA GTT AAT GAT TCT CTC AGA GAG
C/EBP sense	GAT CCT GCA GAT TGC GCA ATC TGC AA

Oligonucleotide	**Sequence (5' – 3')**
C/EBP as	GAT CTT GCA GAT TGC GCA ATC TGC AG
AN15	GAT CCT ACG TTG TTA TTT GTT TTT TTC GA
AN16	GAT CTC GAA AAA AAC AAA TAA CAA CGT AG

Quantitative RT-PCR

TQ-CYP2B6FOR	GCT GAA CTT GTT CTA CCA GAC TTT TTC
TQ-CYP2B6REV	GAA AGT ATT TCA AGA AGC CAG AGA AGA G
CYP2B6 MGB-probe	FAM-TGT ATT CGG CCA GCT GT-MGBNFQ

Copy number assay

2B6(15748)F	TGT ATT CGG CCA GGT CAG G
2B6(15896)R	CCT GAT TCT TCA CAT GTC TGC G
2B6in4(15800)	FAM-TGA ACA CCC AGA ACA CAC GAG AAA AGG A-TAMRA
alb ex12 for	TGT TGC ATG AGA AAA CGC CA
alb ex12 rev	GTC GCC TGT TCA ACC AAG GAT
alb ex12 probe	VIC-AAG TGA CAG AGT CAC CAA ATG CTG CAC AG-TAMRA

Table 12: Oligonucleotides used in this study

VI REFERENCES

Antonarakis SE and the Nomenclature Working Group (1998) Recommendations for a nomenclature system for human gene mutations. *Hum Mutat* **11**: 1-3.

Ariyoshi N, Miyazaki M, Toide K, Sawamura Y and Kamataki T (2001) A single nucleotide polymorphism of CYP2b6 found in Japanese enhances catalytic activity by autoactivation. *Biochem Biophys Res Commun* **281**: 1256-1260.

Bosma PJ, Chowdhury JR, Bakker C, Gantla S, de Boer A, Oostra BA, Lindhout D, Tytgat GN, Jansen PL and Oude Elferink RP (1995) The genetic basis of the reduced expression of bilirubin UDP-glucuronosyltransferase 1 in Gilbert's syndrome. *N Engl J Med* **333**: 1171-1175.

Cao Z, Umek RM and McKnight SL (1991) Regulated expression of three C/EBP isoforms during adipose conversion of 3T3-L1 cells. *Genes Dev* **5**: 1538-1552.

Code EL, Crespi CL, Penman BW, Gonzalez FJ, Chang TK and Waxman DJ (1997) Human cytochrome P4502B6: interindividual hepatic expression, substrate specificity, and role in procarcinogen activation. *Drug Metab Dispos* **25**: 985-993.

Court MH, Duan SX, Hesse LM, Venkatakrishnan K and Greenblatt DJ (2001) Cytochrome P-450 2B6 is responsible for interindividual variability of propofol hydroxylation by human liver microsomes. *Anesthesiology* **94**: 110-119.

Csajka C, Marzolini C, Fattinger K, Decosterd LA, Fellay J, Telenti A, Biollaz J and Buclin T (2003) Population pharmacokinetics and effects of efavirenz in patients with human immunodeficiency virus infection. *Clin Pharmacol Ther* **73**: 20-30.

Czerwinski M, McLemore TL, Gelboin HV and Gonzalez FJ (1994) Quantification of CYP2B7, CYP4B1, and CYPOR messenger RNAs in normal human lung and lung tumors. *Cancer Res* **54**: 1085-1091.

Danielson PB (2002) The cytochrome P450 superfamily: biochemistry, evolution and drug metabolism in humans. *Curr Drug Metab* **3**: 561-597.

Dorko K, Freeswick PD, Bartoli F, Cicalese L, Bardsley BA, Tzakis A and Nussler AK (1994) A new technique for isolating and culturing human hepatocytes from whole or split livers not used for transplantation. *Cell Transplant* **3**: 387-395.

Ducharme MP, Bernstein ML, Granvil CP, Gehrcke B and Wainer IW (1997) Phenytoin-induced alteration in the N-dechloroethylation of ifosfamide stereoisomers. *Cancer Chemother Pharmacol* **40**: 531-533.

Ekins S, Vandenbranden M, Ring BJ, Gillespie JS, Yang TJ, Gelboin HV and Wrighton SA (1998) Further characterization of the expression in liver and catalytic activity of CYP2B6. *J Pharmacol Exp Ther* **286**: 1253-1259.

Endrizzi K, Fischer J, Klein K, Schwab M, Nussler A, Neuhaus P, Eichelbaum M and Zanger UM (2002) Discriminative quantification of cytochrome P4502D6 and 2D7/8 pseudogene expression by TaqMan real-time reverse transcriptase polymerase chain reaction. *Anal Biochem* **300**: 121-31.

Estabrook RW (2003) A passion for P450s (rememberances of the early history of research on cytochrome P450). *Drug Metab Dispos* **31**: 1461-1473.

Faucette SR, Hawke RL, LeCluyse EL, Shord SS, Yan B, Laethem RM and Lindley CM (2000) Validation of bupropion hydroxylation as a selective marker of human cytochrome P450 2B6 catalytic activity. *Drug Metab Dispos* **28**: 1222-1230.

Faucette SR, Wang H, Hamilton GA, Jolley SL, Gilbert D, Lindley C, Yan B, Negishi M and LeCluyse EL (2004) Regulation of CYP2B6 in primary human hepatocytes by prototypical inducers. *Drug Metab Dispos* **32**: 348-358.

Furukawa M, Nishimura M, Ogino D, Chiba R, Ikai I, Ueda N, Naito S, Kuribayashi S, Moustafa MA, Uchida T, Sawada H, Kamataki T, Funae Y and Fukumoto M (2004) Cytochrome p450 gene expression levels in peripheral blood mononuclear cells in comparison with the liver. *Cancer Sci* **95**: 520-529.

Futatsugawa Y, Kubota T, Ishiguro A, Suzuki H, Ishikawa H and Iga T (2004) PCR-based haplotype determination to distinguish CYP2B6*1/*7 and *5/*6. *Clin Chem* **50**: 1472-1473.

Gervot L, Rochat B, Gautier JC, Bohnenstengel F, Kroemer H, de Berardinis V, Martin H, Beaune P and de Waziers I (1999) Human CYP2B6: expression, inducibility and catalytic activities. *Pharmacogenetics* **9**: 295-306.

Gomez-Foix AM, Coats WS, Baque S, Alam T, Gerard RD and Newgard CB (1992) Adenovirus-mediated transfer of the muscle glycogen phosphorylase gene into hepatocytes confers altered regulation of glycogen metabolism. *J Biol Chem* **267**: 25129-25134.

Goodwin B, Moore LB, Stoltz CM, McKee DD and Kliewer SA (2001) Regulation of the human CYP2B6 gene by the nuclear pregnane X receptor. *Mol Pharmacol* **60**: 427-431.

Haas DW, Ribaudo HJ, Kim RB, Tierney C, Wilkinson GR, Gulick RM, Clifford DB, Hulgan T, Marzolini C and Acosta EP (2004) Pharmacogenetics of efavirenz and central nervous system side effects: an Adult AIDS Clinical Trials Group study. *Aids* **18**: 2391-2400.

Hardy GH (1908) Mendelian proportions in a mixed population. *Science* **28**: 49-50.

Hasse B, Gunthard HF, Bleiber G and Krause M (2005) Efavirenz intoxication due to slow hepatic metabolism. *Clin Infect Dis* **40**: e22-e23.

Heder AF, Hirsch-Ernst KI, Bauer D, Kahl GF and Desel H (2001) Induction of cytochrome P450 2B1 by pyrethroids in primary rat hepatocyte cultures. *Biochem Pharmacol* **62**: 71-9.

Hesse LM, He P, Krishnaswamy S, Hao Q, Hogan K, von Moltke LL, Greenblatt DJ and Court MH (2004) Pharmacogenetic determinants of interindividual variability in bupropion hydroxylation by cytochrome P450 2B6 in human liver microsomes. *Pharmacogenetics* **14**: 225-238.

Hiratsuka M, Takekuma Y, Endo N, Narahara K, Hamdy SI, Kishikawa Y, Matsuura M, Agatsuma Y, Inoue T and Mizugaki M (2002) Allele and genotype frequencies of CYP2B6 and CYP3A5 in the Japanese population. *Eur J Clin Pharmacol* **58**: 417-421.

Hirotsune S, Yoshida N, Chen A, Garrett L, Sugiyama F, Takahashi S, Yagami K, Wynshaw-Boris A and Yoshiki A (2003) An expressed pseudogene regulates the messenger-RNA stability of its homologous coding gene. *Nature* **423**: 91-96.

Hoffman SM, Nelson DR and Keeney DS (2001) Organization, structure and evolution of the CYP2 gene cluster on human chromosome 19. *Pharmacogenetics* **11**: 687-698.

Hoffmann M, Mager WH, Scholte BJ, Civil A and Planta RJ (1992) Analysis of the promoter of the cytochrome P-450 2B2 gene in the rat. *Gene Expr* **2**: 353-363.

Honkakoski P, Moore R, Gynther J and Negishi M (1996) Characterization of phenobarbital-inducible mouse Cyp2b10 gene transcription in primary hepatocytes. *J Biol Chem* **271**: 9746-9753.

Hosking L, Lumsden S, Lewis K, Yeo A, McCarthy L, Bansal A, Riley J, Purvis I and Xu CF (2004) Detection of genotyping errors by Hardy-Weinberg equilibrium testing. *Eur J Hum Genet* **12**: 395-399.

Ingelman-Sundberg M (1999) Duplication, multiduplication, and amplification of genes encoding drug-metabolizing enzymes: evolutionary, toxicological, and clinical pharmacological aspects. *Drug Metab Rev* **31**: 449-459.

Iwasaki M, Yoshimura Y, Asahi S, Saito K, Sakai S, Morita S, Takenaka O, Inoda T, Kashiyama E, Aoyama A, Nakabayashi T, Omori S, Kuwabara T, Izumi T, Nakamura K, Takanaka K, Nakayama Y, Takeuchi M, Nakamura H, Kametani S, Terauchi Y, Hashizume T, Nagayama S, Kume T, Achira M, Kawai H, Kawashiro T, Nakamura A, Nakai Y, Kagayama A, Shiraga T, Niwa T, Yoshimura T, Morita J, Ohsawa F, Tani M, Osawa N, Ida K and Noguchi K (2004) Functional characterization of single nucleotide polymorphisms with amino acid substitution in CYP1A2, CYP2A6, and CYP2B6 found in the Japanese population. *Drug Metab Pharmacokinet* **19**: 444-452.

Jacob RM, Johnstone EC, Neville MJ and Walton RT (2004) Identification of CYP2B6 sequence variants by use of multiplex PCR with allele-specific genotyping. *Clin Chem* **50**: 1372-1377.

Jakobsson J, Karypidis H, Johansson JE, Roh HK, Rane A and Ekstrom L (2004) A functional C-G polymorphism in the CYP7B1 promoter region and its different distribution in Orientals and Caucasians. *Pharmacogenomics J* **4**: 245-250.

Janmohamed A, Dolphin CT, Phillips IR and Shephard EA (2001) Quantification and cellular localization of expression in human skin of genes encoding flavin-containing monooxygenases and cytochromes P450. *Biochem Pharmacol* **62**: 777-86.

Jean A, Reiss A, Desrochers M, Dubois S, Trottier E, Trottier Y, Wirtanen L, Adesnik M, Waxman DJ and Anderson A (1994) Rat liver cytochrome P450 2B3: structure of the CYP2B3 gene and immunological identification of a constitutive P450 2B3-like protein in rat liver. *DNA Cell Biol* **13**: 781-792.

Jinno H, Tanaka-Kagawa T, Ohno A, Makino Y, Matsushima E, Hanioka N and Ando M (2003) Functional characterization of cytochrome P450 2B6 allelic variants. *Drug Metab Dispos* **31**: 398-403.

Jover R, Bort R, Gomez-Lechon MJ and Castell JV (1998) Re-expression of C/EBP alpha induces CYP2B6, CYP2C9 and CYP2D6 genes in HepG2 cells. *FEBS Lett* **431**: 227-30.

Jover R, Bort R, Gomez-Lechon MJ and Castell JV (2002) Down-regulation of human CYP3A4 by the inflammatory signal interleukin-6: molecular mechanism and transcription factors involved. *FASEB J* **16**: 1799-1801.

Ketter TA, Jenkins JB, Schroeder DH, Pazzaglia PJ, Marangell LB, George MS, Callahan AM, Hinton ML, Chao J and Post RM (1995) Carbamazepine but not valproate induces bupropion metabolism. *J Clin Psychopharmacol* **15**: 327-333.

Kirchheiner J, Klein C, Meineke I, Sasse J, Zanger UM, Murdter TE, Roots I and Brockmoller J (2003) Bupropion and 4-OH-bupropion pharmacokinetics in relation to genetic polymorphisms in CYP2B6. *Pharmacogenetics* **13**: 619-626.

Klingenberg M (1958) Pigments of rat liver microsomes. *Arch Biochem Biophys* **75**: 376-386.

Kohle C, Mohrle B, Munzel PA, Schwab M, Wernet D, Badary OA and Bock KW (2003) Frequent co-occurrence of the TATA box mutation associated with Gilbert's syndrome (UGT1A1*28) with other polymorphisms of the UDP-glucuronosyltransferase-1 locus (UGT1A6*2 and UGT1A7*3) in Caucasians and Egyptians. *Biochem Pharmacol* **65**: 1521-1527.

Kuo CJ, Conley PB, Hsieh CL, Francke U and Crabtree GR (1990) Molecular cloning, functional expression, and chromosomal localization of mouse hepatocyte nuclear factor 1. *Proc Natl Acad Sci U S A* **87**: 9838-9842.

Lakso M, Masaki R, Noshiro M and Negishi M (1991) Structures and characterization of sex-specific mouse cytochrome P-450 genes as members within a large family. Duplication boundary and evolution. *Eur J Biochem* **195**: 477-486.

Lamba V, Lamba J, Yasuda K, Strom S, Davila J, Hancock ML, Fackenthal JD, Rogan PK, Ring B, Wrighton SA and Schuetz EG (2003) Hepatic CYP2B6 Expression: Gender and Ethnic Differences and Relationship to CYP2B6 Genotype and CAR (Constitutive Androstane Receptor) Expression. *J Pharmacol Exp Ther* **307**: 906-922.

Lang T, Klein K, Fischer J, Nussler AK, Neuhaus P, Hofmann U, Eichelbaum M, Schwab M and Zanger UM (2001) Extensive genetic polymorphism in the human CYP2B6 gene with impact on expression and function in human liver. *Pharmacogenetics* **11**: 399-415.

Lang T, Klein K, Richter T, Zibat A, Kerb R, Eichelbaum M, Schwab M and Zanger UM (2004) Multiple Novel Nonsynonymous CYP2B6 Gene Polymorphisms in Caucasians: Demonstration of Phenotypic Null Alleles. *J Pharmacol Exp Ther* **311**: 34-41.

Mendel DB, Khavari PA, Conley PB, Graves MK, Hansen LP, Admon A and Crabtree GR (1991) Characterization of a cofactor that regulates dimerization of a mammalian homeodomain protein. *Science* **254**: 1762-7.

Miksys S, Lerman C, Shields PG, Mash DC and Tyndale RF (2003) Smoking, alcoholism and genetic polymorphisms alter CYP2B6 levels in human brain. *Neuropharmacology* **45**: 122-132.

Mimura M, Baba T, Yamazaki H, Ohmori S, Inui Y, Gonzalez FJ, Guengerich FP and Shimada T (1993) Characterization of cytochrome P-450 2B6 in human liver microsomes. *Drug Metab Dispos* **21**: 1048-1056.

Nelson DR, Koymans L, Kamataki T, Stegeman JJ, Feyereisen R, Waxman DJ, Waterman MR, Gotoh O, Coon MJ, Estabrook RW, Gunsalus IC and Nebert DW (1996) P450 superfamily: update on new sequences, gene mapping, accession numbers and nomenclature. *Pharmacogenetics* **6**: 1-42.

Nelson DR, Zeldin DC, Hoffman SM, Maltais LJ, Wain HM and Nebert DW (2004) Comparison of cytochrome P450 (CYP) genes from the mouse and human genomes, including nomenclature recommendations for genes, pseudogenes and alternative-splice variants. *Pharmacogenetics* **14**: 1-18.

Neurath M, Ma X and Pettersson S (1997) *DNA/Protein-Interaktionen*. Spektrum, Akad. Verl., Heidelberg.

Pai HV, Kommaddi RP, Chinta SJ, Mori T, Boyd MR and Ravindranath V (2004) A frameshift mutation and alternate splicing in human brain generate a functional form of the pseudogene cytochrome P4502D7 that demethylates codeine to morphine. *J Biol Chem* **279**: 27383-27389.

Park Y and Kemper B (1996) The CYP2B1 proximal promoter contains a functional C/EBP regulatory element. *DNA Cell Biol* **15**: 693-701.

Pitarque M, von Richter O, Oke B, Berkkan H, Oscarson M and Ingelman-Sundberg M (2001) Identification of a single nucleotide polymorphism in the TATA box of the CYP2A6 gene: impairment of its promoter activity. *Biochem Biophys Res Commun* **284**: 455-460.

Quandt K, Frech K, Karas H, Wingender E and Werner T (1995) MatInd and MatInspector: new fast and versatile tools for detection of consensus matches in nucleotide sequence data. *Nucleic Acids Res* **23**: 4878-4884.

Rao Y, Hoffmann E, Zia M, Bodin L, Zeman M, Sellers EM and Tyndale RF (2000) Duplications and defects in the CYP2A6 gene: identification, genotyping, and in vivo effects on smoking. *Mol Pharmacol* **58**: 747-55.

Richter T, Murdter TE, Heinkele G, Pleiss J, Tatzel S, Schwab M, Eichelbaum M and Zanger UM (2004) Potent mechanism-based inhibition of human CYP2B6 by clopidogrel and ticlopidine. *J Pharmacol Exp Ther* **308**: 189-197.

Rotger M, Colombo S, Furrer H, Bleiber G, Buclin T, Lee BL, Keiser O, Biollaz J, Decosterd L, Telenti A and the Swiss HIV Cohort Study (2005) Influence of CYP2B6 polymorphism on plasma and intracellular concentrations and toxicity of efavirenz and nevirapine in HIV-infected patients. *Pharmacogenetics & Genomics* **15**: 1-5.

Roy P, Yu LJ, Crespi CL and Waxman DJ (1999) Development of a substrate-activity based approach to identify the major human liver P-450 catalysts of cyclophosphamide and

ifosfamide activation based on cDNA-expressed activities and liver microsomal P-450 profiles. *Drug Metab Dispos* **27**: 655-666.

Schaeffeler E, Schwab M, Eichelbaum M and Zanger UM (2003) CYP2D6 genotyping strategy based on gene copy number determination by TaqMan real-time PCR. *Hum Mutat* **22**: 476-485.

Schenkman JB and Jansson I (2003) The many roles of cytochrome b5. *Pharmacol Ther* **97**: 139-152.

Schreiber E, Matthias P, Muller MM and Schaffner W (1989) Rapid detection of octamer binding proteins with 'mini-extracts', prepared from a small number of cells. *Nucleic Acids Res* **17**: 6419.

Seglen PO (1976) Preparation of isolated rat liver cells. *Methods Cell Biol* **13**: 29-83.

Shimada T, Yamazaki H, Mimura M, Inui Y and Guengerich FP (1994) Interindividual variations in human liver cytochrome P-450 enzymes involved in the oxidation of drugs, carcinogens and toxic chemicals: studies with liver microsomes of 30 Japanese and 30 Caucasians. *J Pharmacol Exp Ther* **270**: 414-423.

Smith PK, Krohn RI, Hermanson GT, Mallia AK, Gartner FH, Provenzano MD, Fujimoto EK, Goeke NM, Olson BJ and Klenk DC (1985) Measurement of protein using bicinchoninic acid. *Anal Biochem* **150**: 76-85.

Stephens M, Smith NJ and Donnelly P (2001) A new statistical method for haplotype reconstruction from population data. *Am J Hum Genet* **68**: 978-989.

Stresser DM and Kupfer D (1999) Monospecific antipeptide antibody to cytochrome P-450 2B6. *Drug Metab Dispos* **27**: 517-525.

Suzuki Y, Yamashita R, Nakai K and Sugano S (2002) DBTSS: DataBase of human Transcriptional Start Sites and full-length cDNAs. *Nucleic Acids Res* **30**: 328-331.

Svensson US and Ashton M (1999) Identification of the human cytochrome P450 enzymes involved in the in vitro metabolism of artemisinin. *Br J Clin Pharmacol* **48**: 528-535.

Swales K, Kakizaki S, Yamamoto Y, Inoue K, Kobayashi K and Negishi M (2005) Novel CAR-mediated mechanism for synergistic activation of two distinct elements within the human cytochrome P450 2B6 gene in HepG2 cells. *J Biol Chem* **280**: 3458-3466.

Takebe Y, Seiki M, Fujisawa J, Hoy P, Yokota K, Arai K, Yoshida M and Arai N (1988) SR alpha promoter: an efficient and versatile mammalian cDNA expression system composed of the simian virus 40 early promoter and the R-U5 segment of human T-cell leukemia virus type 1 long terminal repeat. *Mol Cell Biol* **8**: 466-472.

Torrents D, Suyama M, Zdobnov E and Bork P (2003) A genome-wide survey of human pseudogenes. *Genome Res* **13**: 2559-2567.

Tsuchiya K, Gatanaga H, Tachikawa N, Teruya K, Kikuchi Y, Yoshino M, Kuwahara T, Shirasaka T, Kimura S and Oka S (2004) Homozygous CYP2B6 *6 (Q172H and K262R)

correlates with high plasma efavirenz concentrations in HIV-1 patients treated with standard efavirenz-containing regimens. *Biochem Biophys Res Commun* **319**: 1322-1326.

Venkatakrishnan K, von Moltke LL, Court MH, Harmatz JS, Crespi CL and Greenblatt DJ (2000) Comparison between cytochrome P450 (CYP) content and relative activity approaches to scaling from cDNA-expressed CYPs to human liver microsomes: ratios of accessory proteins as sources of discrepancies between the approaches. *Drug Metab Dispos* **28**: 1493-1504.

Wade DP, Lindahl GE and Lawn RM (1994) Apolipoprotein(a) gene transcription is regulated by liver-enriched trans-acting factor hepatocyte nuclear factor 1 alpha. *J Biol Chem* **269**: 19757-19765.

Wang H, Faucette S, Sueyoshi T, Moore R, Ferguson S, Negishi M and LeCluyse EL (2003) A novel distal enhancer module regulated by pregnane X receptor/constitutive androstane receptor is essential for the maximal induction of CYP2B6 gene expression. *J Biol Chem* **278**: 14146-14152.

Ward BA, Gorski JC, Jones DR, Hall SD, Flockhart DA and Desta Z (2003) The cytochrome P450 2B6 (CYP2B6) is the main catalyst of efavirenz primary and secondary metabolism: implication for HIV/AIDS therapy and utility of efavirenz as a substrate marker of CYP2B6 catalytic activity. *J Pharmacol Exp Ther* **306**: 287-300.

Wolbold R, Klein K, Burk O, Nussler AK, Neuhaus P, Eichelbaum M, Schwab M and Zanger UM (2003) Sex is a major determinant of CYP3A4 expression in human liver. *Hepatology* **38**: 978-988.

Xie HJ, Yasar U, Lundgren S, Griskevicius L, Terelius Y, Hassan M and Rane A (2003) Role of polymorphic human CYP2B6 in cyclophosphamide bioactivation. *Pharmacogenomics J* **3**: 53-61.

Xu J, Turner A, Little J, Bleecker ER and Meyers DA (2002) Positive results in association studies are associated with departure from Hardy-Weinberg equilibrium: hint for genotyping error? *Hum Genet* **111**: 573-574.

Yamanaka H, Nakajima M, Katoh M, Hara Y, Tachibana O, Yamashita J, McLeod HL and Yokoi T (2004) A novel polymorphism in the promoter region of human UGT1A9 gene (UGT1A9*22) and its effects on the transcriptional activity. *Pharmacogenetics* **14**: 329-332.

Yamano S, Nhamburo PT, Aoyama T, Meyer UA, Inaba T, Kalow W, Gelboin HV, McBride OW and Gonzalez FJ (1989) cDNA cloning and sequence and cDNA-directed expression of human P450 IIB1: identification of a normal and two variant cDNAs derived from the CYP2B locus on chromosome 19 and differential expression of the IIB mRNAs in human liver. *Biochemistry* **28**: 7340-7348.

Yang TJ, Krausz KW, Shou M, Yang SK, Buters JT, Gonzalez FJ and Gelboin HV (1998) Inhibitory monoclonal antibody to human cytochrome P450 2B6. *Biochem Pharmacol* **55**: 1633-1640.

Yule SM, Boddy AV, Cole M, Price L, Wyllie R, Tasso MJ, Pearson AD and Idle JR (1996) Cyclophosphamide pharmacokinetics in children. *Br J Clin Pharmacol* **41**: 13-19.

Zanger UM, Raimundo S and Eichelbaum M (2004) Cytochrome P450 2D6: overview and update on pharmacology, genetics, biochemistry. *Naunyn Schmiedebergs Arch Pharmacol* **369**: 23-37.

Zukunft J, Lang T, Richter T, Hirsch-Ernst KI, Nussler AK, Klein K, Schwab M, Eichelbaum M and Zanger UM (2005) A Natural CYP2B6 TATA Box Polymorphism (-82T-> C) Leading to Enhanced Transcription and Relocation of the Transcriptional Start Site. *Mol Pharmacol* **67**: 1772-1782.

DANKSAGUNGEN

Die vorliegende Dissertation wurde von März 2002 bis April 2005 am Dr. Margarete Fischer-Bosch-Institut für Klinische Pharmakologie in Stuttgart angefertigt. An dieser Stelle bedanke ich mich bei allen Mitarbeitern des Instituts für die gute Zusammenarbeit und freundschaftliche Atmosphäre.

Mein besonderer Dank gilt meinem Doktorvater PD Dr. Uli Zanger. Seine kreativen Ideen und Impulse konnten mich immer wieder motivieren und trugen wesentlich zur fristgerechten Fertigstellung meiner Doktorarbeit bei. Ebenso danke ich ihm für die Ermöglichung meiner Teilnahme an mehreren internationalen Kongressen.

Ich danke Herrn Professor Dr. Michel Eichelbaum für die Möglichkeit, die Doktorarbeit an seinem Institut anzufertigen, und für sein stetiges Interesse an deren Fortkommen. Bei Herrn Professor Dr. Karl-Walter Bock von der Universität Tübingen bedanke ich mich für die Begleitung und Begutachtung meiner Dissertation.

Den Kollegen der Arbeitsgruppe Zanger/Schwab danke ich für die gute Zusammenarbeit. Bei Dr. Oliver Burk bedanke ich mich herzlich für seine ständige Diskussionbereitschaft. Herrn Dr. Thomas Lang, Frau PD Dr. Karen Hirsch-Ernst sowie den Herren PD Dr. Andreas Nüssler und Professor Dr. Peter Neuhaus sei an dieser Stelle für ihre externen Beiträge zu meiner Dissertation gedankt.

Bei meinen Bürokollegen, den Dres. Siegfried Drescher, Kari Kivistö und Werner Schroth, bedanke ich mich für die gute Arbeitsatmosphäre und zahlreiche bereichernde Gespräche. Ebenso geht ein herzliches Dankeschön an die "Kaffeerunde" für die fruchtbare arbeitsgruppenübergreifende Kommunikation.

Zum Schluss danke ich herzlich meiner lieben Frau Tatjana, meinen Eltern, Siegrun und Peter Stütz, und meinen Großeltern, Charlotte und Hans Klink, die mich stets begleitet und unterstützt haben.

Meine akademischen Lehrer waren die Damen und Herren:

Ammon, Bechthold, Derendorf, Drews, Eich, Eichelbaum, Heide, Hiller, Kivistö, Kovar, Lipp, Schäfer-Korting, Schmidt, Schultz, Schunack, Šumski, Ward, Zanger.

LEBENSLAUF

Jörg Alexander Zukunft, geb. Stütz, geboren am 13. Februar 1973 in Pforzheim; verheiratet mit Tatjana Zukunft, ein Kind (geboren am 14. Mai 2004)

07/1984 – 05/1992	Gymnasium Neuenbürg Abitur
06/1992 – 09/1993	Behinderten-Initiative ’76 e.V., Pforzheim Zivildienst
10/1993 – 07/1995	Eberhard-Karls-Universität Tübingen Studium der Biochemie
10/1995 – 07/1996	Eberhard-Karls-Universität Tübingen Studium der Pharmazie 1. Staatsexamen
10/1996 – 07/1997	Freie Universität Berlin Studium der Pharmazie
10/1997 – 02/1998	Auslandsaufenthalt in Mexiko
04/1998 – 10/1999	Eberhard-Karls-Universität Tübingen Studium der Pharmazie 2. Staatsexamen
11/1999 – 04/2000	Praktikum in der Hölderlin-Apotheke, Tübingen
05/2000 – 11/2000	Praktikum an der University of Florida, Gainesville
12/2000	3. Staatsexamen
01/2001	Erhalt der Approbation als Apotheker
02/2001 – 01/2002	Sonnen-Apotheke Pforzheim Tätigkeit als Offizinapotheker
03/2002 – 04/2005	Dr. Margarete Fischer-Bosch-Institut für Klinische Pharmakologie, Stuttgart Promotion